

1979

Synthesis and reactions of selected organodichromium compounds

Michael Charles Pohl
Iowa State University

Follow this and additional works at: <https://lib.dr.iastate.edu/rtd>

 Part of the [Inorganic Chemistry Commons](#)

Recommended Citation

Pohl, Michael Charles, "Synthesis and reactions of selected organodichromium compounds " (1979). *Retrospective Theses and Dissertations*. 6667.
<https://lib.dr.iastate.edu/rtd/6667>

This Dissertation is brought to you for free and open access by the Iowa State University Capstones, Theses and Dissertations at Iowa State University Digital Repository. It has been accepted for inclusion in Retrospective Theses and Dissertations by an authorized administrator of Iowa State University Digital Repository. For more information, please contact digirep@iastate.edu.

INFORMATION TO USERS

This was produced from a copy of a document sent to us for microfilming. While the most advanced technological means to photograph and reproduce this document have been used, the quality is heavily dependent upon the quality of the material submitted.

The following explanation of techniques is provided to help you understand markings or notations which may appear on this reproduction.

1. The sign or "target" for pages apparently lacking from the document photographed is "Missing Page(s)". If it was possible to obtain the missing page(s) or section, they are spliced into the film along with adjacent pages. This may have necessitated cutting through an image and duplicating adjacent pages to assure you of complete continuity.
2. When an image on the film is obliterated with a round black mark it is an indication that the film inspector noticed either blurred copy because of movement during exposure, or duplicate copy. Unless we meant to delete copyrighted materials that should not have been filmed, you will find a good image of the page in the adjacent frame.
3. When a map, drawing or chart, etc., is part of the material being photographed the photographer has followed a definite method in "sectioning" the material. It is customary to begin filming at the upper left hand corner of a large sheet and to continue from left to right in equal sections with small overlaps. If necessary, sectioning is continued again—beginning below the first row and continuing on until complete.
4. For any illustrations that cannot be reproduced satisfactorily by xerography, photographic prints can be purchased at additional cost and tipped into your xerographic copy. Requests can be made to our Dissertations Customer Services Department.
5. Some pages in any document may have indistinct print. In all cases we have filmed the best available copy.

University
Microfilms
International

300 N. ZEEB ROAD, ANN ARBOR, MI 48106
18 BEDFORD ROW, LONDON WC1R 4EJ, ENGLAND

7924265

POHL, MICHAEL CHARLES
SYNTHESIS AND REACTIONS OF SELECTED
ORGANODICHRONIUM COMPOUNDS.

IOWA STATE UNIVERSITY, PH.D., 1979

University
Microfilms
International 300 N. ZEEB ROAD, ANN ARBOR, MI 48106

PLEASE NOTE:

In all cases this material has been filmed in the best possible way from the available copy. Problems encountered with this document have been identified here with a check mark .

1. Glossy photographs _____
2. Colored illustrations _____
3. Photographs with dark background _____
4. Illustrations are poor copy _____
5. Print shows through as there is text on both sides of page _____
6. Indistinct, broken or small print on several pages throughout

7. Tightly bound copy with print lost in spine _____
8. Computer printout pages with indistinct print _____
9. Page(s) _____ lacking when material received, and not available
from school or author _____
10. Page(s) _____ seem to be missing in numbering only as text
follows _____
11. Poor carbon copy _____
12. Not original copy, several pages with blurred type _____
13. Appendix pages are poor copy _____
14. Original copy with light type _____
15. Curling and wrinkled pages _____
16. Other _____

Synthesis and reactions of selected
organodichromium compounds

by

Michael Charles Pohl

A Dissertation Submitted to the
Graduate Faculty in Partial Fulfillment of
The Requirements for the Degree of
DOCTOR OF PHILOSOPHY

Department: Chemistry
Major: Inorganic Chemistry

Approved:

Signature was redacted for privacy.

In Charge of Major Work

Signature was redacted for privacy.

For the Major Department

Signature was redacted for privacy.

For the Graduate College

Iowa State University
Ames, Iowa

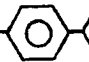
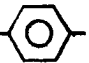
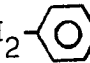
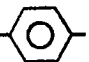
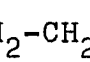
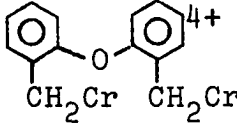

1979

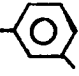
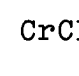
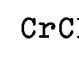
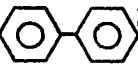
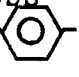
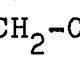
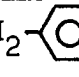
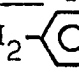
TABLE OF CONTENTS

	Page
INTRODUCTION	1
HISTORICAL	5
EXPERIMENTAL	11
Materials	11
Dibromoxylenes	11
4,4'-Bis(bromomethyl)biphenyl; 4,4'-bis(bromo- methyl)diphenylmethane; 4,4'-bis(bromomethyl)- 1,2-diphenylethane	11
4,4'-Bis(bromomethyl)diphenyl ether	13
2,4-Bis(bromomethyl)toluene	15
p-Phenylbenzyl bromide	16
p-(Bromomethyl)benzyl alcohol	16
p-(Hydroxymethyl)benzyl cobaloxime	18
p-Xylene dicobaloxime	19
Organodichromium compounds	19
Organochromium compounds	20
Organomercury compounds	21
Base decomposition products	23
Poly-p-xylylene	24
Organic product isolation	24
Inorganic reagents	25
Other materials	26

Methods	27
Kinetics	27
Analyses	30
Stoichiometry experiments	31
Electrolysis	32
Photolyses	33
Analog computer experiments	33
RESULTS	36
Characterization of Compounds	36
DISCUSSION	109
BIBLIOGRAPHY	167
ACKNOWLEDGEMENTS	173

LIST OF FIGURES

	Page
Figure 1. Structures of the organodichromium cations	3
Figure 2. Structures of the organochromium cations	4
Figure 3. The analog computer wiring diagram	35
Figure 4. ^1H NMR spectra of 4,4'-bis(bromomethyl)-biphenyl	41
Figure 5. ^1H NMR spectra of 4,4'-bis(bromomethyl)-diphenylmethane	42
Figure 6. ^1H NMR spectra of 4,4'-bis(bromomethyl)-1,2-diphenylethane	43
Figure 7. ^1H NMR spectra of 2,4-bis(bromomethyl)-toluene	44
Figure 8. ^1H NMR spectra of p-(bromomethyl)benzyl alcohol	45
Figure 9. ^1H NMR spectra of p-(hydroxymethyl)-benzylcobaloxime	47
Figure 10. ^1H NMR spectra of the base decomposition product of CrCH_2 -  - $\text{CH}_2\text{Cr}^{4+}$	52
Figure 11. ^1H NMR spectra of the base decomposition product of CrCH_2 -  - CH_2 -  - $\text{CH}_2\text{Cr}^{4+}$	53
Figure 12. ^1H NMR spectra of the base decomposition product of CrCH_2 -  - CH_2 - CH_2 -  - $\text{CH}_2\text{Cr}^{4+}$	54
Figure 13. ^1H NMR spectra of the base decomposition product of  $^{4+}$	55
Figure 14. ^1H NMR spectra of the base decomposition product of CrCH_2 -  - $\text{CH}_2\text{OH}^{2+}$	56

- Figure 15. ^1H NMR spectra of the base decomposition product of CrCH_2 -- $\text{CH}_2\text{Br}^{2+}$ 57
- Figure 16. IR spectra of authentic poly-p-xylylene 59
- Figure 17. IR spectra of poly-p-xylylene from the electrochemical preparation 60
- Figure 18. IR spectra of polymer from Fe^{3+} decomposition of CrCH_2 -- $\text{CH}_2\text{Cr}^{4+}$ 61
- Figure 19. IR spectra of polymer from Fe^{3+} decomposition of CrCH_2 -- $\text{CH}_2\text{OH}^{2+}$ 62
- Figure 20. IR spectra of a film of poly-p-xylylene 63
- Figure 21. ^1H NMR spectra of the product of reaction of CrCH_2 -- $^{2+}$ with Fe^{3+} 65
- Figure 22. A plot of k_{obs} versus $[\text{Fe}^{3+}]$ for the reaction of CrCH_2 -- CH_2 - CH_2 -- $\text{CH}_2\text{Cr}^{4+}$ 73
- Figure 23. Test of the trial rate equation 2.42 for reaction of V^{3+} and Cr^{2+} by a plot of $1/k_{\text{app}}$ (25°C) versus $[\text{H}^+]$ 75
- Figure 24. A plot of k_{obs} versus $[\text{Fe}^{3+}]$ for the reaction of CrCH_2 -- $\text{CH}_2\text{Br}^{2+}$ at 0.1 M H^+ 79
- Figure 25. A plot of k_{obs} versus $[\text{Fe}^{3+}]$ for the reaction of CrCH_2 -- $\text{CH}_2\text{Br}^{2+}$ at 0.1 M $\text{HClO}_4/0.3$ M NaClO_4 80

- Figure 26. A plot of absorbance versus time for
 $A \xrightarrow{k_1} B \xrightarrow{k_2} C$ with $[A]_0 = 1.0$,
 $[B]_0 = [C]_0 = 0$, $k_1 = 0.50$, $k_2 = 0.25$,
 $\epsilon_A = 1.0$, $\epsilon_B = 1.0$, $\epsilon_C = 0$ 81
- Figure 27. A plot of $\ln|D_t - D_\infty|$ versus time for
 $A \xrightarrow{k_1} B \xrightarrow{k_2} C$ with $[A]_0 = 1.0$,
 $[B]_0 = [C]_0 = 0$, $k_1 = 0.50$, $k_2 = 0.25$,
 $\epsilon_A = 1.0$, $\epsilon_B = 1.0$, $\epsilon_C = 0$ 82
- Figure 28. A plot of absorbance versus time for
 $A \xrightarrow{k_1} B \xrightarrow{k_2} C$ with $[A]_0 = 1.0$,
 $[B]_0 = [C]_0 = 0$, $k_1 = 0.50$, $k_2 = 0.25$,
 $\epsilon_A = 1.0$, $\epsilon_B = 0.6$, $\epsilon_C = 0$ 83
- Figure 29. A plot of $\ln|D_t - D_\infty|$ versus time for
 $A \xrightarrow{k_1} B \xrightarrow{k_2} C$ with $[A]_0 = 1.0$,
 $[B]_0 = [C]_0 = 0$, $k_1 = 0.50$, $k_2 = 0.25$,
 $\epsilon_A = 1.0$, $\epsilon_B = 0.6$, $\epsilon_C = 0$ 84
- Figure 30. A plot of $[A]$, $[B]$ and $[C]$ versus time
 $A \xrightarrow{k_1} B \xrightarrow{k_2} C$ with $[A]_0 = 1.0$,
 $[B]_0 = [C]_0 = 0$, $k_1 = 0.50$, $k_2 = 0.25$,
 $\epsilon_A = 1.0$, $\epsilon_B = 0.5$, $\epsilon_C = 0$ 85
- Figure 31. A plot of absorbance versus time for
 $A \xrightarrow{k_1} B \xrightarrow{k_2} C$ with $[A]_0 = 1.0$,
 $[B]_0 = [C]_0 = 0$, $k_1 = 0.50$, $k_2 = 0.25$,
 $\epsilon_A = 1.0$, $\epsilon_B = 0.5$, $\epsilon_C = 0$ 86

- Figure 32. A plot of $\ln|D_t - D_\infty|$ versus time for
 $A \xrightarrow{k_1} B \xrightarrow{k_2} C$ with $[A]_0 = 1.0$,
 $[B]_0 = [C]_0 = 0$, $k_1 = 0.50$, $k_2 = 0.25$,
 $\epsilon_A = 1.0$, $\epsilon_B = 0.50$, $\epsilon_C = 0$ 87
- Figure 33. A plot of absorbance versus time for
 $A \xrightarrow{k_1} B \xrightarrow{k_2} C$ with $[A]_0 = 1.0$,
 $[B]_0 = [C]_0 = 0$, $k_1 = 0.50$, $k_2 = 0.25$,
 $\epsilon_A = 1.0$, $\epsilon_B = 0.4$, $\epsilon_C = 0$ 88
- Figure 34. A plot of $\ln|D_t - D_\infty|$ versus time for
 $A \xrightarrow{k_1} B \xrightarrow{k_2} C$ with $[A]_0 = 1.0$,
 $[B]_0 = [C]_0 = 0$, $k_1 = 0.50$, $k_2 = 0.25$,
 $\epsilon_A = 1.0$, $\epsilon_B = 0.4$, $\epsilon_C = 0$ 89
- Figure 35. A plot of absorbance versus time for
 $A \xrightarrow{k_1} B \xrightarrow{k_2} C$ with $[A]_0 = 1.0$,
 $[B]_0 = [C]_0 = 0$, $k_1 = 0.50$, $k_2 = 0.25$,
 $\epsilon_A = 1.0$, $\epsilon_B = 0.1$, $\epsilon_C = 0$ 90
- Figure 36. A plot of absorbance versus time for
 $A \xrightarrow{k_1} B \xrightarrow{k_2} C$ with $[A]_0 = 1.0$,
 $[B]_0 = [C]_0 = 0$, $k_1 = 1.00$, $k_2 = 0.25$,
 $\epsilon_A = 1.0$, $\epsilon_B = 0.5$, $\epsilon_C = 0$ 93
- Figure 37. A plot of $\ln|D_t - D_\infty|$ versus time for
 $A \xrightarrow{k_1} B \xrightarrow{k_2} C$ with $[A]_0 = 1.0$,
 $[B]_0 = [C]_0 = 0$, $k_1 = 1.00$, $k_2 = 0.25$,
 $\epsilon_A = 1.0$, $\epsilon_B = 0.5$, $\epsilon_C = 0$ 94

- Figure 38. A plot of absorbance versus time for
 $A \xrightarrow{k_1} B \xrightarrow{k_2} C$ with $[A]_0 = 1.0$,
 $[B]_0 = [C]_0 = 0$, $k_1 = 1.00$, $k_2 = 0.125$,
 $\epsilon_A = 1.0$, $\epsilon_B = 0.5$, $\epsilon_C = 0$ 95
- Figure 39. A plot of $\ln|D_t - D_\infty|$ versus time for
 $A \xrightarrow{k_1} B \xrightarrow{k_2} C$ with $[A]_0 = 1.0$,
 $[B]_0 = [C]_0 = 0$, $k_1 = 1.00$, $k_2 = 0.125$,
 $\epsilon_A = 1.0$, $\epsilon_B = 0.5$, $\epsilon_C = 0$ 96
- Figure 40. A plot of $[A]$, $[B]$ and $[C]$ versus time
for $A \xrightarrow{k_1} B \xrightarrow{k_2} C$ with $[A]_0 = 1.0$,
 $[B]_0 = [C]_0 = 0$, $k_1 = 1.00$, $k_2 = 0.033$,
 $\epsilon_A = 1.0$, $\epsilon_B = 0.5$, $\epsilon_C = 0$ 97
- Figure 41. A plot of absorbance versus time for
 $A \xrightarrow{k_1} B \xrightarrow{k_2} C$ with $[A]_0 = 1.0$,
 $[B]_0 = [C]_0 = 0$, $k_1 = 1.00$, $k_2 = 0.033$,
 $\epsilon_A = 1.0$, $\epsilon_B = 0.5$, $\epsilon_C = 0$ 98
- Figure 42. A plot of $\ln|D_t - D_\infty|$ versus time for
 $A \xrightarrow{k_1} B \xrightarrow{k_2} C$ with $[A]_0 = 1.0$,
 $[B]_0 = [C]_0 = 0$, $k_1 = 1.00$, $k_2 = 0.033$,
 $\epsilon_A = 1.0$, $\epsilon_B = 0.5$, $\epsilon_C = 0$ 99
- Figure 43. A plot of Δ versus time for $A \xrightarrow{k_1} B \xrightarrow{k_2} C$
with $[A]_0 = 1.0$, $[B]_0 = [C]_0 = 0$, $k_1 = 1.00$,
 $k_2 = 0.033$, $\epsilon_A = 1.0$, $\epsilon_B = 0.5$, $\epsilon_C = 0$ 100
- Figure 44. A plot of k_1 versus σ_p for the decomposition
of substituted benzyl-chromium cation
and oxidizing agents 113
- Figure 45. A plot of k_2/k_1 versus ϕ where $\phi = \epsilon_B/\epsilon_C$ 133

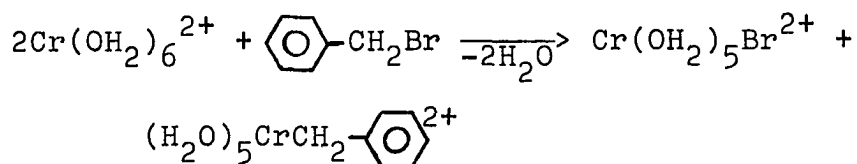
LIST OF TABLES

	Page
Table 1. Characterization of the organic bromides and dibromides	37
Table 2. Characterization of the cobaloximes	46
Table 3. Characterization of the organic products of the base decomposition reaction	50
Table 4. Elemental analyses of poly-p-xylylene samples	58
Table 5. The kinetics of the reaction of $\text{CrCH}_2\text{-}\langle\bigcirc\rangle\text{-CH}_2\text{Cr}^{4+}$ with oxidizing agents	66
Table 6. The kinetics of the reaction of $\text{CrCH}_2\text{-}\langle\bigcirc\rangle\text{-CH}_2\text{Cr}^{4+}$ with oxidizing agents	68
Table 7. The kinetics of the reaction of $\text{CrCH}_2\text{-}\langle\bigcirc\rangle\text{-CH}_2\text{-CH}_2\text{-}\langle\bigcirc\rangle\text{-CH}_2\text{Cr}^{4+}$ with oxidizing agents	69
Table 8. The kinetics of the reaction of $\text{CrCH}_2\text{-}\langle\bigcirc\rangle\text{-CH}_2\text{-}\langle\bigcirc\rangle\text{-CH}_2\text{Cr}^{4+}$ with oxidizing agents	70
Table 9. The treatment of data for the rate law $k_{\text{app}} = k_1 + k_2 [X]$	74
Table 10. The kinetics of the reaction of $\text{CrCH}_2\text{-}\langle\bigcirc\rangle\text{-CH}_2\text{OH}^{2+}$ with oxidizing agents	75
Table 11. The kinetics of the reaction of $\text{CrCH}_2\text{-}\langle\bigcirc\rangle\text{-CH}_2\text{Br}^{2+}$ with oxidizing agents	77

Table 12.	The kinetics of the reaction of $\text{CrCH}_2\text{-}\langle\text{O}\rangle\text{-}\langle\text{O}\rangle^{2+}$ with oxidizing agents	78
Table 13.	Rate law derivation for statistical kinetics	92
Table 14.	The determination of ϵ for organochromium and organodichromium compounds	102
Table 15.	The stoichiometry of the reaction of Fe^{3+} and organodichromium compounds	103
Table 16.	The decomposition products of organodichromium cations	106
Table 17.	The decomposition products of organochromium cations	108
Table 18.	The organic products of the reaction of benzyl-chromium and oxidizing agents	123
Table 19.	The anticipated organic products of the reaction of $\text{CrCH}_2\text{-}\langle\text{O}\rangle\text{-CH}_2\text{Cr}^{4+}$ and oxidizing agents	124

INTRODUCTION

This thesis is concerned with organometallic compounds which contain two metal-carbon bonds in the same molecule. The central focus is on molecules containing two carbon-chromium bonds, but one containing carbon-cobalt bonds will also be investigated. Perhaps the simplest method of forming carbon-chromium bonds is to react Cr^{2+} with an activated organic halide. Such a method is shown below for the formation of the benzyl-chromium cation.¹ By analogy,



if one had two benzylic bromides in the same molecule, then reaction with four moles of chromous ion should produce an organometallic compound with two carbon-chromium bonds. This

¹A convention used throughout this work concerns the notation for metal ions in solution. In general, the metal ions are six coordinate, as shown, but the water molecules in the primary coordination sphere will not be shown. For example, Cr^{3+} refers to the hexaquo species $(\text{H}_2\text{O})_6\text{Cr}^{3+}$, and CrR^{2+} refers to the pentaquo organochromium(III) species, $(\text{H}_2\text{O})_5\text{CrR}^{2+}$.

method has been employed to synthesize a number of organo-dichromium compounds which are illustrated in Figure 1. During the course of this project, it became necessary to study several organochromium compounds, and their structures are shown in Figure 2. This thesis will deal with the isolation, characterization, and reactions of these organochromium compounds.

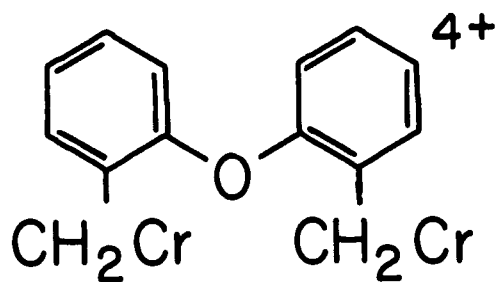
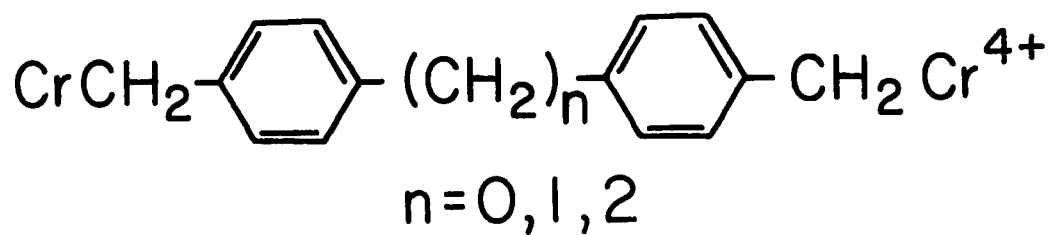
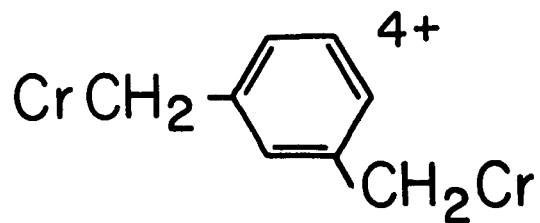
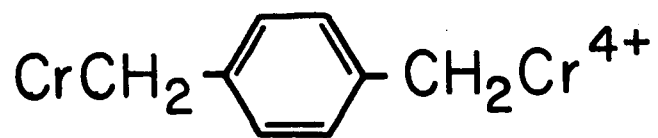


Figure 1. Structures of the organodichromium cations

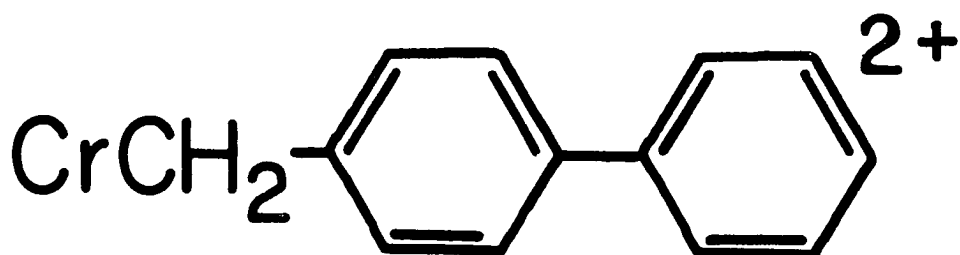
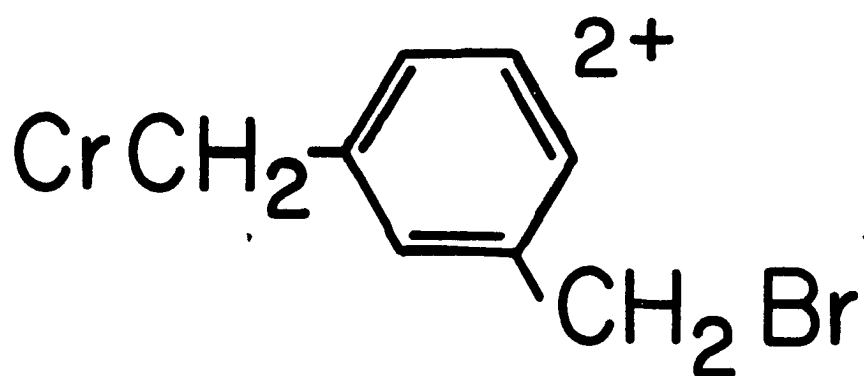
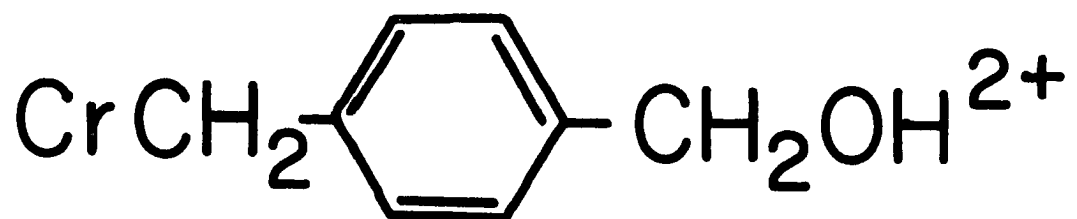
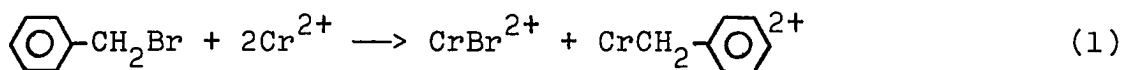


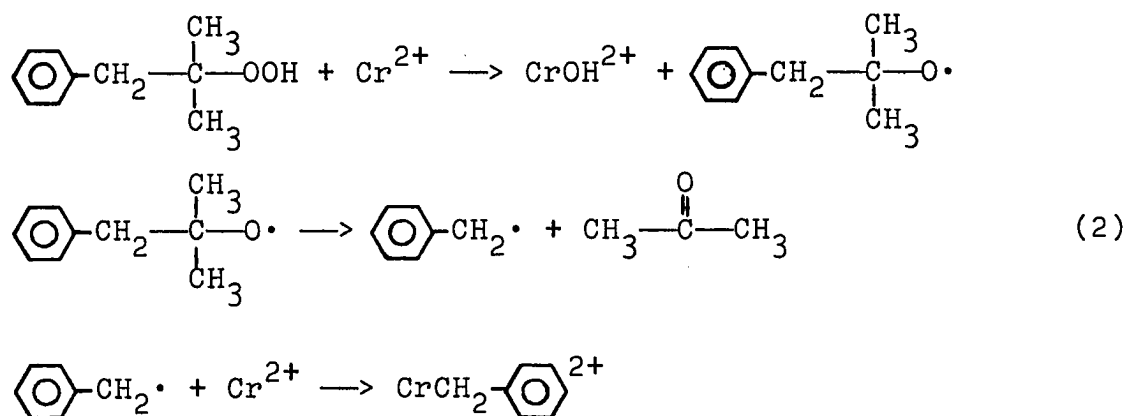
Figure 2. Structures of the organochromium cations

HISTORICAL

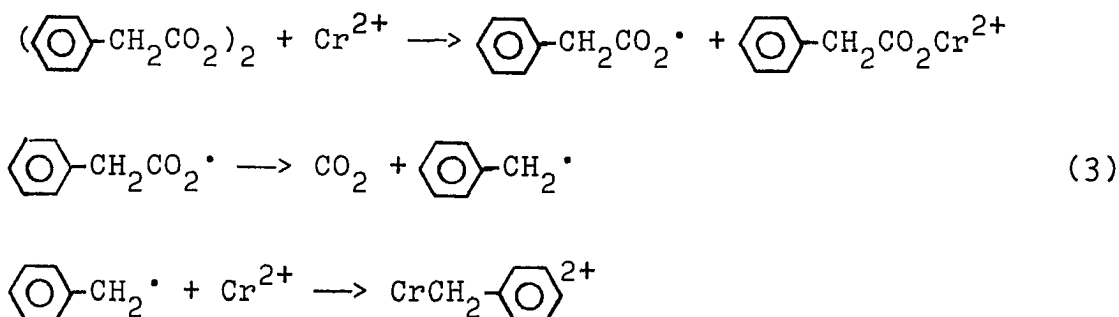
Organochromium(III) complexes of the form $(\text{H}_2\text{O})_5\text{CrR}^{2+}$, containing metal-carbon sigma bonds, were first synthesized by Anet and LeBlanc (1). They synthesized the benzylchromium(III) cation according to equation 1. This method



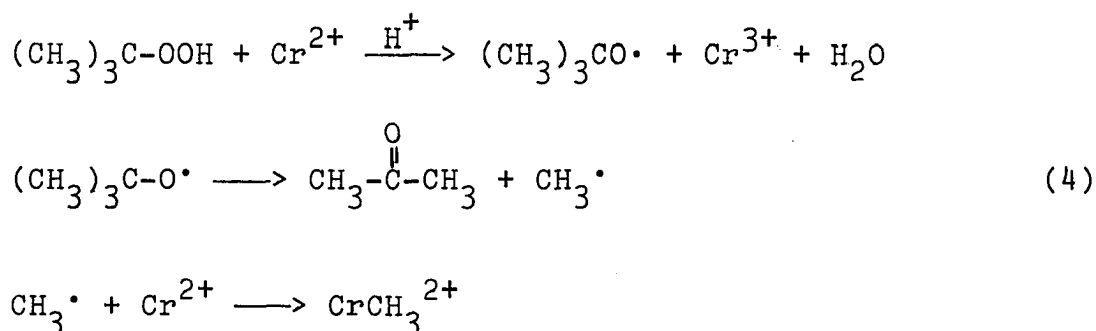
works well for activated organic halides such as benzyl bromide, but is not applicable to general alkyl halides. As a result, new schemes had to be developed to prepare other organochromium(III) complexes. One of the new routes was to react organic hydroperoxides with Cr^{2+} . An example is the reaction which Kochi and Davis (2) used to produce benzylchromium(III) cation. The mechanism proceeded according to equation 2. If an organic peroxide was used in place of the



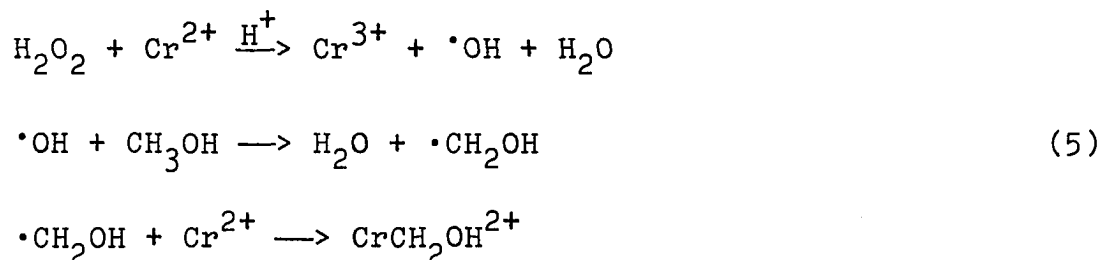
hydroperoxide, the reaction proceeded according to equation 3. The same type of procedure is applicable to the



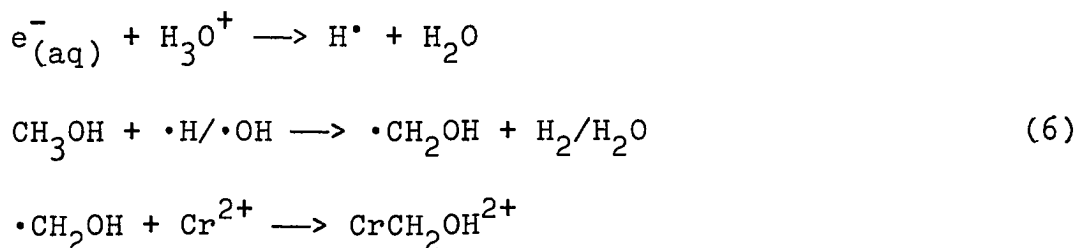
production of methyl-chromium(III). The mechanism proposed by Ardon, Woolmington and Pernick (3) is shown in equation 4.



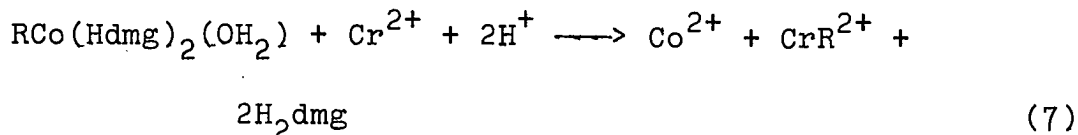
Schmidt, Swinehart and Taube (4) have used Cr^{2+} , H_2O_2 , and organic substrates in an analogous manner to produce alkyl-chromium(III) ions. Their mechanism for the production of (hydroxymethyl)-chromium(III) ions is shown in equation 5.



These chemical procedures suggest that the key is forming the desired radical in the presence of Cr^{2+} . In support of this idea Cohen and Meyerstein (5) have shown that radicals produced by pulse radiolysis will quickly couple with Cr^{2+} . Their reaction is illustrated in equation 6 for the production of (hydroxymethyl)-chromium(III) ions. A more

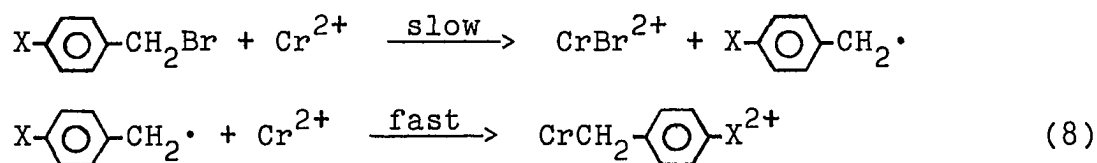


novel route to these types of compounds has been developed by Espenson and Shveima (6). The method involves the reaction of organoaquocobaloximes (7) with Cr^{2+} . The reaction is illustrated for RCr^{2+} in equation 7.



Of the alkyl-chromium(III) ions prepared by these various routes, the most thoroughly studied is the benzyl-chromium(III) ion. The first extensive study of the cation was performed by Kochi and Davis (2). They prepared and characterized a whole series of substituted benzyl-chromium(III) cations. Attempts were made to grow single crystals, but they all failed. As a result, the species

were all identified as cations in solution. The species were identified by their ultraviolet and visible spectra, the kinetics of their formation, decomposition products, and kinetics of decomposition. The mechanism of the formation reaction was shown to follow the steps shown in equation 8. Their data for various substituents indicated

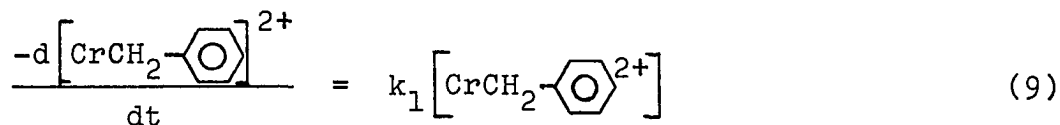


a total lack of any linear free-energy correlation.

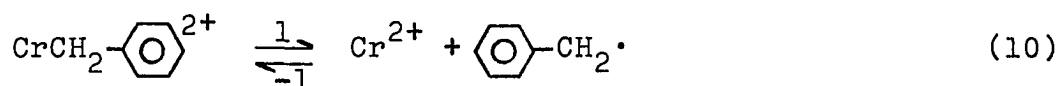
The thorough study of the decomposition reaction of these benzyl-chromium(III) cations was performed by Kochi and Buchanan (8). The decomposition was performed in ethanol-water solutions containing perchloric acid. The major organic product was toluene with only small amounts of bibenzyl. If benzyl-chromium(III) is reacted with substituted benzyl bromide, a mixture of toluene, substituted toluene and bibenzyls is obtained. Some speculation is given as to the mechanism, but no definitive answers are given.

The first definitive work on the mechanism of decomposition came from Nohr and Espenson (9). Their work dealt primarily with the reaction of oxidizing agents with benzyl-chromium(III). They have shown the reaction to be

independent of the concentration as well as the nature of the oxidant. The observed rate law is given in equation 9.

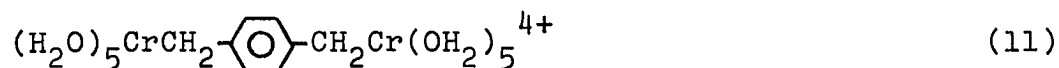


The mechanism which fits these kinetics is termed $S_H 1$ homolysis and is given in equation 10. All oxidants scavenge



Cr^{2+} and/or the organic radical. Therefore, the back reaction is unimportant, and so the experimentally obtained k_1 is equal to the forward rate of the reaction depicted in equation 10. In addition they have shown that for para-substituents there exists a good linear free-energy correlation between $\log k_1$ and σ_p .

Lunk and Youngman (10) used chromium(II) salts to couple difunctional halides such as α,α' -dibromo-p-xylene. They did not attempt to do any mechanistic work, but our experience suggested the formation of benzyl-chromium(III) bonds. It suggested to us the possibility of the formation of an organodichromium cation such as the one depicted in equation 11. In this project the organodichromium cation



shown, as well as several others, will be examined. This work characterizes these compounds and studies their modes of reaction with various reagents,

EXPERIMENTAL

Materials

Dibromoxylenes

Both the meta- and para- isomer of α,α' -dibromoxylene were obtained from Aldrich Chemical Company. They were 98% pure, but both contained light brown material and so required purification prior to use. The para- isomer was recrystallized as white needles from chloroform. The meta- isomer was sublimed (0.5 mm, 60-65°C) as white crystals. The analyses of both compounds matched those of the authentic compounds (11).

4,4'-Bis(bromomethyl)biphenyl; 4,4'-bis(bromomethyl)diphenylmethane; 4,4'-bis(bromomethyl)-1,2-diphenylethane

All three compounds were prepared in the same manner and so their syntheses will be described together (12). 1,2-Diphenylethane (25.0 g, 0.137 mol), or diphenylmethane (23.0 g, 0.137 mol), or biphenyl (21.1 g, 0.137 mol) was added to a mixture of 21.0 g paraformaldehyde, 54.0 ml of 48% hydrobromic acid, 40.5 ml 85% phosphoric acid, and 66.0 ml of glacial acetic acid. The solution was stirred and gently warmed in a two-necked round-bottom flask to which was attached a reflux condenser. When the solution reached 95°C, gaseous HBr (13) was bubbled into the solution through a gas dispersion tube. The solution was maintained

between 95-110°C for 5 hours. At that time the gaseous HBr was removed and the solution allowed to cool to room temperature overnight. The mixture was then poured into 600 ml of distilled water and the resulting pasty precipitate separated by gravity filtration. The purification of the three compounds followed different procedures, and so they will be described separately.

The 4,4'-bis(bromomethyl)biphenyl was in the form of a yellow-white sticky mass. The solid was dissolved in pure acetone and then reprecipitated by adding distilled water up to 50% of the initial volume of the acetone. The colorless needles were collected after cooling the solution in an ice bath for 20 minutes to assure complete precipitation. This procedure was repeated twice to obtain highest purity material. The resulting product had properties identical to the authentic material (14).

The 4,4'-bis(bromomethyl)diphenylmethane was in the form of a colorless solid coated with an oily material. This material was dissolved in benzene and then washed with several 100 ml portions of ~ 1.0 M NaOH followed by several 100 ml portions of distilled water. The resulting benzene solution was then cooled and the solid precipitated. The impure compound was then recrystallized twice from hot benzene to obtain pure material (12).

The 4,4'-bis(bromomethyl)-1,2-diphenylethane was in the form of a yellow-orange sticky solid. This solid was dissolved in CCl_4 and chromatographed on silica gel with CCl_4 as eluent. The CCl_4 was evaporated and the resulting crystals were a pale yellow color. This solid was then placed on a Coors porous plate and a powder funnel was inverted over the crystals. Six 2 ml portions of hexane were squirted around the base of the powder funnel. The entire apparatus was placed in the dark room for a week. At the end of that time the yellow liquid had been absorbed into the plate, and the white crystals remained on top of the plate. The crystals were removed from the plate and recrystallized from diethyl ether to produce the pure product (12).

4,4'-Bis(bromomethyl)diphenyl ether

The 4,4'- as well as the other five isomeric compounds can be synthesized by the same procedure (15). The exact procedure will be given only for the 4,4' isomer. To a one-necked, 250 ml, standard taper flask was added 35.18 g (0.324 moles) of p-cresol, 78.17 g (0.324 moles) KOH, and 55.5 g (0.324 moles) p-bromotoluene. The suspension was gently heated and 1.0 g of copper powder and a catalytic amount of cuprous chloride was added. The mixture was then heated to 140°C at which point the water produced by the reaction was boiled off through the uncooled condenser. The

heating was continued for 4 hours. The oil bath was then removed and the solution allowed to crystallize. The solid was dissolved in a mixture of 1.0 M NaOH and diethyl ether. The solution volume was adjusted to 300 ml with ether and the solution was washed with six 100 ml portions of 1.0 M NaOH to remove all excess cresol. The ether layer was then washed with two 100 ml portions of water. The final portion was checked for neutrality with pH paper. The ether was then dried over MgSO_4 and the MgSO_4 was filtered off. The volume of solution was then reduced to 150 ml by bubbling with a stream of nitrogen. At this point, 90 ml of 95% ethanol was added and the volume of the solution reduced to 60 ml by nitrogen bubbling. The solution was placed in a freezer at -5°C and the crystals precipitated after 8 hours. The product was crude 4,4'-dimethyldiphenyl ether. Its melting point, $41-43^\circ\text{C}$, is close to the literature value of 50°C (16). As a result, it was used in impure form in the remainder of the synthesis.

The next step was to brominate the benzylic positions by reaction with N-bromosuccinimide. The N-bromosuccinimide which was used had been recrystallized from ten times its weight of water and dried overnight under vacuum. The reaction was performed on a 10.0 g (0.050 mole) sample of the ether. To this was added 20.4 g (0.115 mole) of N-bromosuccinimide in 250 ml CCl_4 . The reaction was run in a

500 ml one-necked flask fitted with a reflux condensor. The reaction was gently heated to 60°C at which point a few grams of benzoyl peroxide was added. The oil bath was then raised to 130°C and the reaction allowed to run for 3 hours. The insoluble product, succinimide, was filtered from the warm solution and the resulting clear solution allowed to cool to room temperature. At that time it was again filtered to remove any last traces of succinimide. The solution was evaporated to dryness, and the resulting yellow oil was treated with hexane to precipitate the desired product. The yellow solid was twice recrystallized from hot benzene to produce the desired material (16).

The 3,3' isomer was prepared by a similar procedure. The corresponding organodichromium cation was prepared and studied. This work forms the basis for a closely related paper by Marty and Espenson (17). The 2,2' isomer was prepared and analyzed (18). The corresponding organodichromium cation was prepared and a few aspects of its chemistry investigated.

2,4-Bis(bromomethyl)toluene

This compound was prepared by the reaction of two moles of N-bromosuccinimide with one mole of 1,2,4-trimethylbenzene following procedures identical to those described for the bromination of 4,4'-dimethyldiphenyl ether. Following evaporation of the solvent, yellow oily crystals were

obtained. These were separated from the oil by the porous plate procedure previously described for 4,4'-bis(bromomethyl)-1,2-diphenylethane. After 4 to 5 days in the dark, most of the oil had separated. The resulting crystals were then recrystallized from CHCl_3 to produce the authentic compound (19).

p-Phenylbenzyl bromide

This compound was prepared by the reaction of N-bromosuccinimide and p-phenyltoluene. The reaction and purification followed exactly the procedure of Bullpitt and coworkers (20). At the end of the procedure, the crystals were pale yellow instead of white. These crystals were first sublimed (65-70°C, 0.5 mm) to remove all of the yellow material. The white crystals still contained a small amount of nitrogen containing impurity (presumably succinimide), and so the crystals were recrystallized from hot petroleum ether. This produced white needles which matched the authentic compound (20).

p-(Bromomethyl)benzyl alcohol

This material was synthesized in a two-step procedure beginning with α -bromo-p-toluic acid. The first step was the acid catalyzed esterification of the acid group. It was converted to the methyl ester by running the reaction in methanol according to the procedure of Codington and Mosettig

(21). The crystals were dried in a vacuum desiccator prior to use in the second step. The second step was the LAH reduction of the ester group to an alcohol. The procedure followed the general outline of Felkin's method (22). The reaction was performed with exactly a stoichiometric (1:2) ratio of LAH to substrate. In addition, the LAH was dissolved in large quantities (500 ml) of freshly distilled diethyl ether, and was added slowly with vigorous stirring. These precautions maintained the concentration of LAH at low levels at all times to prevent reduction of the benzylic bromide. In spite of all these precautions, a mixture of three products was always obtained. This mixture consisted of unreacted starting material, methyl *p*-(bromomethyl)-benzoate, over-reduced product, *p*-methylbenzyl alcohol, and the desired product, *p*-(bromomethyl)benzyl alcohol. These materials were separated by column chromatography on silica gel with CH_2Cl_2 as eluent. The unreacted starting material was used for a second reduction, while the *p*-methylbenzyl alcohol was discarded. The *p*-(bromomethyl)benzyl alcohol thus obtained was fairly pure from its ^1H NMR, but its melting point was low. It was further purified by recrystallizing it from hot petroleum ether. Although it was a good sample, it had to be analyzed immediately due to its rapid decomposition. This stability problem made it difficult to work with and even more difficult to analyze (23). The

compound had to be used immediately following preparation, or else rechromatographed and analyzed prior to use.

p-(Hydroxymethyl)benzyl cobaloxime

This substituted benzyl cobaloxime was prepared by a method similar to that developed by Anderson and coworkers (24). Cobaltous chloride hexahydrate (11.8 g, 0.05 mole) was dissolved in 185 ml of methanol. To this solution was added 11.6 g (0.1 mole) of dimethylglyoxime. The slurry was stirred for 15 minutes under nitrogen at which time 10 ml of 5.0 M NaOH was added followed by 4.0 g (0.05 mole) of pyridine. After allowing the solution to stir for an additional 30 minutes, the solution was cooled to 5°C with an ice bath. To the chilled solution was added 10 ml of 5.0 M NaOH followed by several additions of NaBH₄. NaBH₄ was added until the solution had turned dark blue indicating the complete conversion to Co(I). At that point, 5.0 g (0.025 mole) of p-(bromomethyl)benzyl alcohol dissolved in a minimum amount of methanol was added dropwise. It was added through a pressure equalizing dropping funnel over the period of 30 minutes. The solution gradually turned orange and was allowed to stir for 1 hour after the final drop of solution was added. The solution contained large amounts of orange solid, but 200 ml of distilled water was added to assure complete precipitation. The orange solid was filtered and washed with several volumes of warm water to remove

inorganic cobalt. The crystals were dried overnight in a vacuum desiccator. The dry orange solid was then dissolved in CH_2Cl_2 and reprecipitated by the addition of hexane. The orange solid was filtered and dried in a vacuum desiccator. This procedure was repeated several times to assure maximum purity.

p-Xylene dicobaloxime

This dicobaloxime was prepared from Co(I) and α,α' -dibromo-p-xylene. The method is exactly the same as previously described for benzyl cobaloxime using larger quantities of Co(I) to react with the second bromide group.

Organodichromium compounds

All organodichromium compounds were synthesized in approximately the same manner, and so only one example will be given. A deaerated acetone (25) solution of α,α' -dibromo-p-xylene (39.6 mg, 0.15 mmol) was reacted with aqueous Cr^{2+} (5.0 ml, 0.2 M) for ~20 minutes at room temperature. During that time the solution changed from pale blue to yellow-green. The reaction mixture was then transferred to the top of a deaerated column of Sephadex SP-C25 (H^+ -form) ion-exchange resin. The column was held at 0°C by circulating ice water through the jacket outside the column. The solution was allowed to run slowly through the resin to allow the organodichromium cation to adhere to the resin.

The column was first eluted with a deaerated solution of 0.1 M HClO_4 . The first compound to be eluted was the excess Cr^{2+} . Excess Cr^{2+} was used to ensure complete reaction with the organic bromide in addition to assuring complete removal of oxygen from the column. Next, Cr^{3+} (formed by the accidental oxidation of Cr^{2+} by oxygen) was eluted. The organodichromium cation was then eluted with a deaerated solution containing 0.9 M NaClO_4 /0.1 M HClO_4 . After all of the yellow organodichromium compound was removed, several green-blue bands remained on the column. These were dimeric Cr(III) compounds arising from oxidation of the excess Cr^{2+} . They were easily removed with 2.0 M NaClO_4 , and the resin regenerated by elution with 0.1 M HClO_4 .

Organochromium compounds

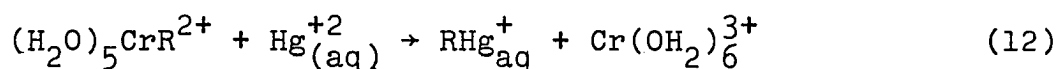
The synthesis of organochromium cations which originated from organic bromides follow the same procedure as the organodichromium compounds except that only half as much Cr^{2+} was used. In addition, the products of interest have a 2+ charge and so were eluted with 0.1 M HClO_4 . They were eluted after Cr^{2+} and before Cr^{3+} .

The synthesis of organochromium cations which originated from organic dibromides followed the general procedure given for α, α' -dibromo-m-xylene. A deaerated acetone solution of α, α' -dibromo-m-xylene (79.2 mg, 0.30 mmol) was reacted with aqueous Cr^{2+} (5.0 ml, 0.2 M) for 15 minutes at room

temperature. At the end of that time, the dark yellow solution was added to 100 ml of deaerated 0.1 M HClO_4 . The unreacted dibromide precipitated gradually and was filtered off in the air. The resulting solution was deaerated and again filtered, this time directly onto the ion-exchange column. Due to the large volume of solution, ~150 ml, plus small amounts of decomposition products, it required 2 to 3 hours to pass all of the solution through the column. The column was then eluted with deaerated 0.1 M HClO_4 . Since the excess Cr^{2+} was destroyed by working in air, the major product, the organochromium, came off first. This was followed by Cr^{3+} , small amounts of the corresponding organodichromium, and finally the Cr(III) dimers.

Organomercury compounds

The reaction used to produce these compounds is listed as equation 12. The procedure was originally used by Leslie

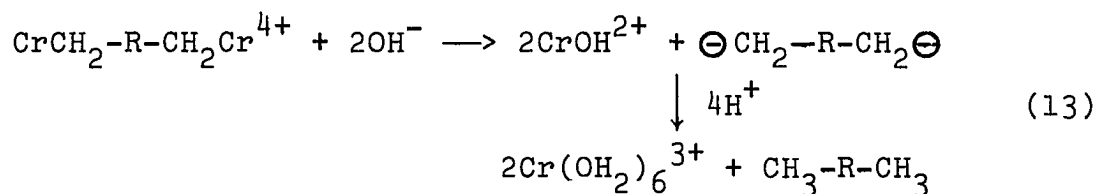


and Espenson (26) to synthesize organomercury compounds. This procedure did not work well for organodimercury compounds and so the procedure of Coombes and Johnson (27) was adopted. Since this procedure works well for organodimercury compounds and is not yet published, it will be given in detail.

A methanol-water solution of the organodichromium cation, $4.0 - 5.0 \times 10^{-3}$ M, was prepared in the usual fashion. The solution was bubbled with air for one minute to destroy the excess Cr^{2+} . This solution was then added to a 25% stoichiometric excess of HgCl_2 in methanol. There was an immediate reaction producing a white precipitate plus a blue Cr(III) solution. To this solution was added an equal volume of distilled water which caused additional precipitate to appear. The precipitate was filtered, washed with several portions of distilled water, and dried by suction from an aspirator. To this impure solid containing Hg_2Cl_2 was added several 20 ml portions of pyridine. This caused disproportionation of the Hg(I) into Hg(0) and Hg(II) . The resulting solid Hg(0) remained on the filter paper while the desired product plus the Hg(II) were dissolved and dripped through the filter paper. The pyridine solution was allowed to drip into 250 ml of 0.01 M HCl . The desired white crystals reprecipitated from solution while the Hg(II) remained in solution. The white crystals were filtered and washed with several portions of distilled water to remove any final traces of Hg(II) . The crystals were dried in a vacuum desiccator overnight prior to analysis (27). If any traces of impurity remained, they could be removed by recrystallization from dimethylsulfoxide.

Base decomposition products

These compounds were prepared to help confirm the structures of the organodichromium cations. The reaction of interest was suggested by Coombes, Johnson and Winterton (28). A balanced equation for the reaction is given in equation 13. This tells little about the mechanism, but



does explain the observed products. The original procedure has been significantly modified, and so the procedure is given in complete detail.

An acetone-water solution of organodichromium cation prepared in usual fashion was added to 30 ml of deaerated saturated Na_2CO_3 solution. The solution turns colorless with a brown suspension floating in it. It is bubbled with nitrogen for 15 minutes at which time concentrated perchloric acid is added with a syringe. Perchloric acid is added slowly over a period of 15-20 minutes to prevent excessive bubbling from the CO_2 produced by the reaction. Perchloric acid addition is stopped when all of the brown material has redissolved and the resultant homogeneous solution has turned blue. The solution which should be slightly acidic (may be checked with pH paper) is then extracted with four 125 ml portions of CCl_4 . These portions are combined,

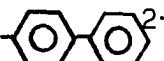
dried over MgSO_4 , and evaporated to dryness. The resulting brown crystals may be analyzed (29) or further purified prior to the analysis.

Poly-p-xylylene

This polymer was produced by the decomposition of several of the organodichromium compounds. This material was collected by filtering the floating particles from solution. The solid was then washed with several portions of water to remove any metals salts from the surface of the polymer. The product was dried in a vacuum desiccator prior to analysis (30). Yields were difficult to determine because a fair portion of the polymer adhered to the reaction vessel. In addition, it was fairly difficult to remove the polymer from the filter paper. Repeated attempts to recrystallize the product from hot benzyl benzoate (31) failed to purify the polymer.

Organic product isolation

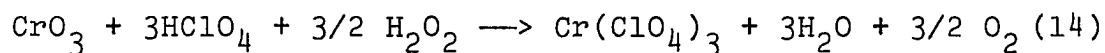
The products of the reaction of organochromium compounds with oxidizing agents were isolated in several cases. All of the compounds investigated produced nonpolymeric water insoluble materials. The procedure was used on samples which were not chromatographed prior to use. The procedure for the organic product resulting from the decomposition of

CrCH_2 - is given as a typical example. To an

acetone-water solution of the organochromium cation was added a two-fold stoichiometric excess of Fe^{3+} . The reaction was allowed to proceed under nitrogen for 2 hours. This assured complete reaction as well as evaporating most of the acetone which permitted easier extraction of the product. After this period of time, ~50 ml of predominantly aqueous solution remained. This solution was extracted with four 50-ml portions of a 90-10 mixture of pentane-diethyl ether. The organic layer is dried over MgSO_4 and evaporated to dryness. The resulting white crystals were collected and analyzed.

Inorganic reagents

$\text{Cr}(\text{ClO}_4)_3$ Pure chromium(III) perchlorate was prepared by the reduction of CrO_3 with H_2O_2 in HClO_4 solution according to equation 14. The trioxide (130 g, 1.3 moles)



was dissolved in 70 ml of distilled water and added to 400 ml of concentrated HClO_4 (4.6 moles). This mixture was cooled to 0°C and an excess of 30% H_2O_2 added slowly with stirring. The solution was then concentrated by evaporation, and the solid $\text{Cr}(\text{ClO}_4)_3$ slowly crystallized from the super-saturated solution. The product was recrystallized from water twice prior to use.

Cr(ClO₄)₂ Solutions of chromium(II) ion were prepared from Cr(ClO₄)₃ by reduction using amalgamated zinc. The zinc reduction was carried out by placing an air-free acid solution of Cr(ClO₄)₃ over freshly-prepared zinc amalgam. (The amalgam was prepared by adding a solution of HgCl₂ in 2.0 M HCl to a few grams of reagent-grade zinc granules which had been cleaned with 2.0 M HCl and washed with distilled water.) The mixture was allowed to react for several hours under nitrogen. The Cr²⁺ was stored in the rubber-capped bottle above the amalgam to prevent decomposition due to oxygen.

Other materials

Solutions of Fe(ClO₄)₃ in HClO₄ were prepared and analyzed by standard literature procedures (32).

Solutions of Hg(ClO₄)₂ were prepared and analyzed by standard procedure (33). Alternatively, the solid trihydrate (G. Frederick Smith Chemical Co.) was dissolved in the appropriate amount of 0.1 M HClO₄ to prepare a solution of desired concentration.

[Co(NH₃)₅Cl](ClO₄)₂ was prepared from [Co(NH₃)₅Cl](Cl)₂ by reacting an aqueous solution of the complex with AgClO₄ in HClO₄. The AgCl is filtered off and the resulting solution evaporated to produce crystals of the desired compound. The [Co(NH₃)₅Cl](Cl)₂ was produced and analyzed by standard procedures (34).

$[\text{Co}(\text{NH}_3)_5\text{Br}](\text{Br})_2$ was prepared by routine procedures (35).

$\text{Co}(\text{ClO}_4)_2$ solutions were prepared by dissolving the hexahydrate (G. Frederick Smith Chemical Co.) in the appropriate amount of aqueous perchloric acid.

All other materials used were reagent grade chemicals and were used without further purification.

Methods

Kinetics

The rate of formation of organodichromium cations from Cr^{2+} and organic dibromides was followed spectrophotometrically at λ 360 nm, a peak for the Cr(III) complex. A solution of the dibromide in ethanol or acetone was placed in a quartz cell, capped by a septum, and deaerated for 20 minutes with nitrogen. Temperature control was achieved by immersing the reaction cell in a small water bath positioned in the light beam of the Cary Model 14 spectrophotometer. This bath had quartz windows, and the water it contained was held at the desired temperature by circulation of water through an external jacket. A small volume of Cr^{2+} solution was added, the cell shaken to ensure homogeneity, and the spectrophotometer turned on to obtain a trace of absorbance versus time. All experiments were carried out in an air-free environment with a pseudo first-order excess of Cr^{2+} present. In all runs, $[\text{H}^+]$ was maintained at 0.1 M.

The rate of decomposition of the organodichromium and organochromium cations was obtained in much the same manner. In this case the oxidizing agent was added in greater than ten-fold excess to the organodichromium solution which was already in the cell. In this case the decrease in absorbance at λ 360 nm was followed as a function of time.

In most every case the trace of absorbance versus time appeared to indicate exponential traces and so was treated as a first-order kinetic trace. Since equation 15 applies to this case, the rate constant, k_{obs} , was determined from a

$$\ln|D_t - D_\infty| = \ln|D_0 - D_\infty| - k_{\text{obs}} t \quad (15)$$

plot of $\ln|D_t - D_\infty|$ versus time. In certain cases it proved difficult to obtain reliable values of D_∞ , and so the method of Guggenheim (36) was employed. This method is described by equation 16 where τ represents a time interval corresponding

$$\ln|D_t - D_{t+\tau}| = \ln\{|D_0 - D_\infty|(1 - e^{-kt})\} - k_{\text{obs}} t \quad (16)$$

to about two or three half-lives. $\ln|D_t - D_{t+\tau}|$ is plotted versus time to obtain $-k_{\text{obs}}$.

In certain rare cases, the plot of $\ln|D_t - D_\infty|$ versus time produced a curved line instead of a straight one. In these cases, the data were handled by resolving the curved line into straight lines whose slopes correspond to two separate rate constants. This was accomplished by allowing the

reactions to run for long periods of time and then plotting $\ln|D_t - D_\infty|$ versus time for the points at the very end of the reaction. The slope of this line was designated $-k_2$ and the y-intercept called β . A value Δ is then calculated from equation 17. Δ is then plotted versus time and the slope

$$\Delta = |D_t - D_\infty| - \beta e^{-k_2 t} \quad (17)$$

of this line is $-k_1$. This method is applicable to spectrophotometric determinations and has been fully described by Wilkins (37). It should be pointed out that although we designated these rate constants k_1 and k_2 , more experiments must be done to assign these to any particular steps in proposed mechanisms (38).

In the decomposition reactions most appeared to follow a rate law similar to that shown in equation 18. In order

$$\frac{-d[\text{organochromium}]}{dt} = k_1[\text{organochromium}] \quad (18)$$

to prove the lack of dependence upon [OXIDIZING AGENT], the concentration was doubled and halved and shown to have no effect upon the rate of the reaction. In a few cases (all Fe^{3+}) there was a slight dependence upon the concentration of the oxidizing agent. In these cases a plot of k_{obs} versus [OXIDIZING AGENT] was made to verify the dependence. The production of a straight line with a nonzero intercept would indicate a two-term rate law such as that shown in equation 19.

$$\frac{-d[\text{organochromium}]}{dt} = (k_1 + k_2[\text{Fe}^{3+}])[\text{organochromium}] \quad (19)$$

Analyses

Chromium(II) solutions were analyzed by the following procedure. An aliquot of Cr^{2+} solution was syringed into a volumetric flask containing a 15-30% excess solution of $\text{Co}(\text{NH}_3)_5\text{Cl}^{2+}$ which had been well purged with nitrogen. The Co^{2+} released was determined spectrophotometrically as the $\text{Co}(\text{NCS})_4^{2-}$ ion by adding an excess of solid NH_4SCN and diluting to the mark with 1:1 acetone-water (39). From the absorbance at λ 623 nm ($\epsilon = 1842$), the 1:1 nature of the reaction, and the dilution factors; the concentration of Cr^{2+} was computed. This same procedure was used to determine the concentration of organodichromium compounds. The only modification was that the reactants had to be allowed to react for 2 hours prior to dilution.

The total concentration of chromium was determined according to the method of Haupt (40). The procedure involved oxidizing all chromium species to chromium(VI) with H_2O_2 in base, heating for 20-30 minutes to decompose the excess H_2O_2 , and diluting to the mark in a volumetric flask. Finally, the absorbance was read at λ 372 nm ($\epsilon = 4830$) and from the dilution factors the total concentration of chromium determined.

The concentration of Na^+ in stock solutions was determined by passing aliquots of the solution through a column of Dowex 50W-X8 cation-exchange resin in the H^+ form. This effected displacement of the H^+ by the Na^+ and the liberated H^+ was titrated with standardized NaOH to the phenolphthalein end-point. The $[\text{H}^+]$ was determined by titration to the phenolphthalein end-point with standardized NaOH.

The ϵ for the organodichromium compounds was determined spectrophotometrically. This was done by determining the absorbance of the solution at λ 360 nm and dividing this number by the $[\text{Cr}^{2+}]$ determined by the reaction with $\text{Co}(\text{NH}_3)_5\text{Cl}^{2+}$. This procedure involved the assumption that each carbon-chromium bond reacted with only one molecule of Co(III). This assumption has been seen to be valid for organochromium cations, was consistent with the observed polymeric product, and produced values for ϵ around 2400. As a result, it was assumed to be the case for these organodichromium cations. Since each molecule contained two carbon-chromium bonds, the ϵ is actually twice the measured value.

Stoichiometry experiments

The stoichiometry was performed for the reaction of Fe^{3+} and several organodichromium cations. The organodichromium was prepared in the usual manner and to it was added an

eight-fold excess of deaerated Fe^{3+} solution. The reaction was allowed to proceed until all of the yellow color disappeared (1 to 2 hours). At the end of this time, the concentration of Fe^{2+} was determined. The determination of $[\text{Fe}^{2+}]$ involved spectrophotometric determination of the Fe^{2+} tris-phenanthroline complex at λ 510 nm (41).

Electrolysis

The electrochemical experiments were performed on a Princeton Applied Research Model 173 Potentiostat/Galvanostat equipped with a Model 179 Digital coulometer. The cell used for electrolysis was equipped with three electrodes. The mercury pool cathode was mechanically stirred and was separated from the SCE reference electrode and the platinum wire anode by glass frits. In all cases the solution was deaerated with nitrogen for 20 minutes prior to the electrolysis in addition to the entire time of the electrolysis.

In a typical experiment (42) a solution of 2.0 g (0.0076 moles) of α,α' -dibromo-*p*-xylene in 100 ml of DMF containing 0.1 M $(\text{NEt}_4)\text{Br}$ was exhaustively electrolyzed at -1.5 V. The resulting precipitate was filtered, washed with several portions of distilled water, and dried in a vacuum desiccator. The product was analyzed in the usual fashion.

Photolyses

All photolyses were performed with a Sorenson Xenon lamp. The photolyses were done in a Pyrex vessel to prevent the complexes from exposure to ultraviolet radiation. The solutions were aqueous-methanol containing 0.1 M HClO_4 plus the substrate at millimolar concentration. The solutions were purged with prepurified nitrogen for 20 minutes prior to irradiation as well as throughout the irradiation. The solution was chilled with an ice bath during photolysis to prevent warming of the solution. The photolysis was stopped when the color of the solution had completely disappeared. The time of the photolysis varied from 20 minutes to 4 hours, depending on the substrate. In the cases where polymer was produced, it was filtered, washed with water, and dried in a vacuum desiccator prior to analysis. In the case of soluble products, the methanol was evaporated, and the resulting water layer extracted with several portions of CHCl_3 . The CHCl_3 solution was then dried over MgSO_4 and evaporated to dryness to obtain the solid product.

Analog computer experiments

These experiments were run on an EAI TR-20 analog computer. The experiments were based on the kinetic scheme

$$A \xrightarrow{k_1} B \xrightarrow{k_2} C.$$

The experiments were wired essentially the same as those of Crossley and Slifkin (43). Several

features were added so that ϵ_A , ϵ_B , and ϵ_C could be entered into the computer. This allowed one to obtain a plot of absorbance versus time as well as the individual concentrations as a function of time. The wiring diagram is shown in Figure 3. The ratio k_1/k_2 was varied from 10 to 0.1, ϵ_A/ϵ_B was varied from 10 to 0.1, $[A]_0 = 1.0$, $[B]_0 = 0$, $[C]_0 = 0$. The computer produced plots of absorbance versus time. These were treated just like normal kinetics and were evaluated as two-stage kinetics as described in the kinetics section. The rate constants determined were then compared to the values given to the computer to assure the correctness of the procedure.

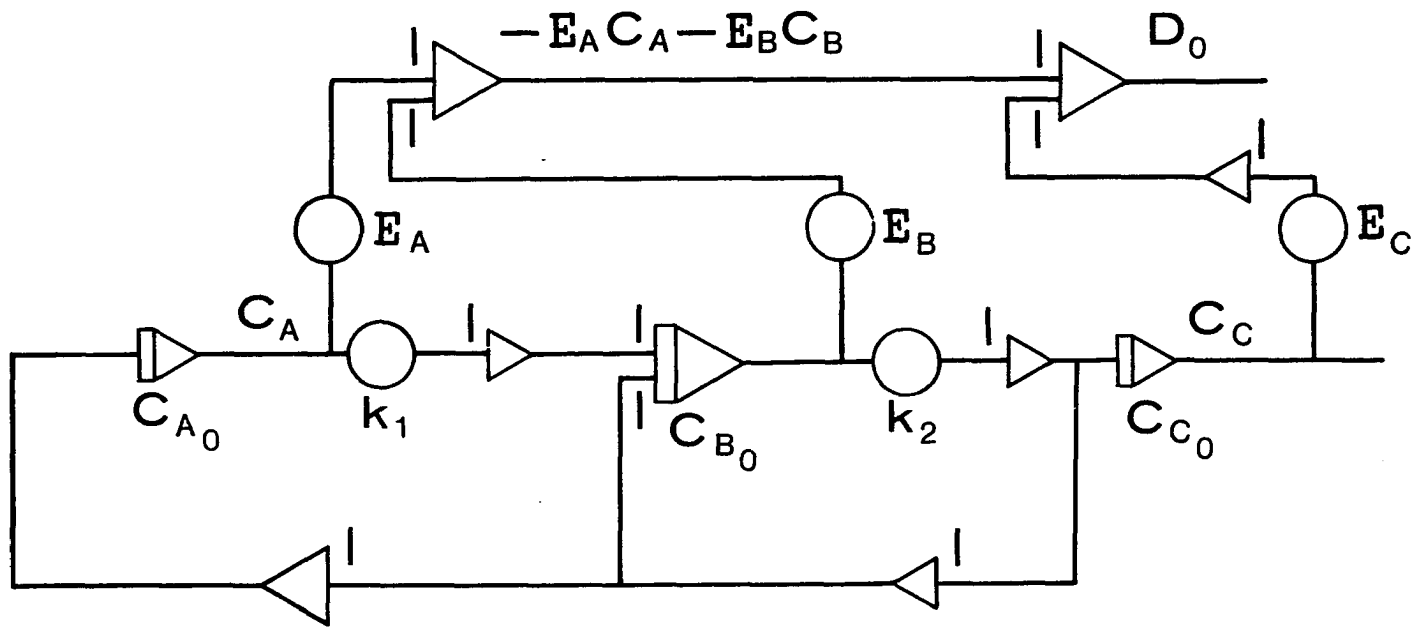


Figure 3. The analog computer wiring diagram

RESULTS

Characterization of Compounds

The analyses of all organic bromides and dibromides are given in Table 1. Most compounds were compounds already in the literature and the synthesized materials proved identical to those reported. Since the compounds analyzed satisfactorily, these were used without fear of side reactions. The only compound which proved troublesome was p-(bromomethyl)benzyl alcohol. This compound proved so unstable that orange contaminants began to appear as shortly as 24 hours after synthesis. This decomposition problem makes some of the results of its chemistry questionable.

The analyses of the cobaloximes which were synthesized are given in Table 2. The analyses were acceptable, but surely not good. The analysis of the dicobaloxime, although not good, did match that obtained by Anderson, Ballard and Johnson (24).

The production of the organochromium and organodichromium cations proceeded exactly as anticipated. The organochromium cations have a 2+ charge and so could be eluted with 0.1 - 0.2 M HClO_4 . On the other hand, the organodichromium cations are 4+ charged and required 0.1 M $\text{HClO}_4/0.9$ M NaClO_4 . In all cases the compounds were yellow with a λ_{max} between 355 - 360 nm. All of the cations also

Table 1. Characterization of the organic bromides and dibromides

Bromide	M.P. ^a °C	
	Actual	Literature
α,α' -Dibromo- <u>m</u> -xylene	75-77	75-77 ^c
α,α' -Dibromo- <u>p</u> -xylene	142-143	142-143 ^c
4,4-Bis(bromomethyl)- biphenyl	167.5-170.5	170 ^e
4,4-Bis(bromomethyl)- diphenylmethane	151.5-153.5	153.5 ^f
4,4'-Bis(bromomethyl)- 1,2-diphenylethane	116-119.5	117-120 ^f
4,4'-Bis(bromomethyl)- diphenyl ether	94-95	93-95 ^g

^aAll values are uncorrected and were determined on the Fisher 355 digital melting point analyses.

^bAll spectra are in CDCl_3 with TMS as the internal standard.

^cReference 11.

^dElemental analysis not performed due to known purity of the sample.

^eReference 14.

^fReference 12.

^gReference 16.

^hSpectra run in CCl_4 with TMS as the internal standard.

¹ H NMR ^b		Elemental Analysis	
Actual	Literature	Actual	Theoretical
δ 7.35(m)	δ 7.35(m) ^c	---	d
δ 4.50(s)	δ 4.52(s)		
δ 7.42(s)	δ 7.40(s) ^c	---	d
δ 4.50(s)	δ 4.48(s)		
See Figure 4	---	49.65%C 3.58%H	49.41%C 3.53%H
See Figure 5	---	50.88%C 3.94%H	50.88%C 3.98%H
See Figure 6	---	52.18%C 4.38%H	52.20%C 4.38%H
δ 7.1(AA'BB',8) ^h	δ 7.05 - δ 0.45 (8H) ^g	47.56%C	47.22%C
δ 4.52(s, 4)	δ 4.56(4H)	3.39%H	3.46%H

Table 1. (Continued)

Bromide	M.P. ^a °C	
	Actual	Literature
2,4-Bis(bromomethyl)-toluene	96.5 - 97.0	97.0 ⁱ
p-Phenylbenzyl bromide	83 - 84	84 - 85 ^j
p-(Bromomethyl)benzyl alcohol	82.5 - 83.0	84.0 ^k

ⁱReference 19.

^jReference 20.

^kReference 23.

^lThe high resolution mass spectra indicated a major peak at 199.98367 and the anticipated mass for $^{12}\text{C}_8^{1}\text{H}_9^{79}\text{Br}^{16}\text{O}$ is 199.98368.

$^1\text{H NMR}^b$		Elemental Analysis	
Actual	Literature	Actual	Theoretical
See Figure 7	---	38.58%C 3.72%H	38.88%C 3.63%H
δ 7.40 - 7.60(m)	δ 7.40 - 7.60 (Ar-H) ^j	63.18%C	63.18%C
δ 4.50(s, 2)	δ 4.48(CH ₂ Br)	4.52%H	4.49%H
See Figure 8 ^l	---	48.23%C 4.51%H	47.79%C 4.51%H

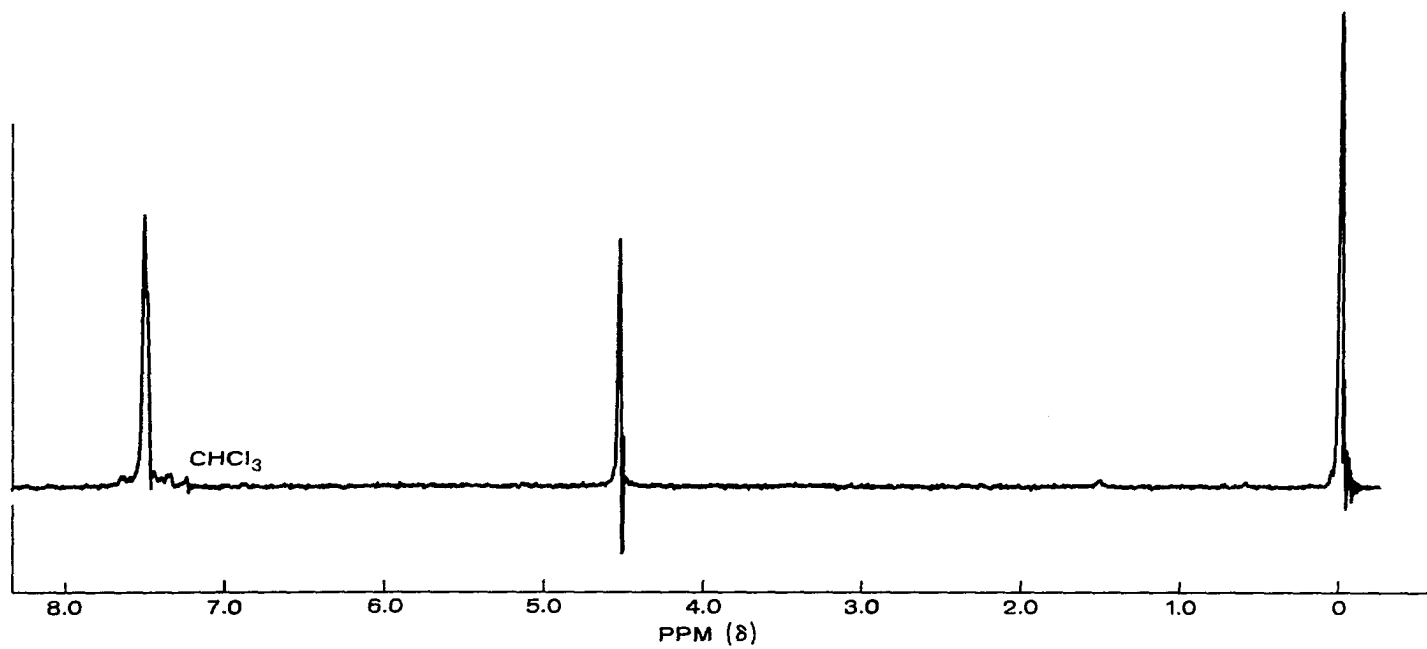


Figure 4. ^1H NMR spectrum of 4,4'-bis(bromomethyl)biphenyl

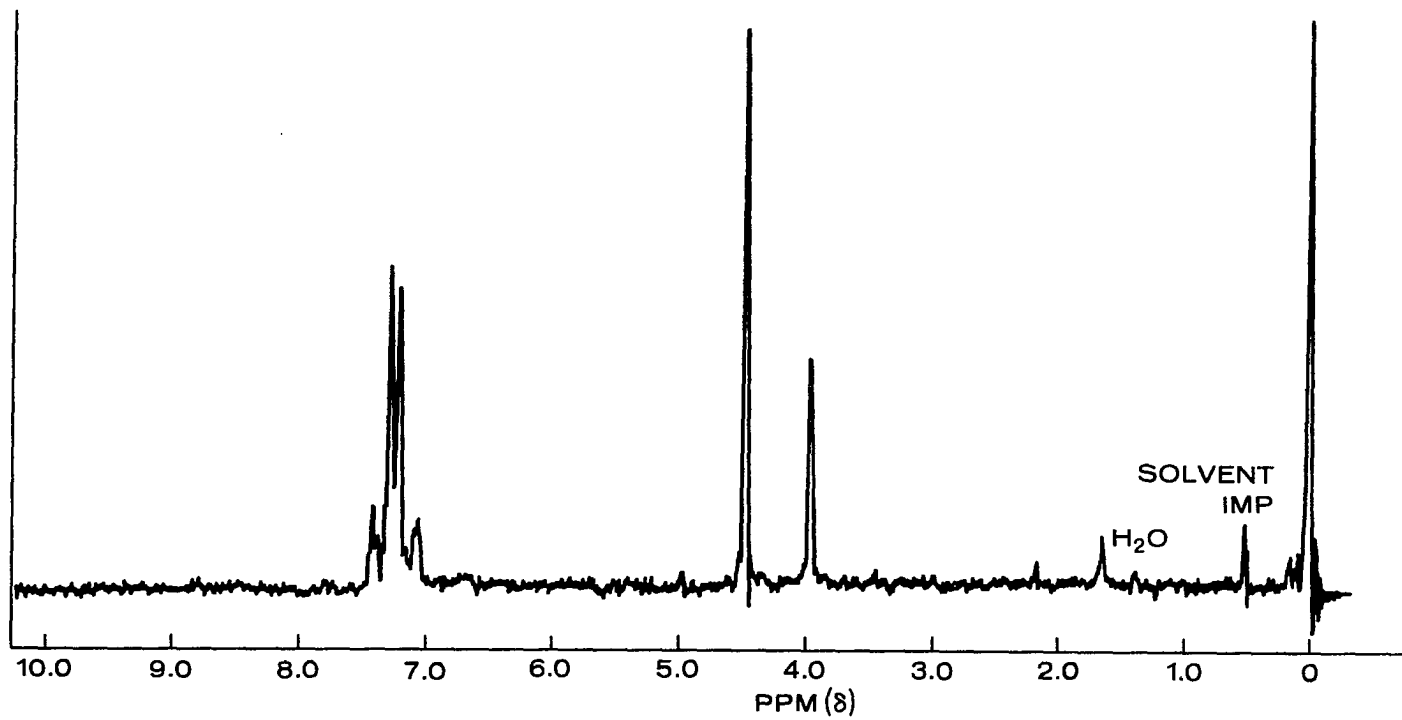


Figure 5. ^1H NMR spectrum of 4,4'-bis(bromomethyl)diphenylmethane

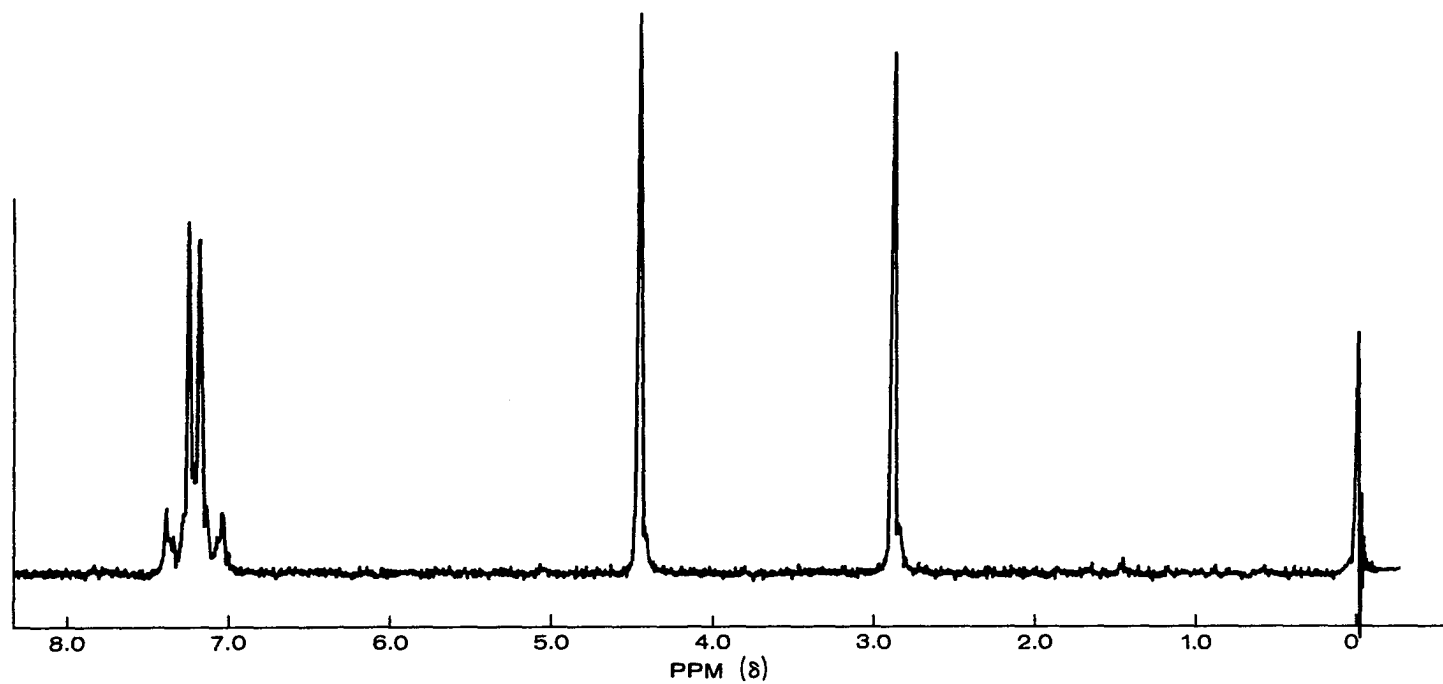


Figure 6. ^1H NMR spectrum of 4,4'-bis(bromomethyl)-1,2-diphenylethane

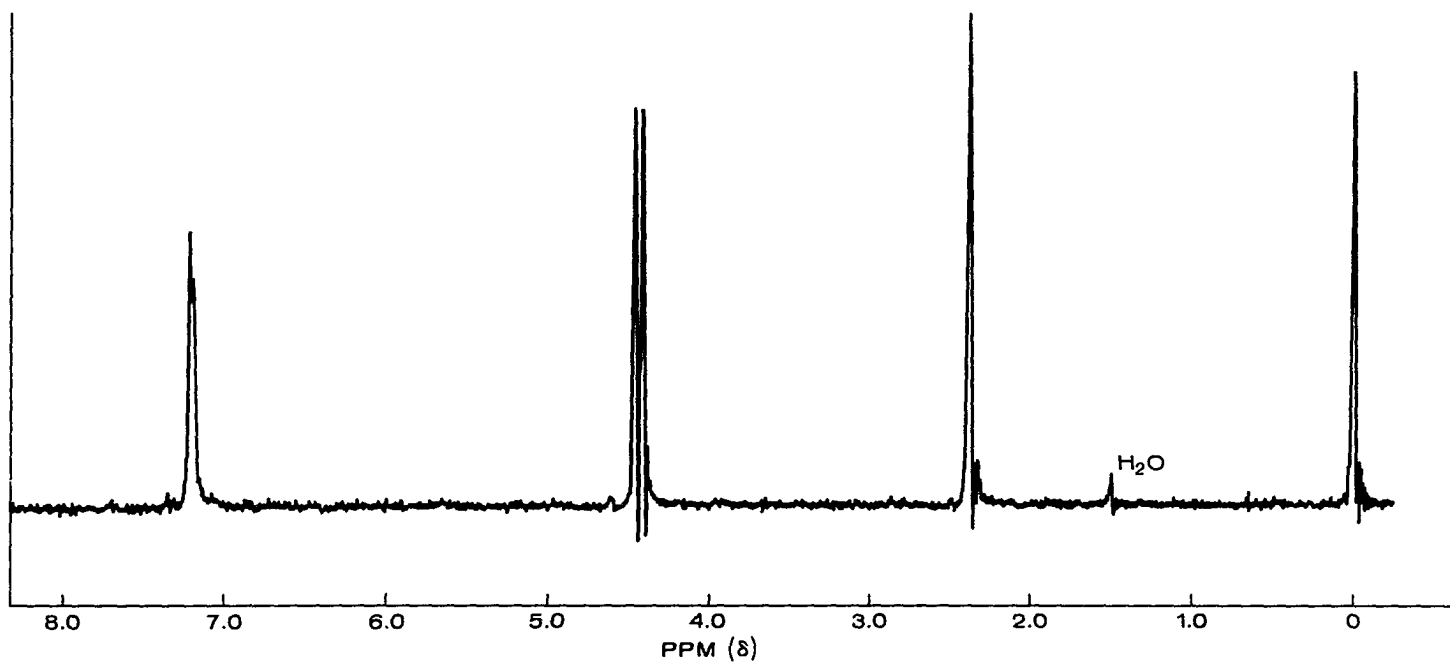


Figure 7. ^1H NMR spectrum of 2,4-bis(bromomethyl)toluene

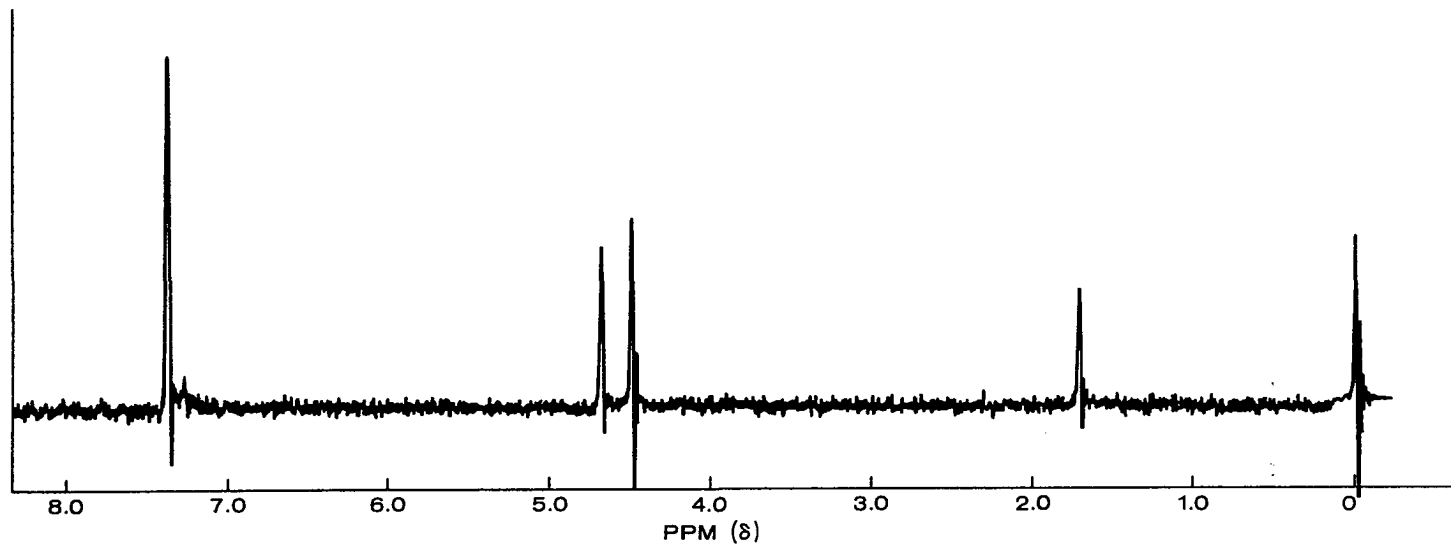


Figure 8. ^1H NMR spectrum of *p*-(bromomethyl)benzyl alcohol

Table 2. Characterization of the cobaloximes

Cobaloxime	¹ H NMR ^a	Elemental Analysis	
		Actual	Theoretical
$ \begin{array}{c} \text{CH}_2 - \text{C}_6\text{H}_4 - \text{CH}_2\text{OH} \\ \\ (\text{Co}) \\ \\ \text{PY} \end{array} $	See Figure 9	51.18%C 5.73%H 14.19%N	51.53%C 5.76%H 14.30%N
$ \begin{array}{cc} \text{CH}_2 - \text{C}_6\text{H}_4 - \text{CH}_2 & \\ & \\ (\text{Co}) & (\text{Co}) \\ & \\ \text{PY} & \text{PY} \end{array} $	δ 6.8(s, 4) δ 2.8(s, 4) δ 1.9(s, 24) ^c	48.61% ^b C 5.80%H 15.36%N	48.68%C 5.51%H 16.66%N

^a¹H NMR spectra were run in CDCl₃ with TMS as an internal standard.

^bClose to the values 47.8%C, 5.7%H and 15.8%N given by Anderson et al. (24).

^cIdentical to the values given by Anderson et al. (24).

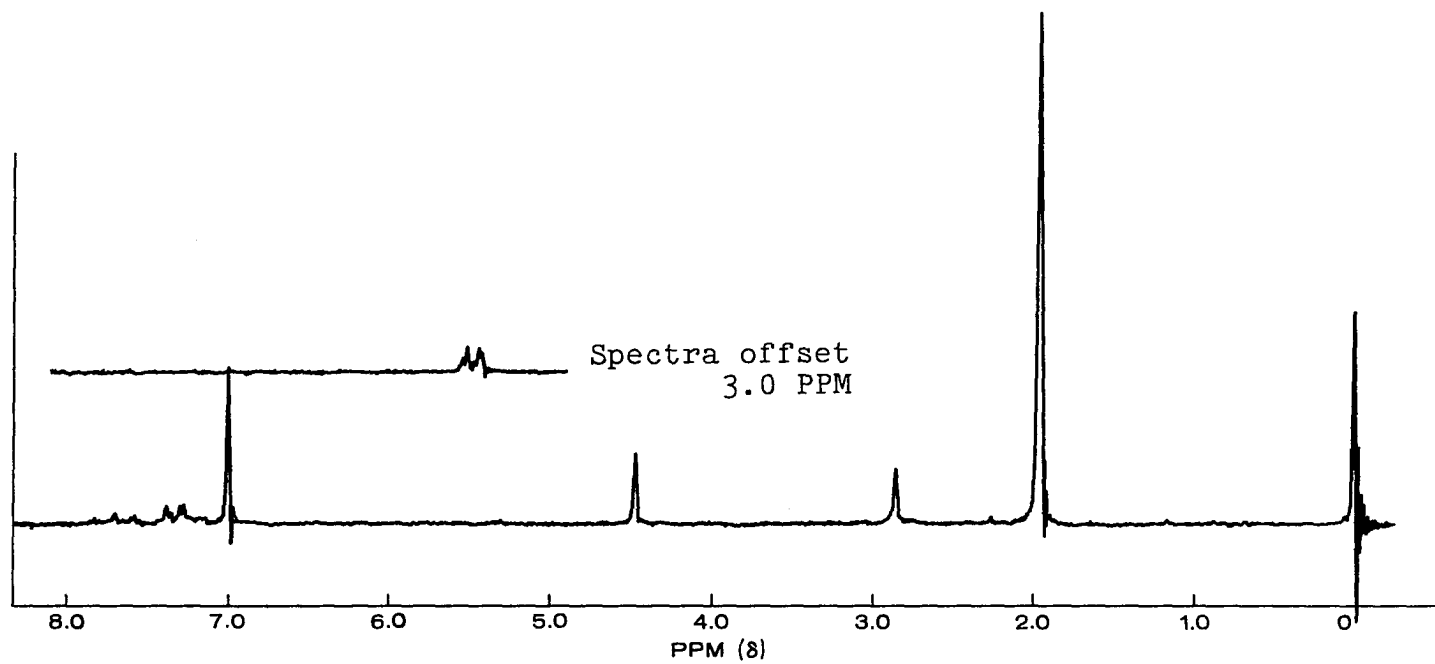


Figure 9. ^1H NMR spectrum of *p*-(hydroxymethyl)benzylcobaloxime

possessed two other strong absorbances in the ultraviolet region. In order to better identify the organodichromium cations, several reactions were run in the hope of identifying the products of the reaction. The products which were anticipated were those which would have come from chemistry identical to that of the benzyl-chromium cation. The few which were successful are mentioned in detail below. In addition to these, several other reactions such as the reaction with bromine, oxidizing agents, and H^+ were attempted. In all of the latter cases the only organic product was polymer, and so they did not constitute a proof for the structure of the organodichromium cations.

The production of organodimercury compounds was attempted for several organodichromium compounds. The only one which produced crystals of the desired product was $CrCH_2-C_6H_4-CH_2Cr^{4+}$. The 1H NMR [δ 2.97 (CH_2 , $J(^1H - ^{199}Hg)$ 296 Hz (adjacent Hg), $J(^1H - ^{199}Hg)$ 11 Hz (meta Hg); δ 7.06 (C_6H_4 complex multiplet))] is very close to that reported by Coombes and Johnson (27). In the other cases the desired reaction appeared to occur, but the desired product decomposed prior to isolation. Many variations were tried to prevent the organodimercury compounds from decomposing, but none were successful for any of the other organodichromium cations.

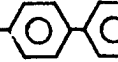
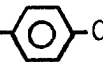
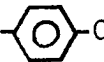
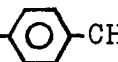
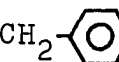
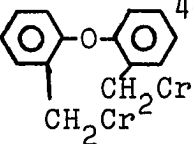
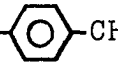

The analyses of the organic products from the base decomposition reaction are given in Table 3. All of these matched the anticipated hydrocarbons very closely. The same procedure was performed on $\text{CrCH}_2\text{-C}_6\text{H}_4\text{-CH}_2\text{Cr}^{4+}$ and $\text{CrCH}_2\text{-C}_6\text{H}_3(\text{CH}_2\text{Cr})\text{-CH}_2\text{Cr}^{4+}$

several times. In all cases, the predominant products were polymers rather than simple organic molecules. Due to this problem, the base decomposition of these organodichromium cations was not further pursued.

Poly-p-xylylene has been prepared by several routes and the material analyzed and compared. In Table 4 are listed the elemental analyses of several preparative samples of the polymer as well as the authentic material (ICN Pharmaceuticals Inc.). In addition, the infrared spectra of all of these materials are shown in Figures 16-19. Figure 20 shows the infrared spectrum of the commercially available polymer film (44). In all cases the polymer did not melt or decompose significantly up to 310°C. The polymer was very insoluble in normal organic solvents, but could be solubilized in hot (>200°C) solvents such as benzyl benzoate. Attempts were made to recrystallize the polymer from such solvents, but the product was no purer than the starting material (45).

The reaction of organodichromium cations with oxidizing agents invariably produced polymeric products. The one

Table 3. Characterization of the organic products of the base decomposition reaction

Organodichromium	Anticipated Product
$\text{CrCH}_2\text{-}$  $\text{-CH}_2\text{Cr}^{4+}$	4,4'-Dimethylbiphenyl
$\text{Cr-CH}_2\text{-}$  $\text{-CH}_2\text{-}$  $\text{-CH}_2\text{Cr}^{4+}$	4,4'-Dimethyldiphenylmethane
$\text{CrCH}_2\text{-}$  $\text{-CH}_2\text{-CH}_2\text{-}$  $\text{-CH}_2\text{Cr}^{4+}$	4,4'-Dimethyl-1,2-diphenyl-ethane
 $^{4+}$ CH_2Cr^2	2,2'-Dimethyldiphenyl ether
$\text{CrCH}_2\text{-}$  $\text{-CH}_2\text{OH}^{2+}$	<u>p</u> -Methylbenzyl alcohol
$\text{CrCH}_2\text{-}$  $\text{-CH}_2\text{Br}^{2+}$	<u>m</u> -(Bromomethyl)toluene

^aSpectra run in CDCl_3 with TMS as the internal standard.

^bReference 11.

^cReference 29.

^dReference 20.

^eThe high resolution mass spectra indicates a strong peak at 122.07303 for $^{12}\text{C}_8^1\text{H}_{10}^{16}\text{O}$ mass is 122.07317.

^fThe high resolution mass spectra indicates a strong peak at 183.98872 for $^{12}\text{C}_8^1\text{H}_9^{70}\text{Br}$ mass is 183.98876.

Anticipated ^1H NMR ^a	Actual NMR
δ 7.31 (AA'BB') ^b δ 2.42 (s)	See Figure 10
δ 6.96 (s) ^c δ 3.81 (s) δ 2.27 (s)	See Figure 11
δ 7.02 (s) ^b δ 2.85 (s) δ 2.30 (s)	See Figure 12
δ 6.60 - 7.30 (m) ^d δ 2.27 (s)	See Figure 13
δ 7.15 (s) ^b δ 4.60 (s) δ 2.35 (s) δ 1.92 (broad)	See Figure 14 ^e
δ 7.10 [s(?)] ^b δ 4.65 (s) δ 2.40 (s) δ 2.25 (broad)	See Figure 15 ^f

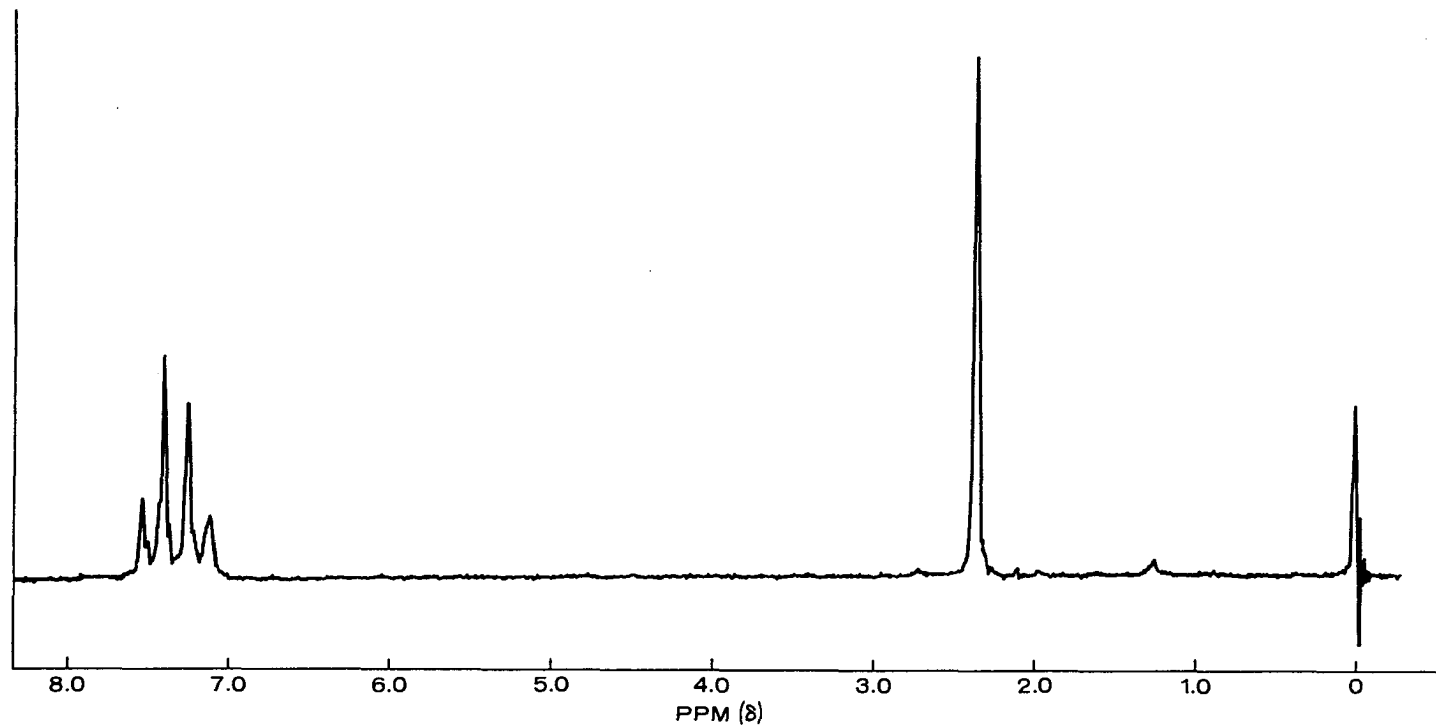
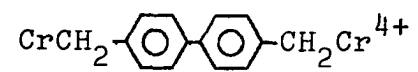


Figure 10. ¹H NMR spectrum of the base decomposition product of



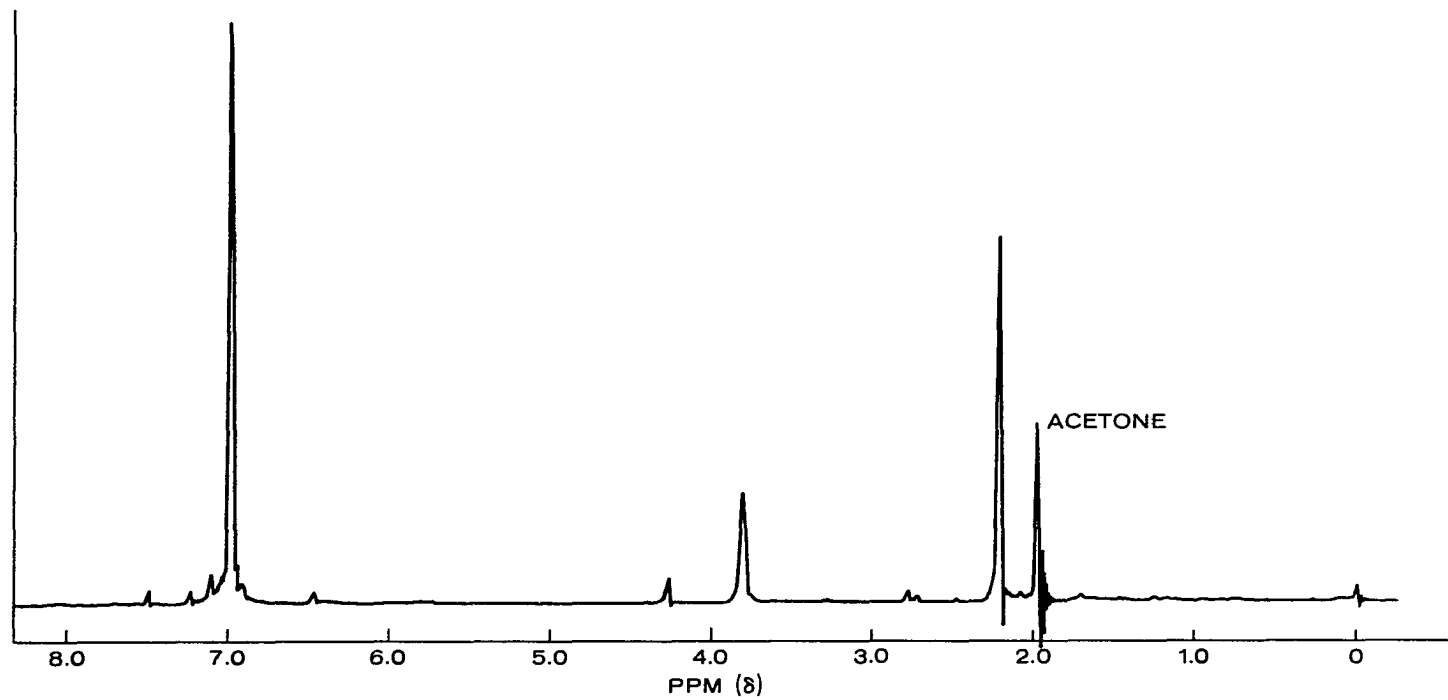


Figure 11. ^1H NMR spectrum of the base decomposition product
of $\text{CrCH}_2-\text{C}_6\text{H}_4-\text{CH}_2-\text{C}_6\text{H}_4-\text{CH}_2\text{Cr}^{4+}$

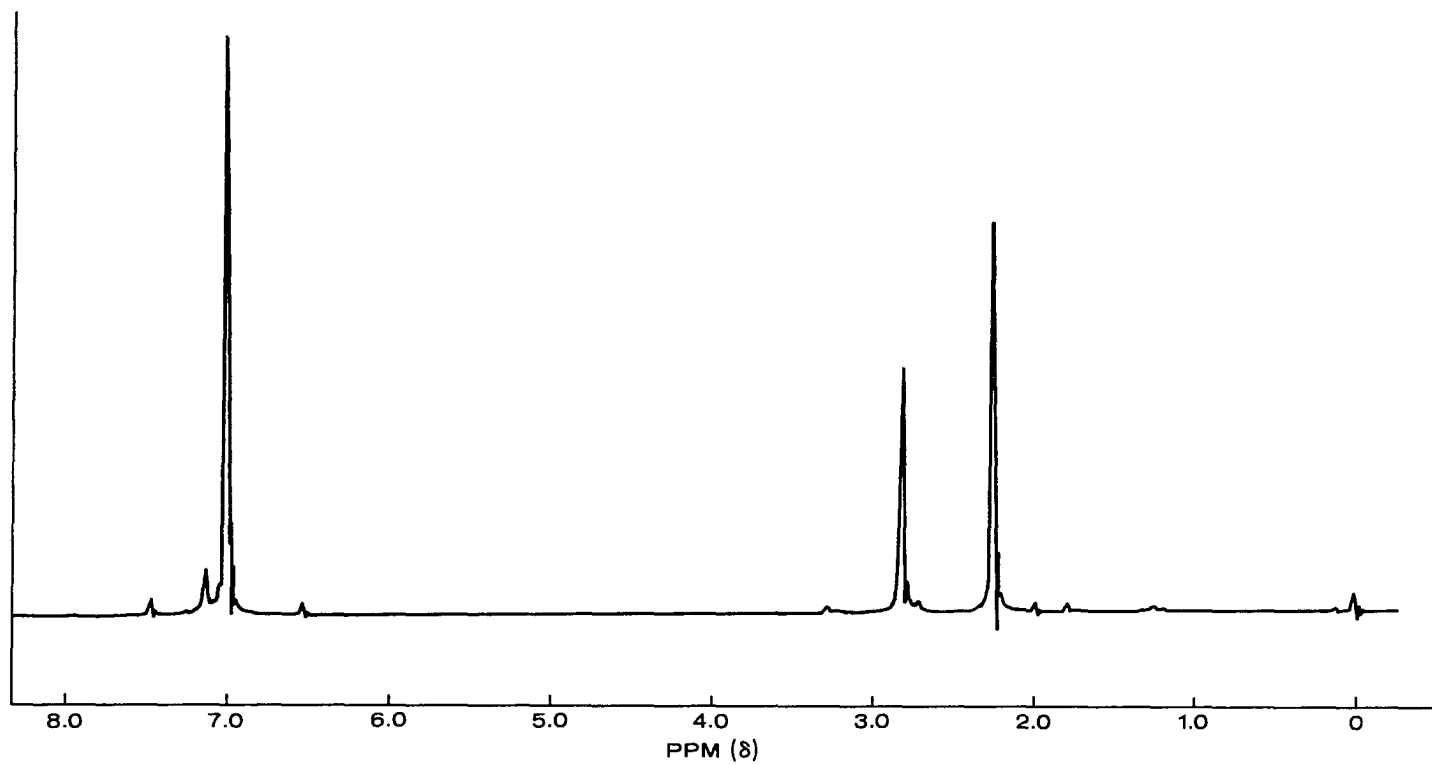
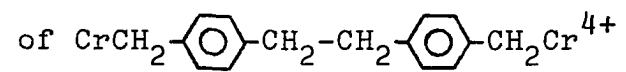


Figure 12. ^1H NMR spectrum of the base decomposition product



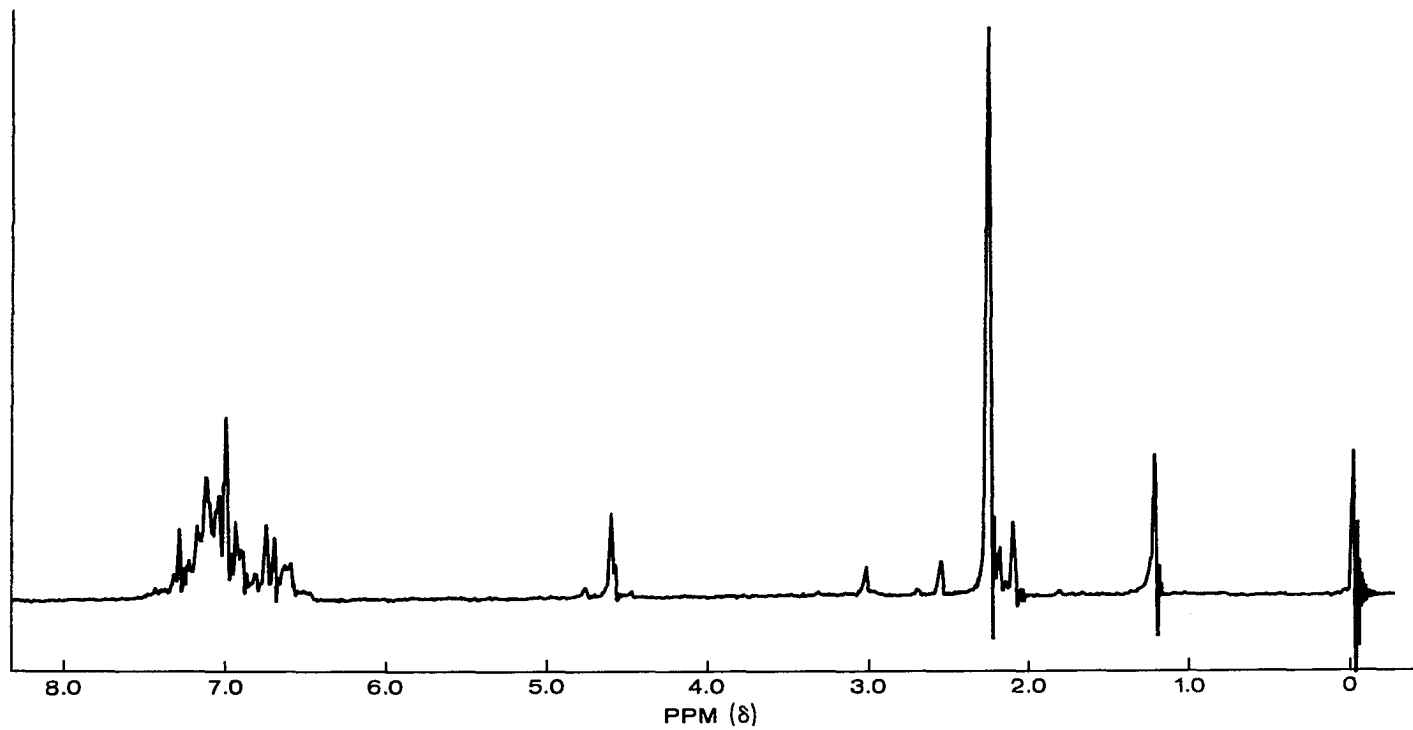
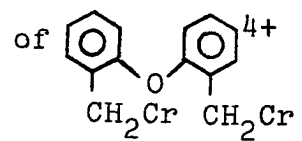


Figure 13. ^1H NMR spectrum of the base decomposition product



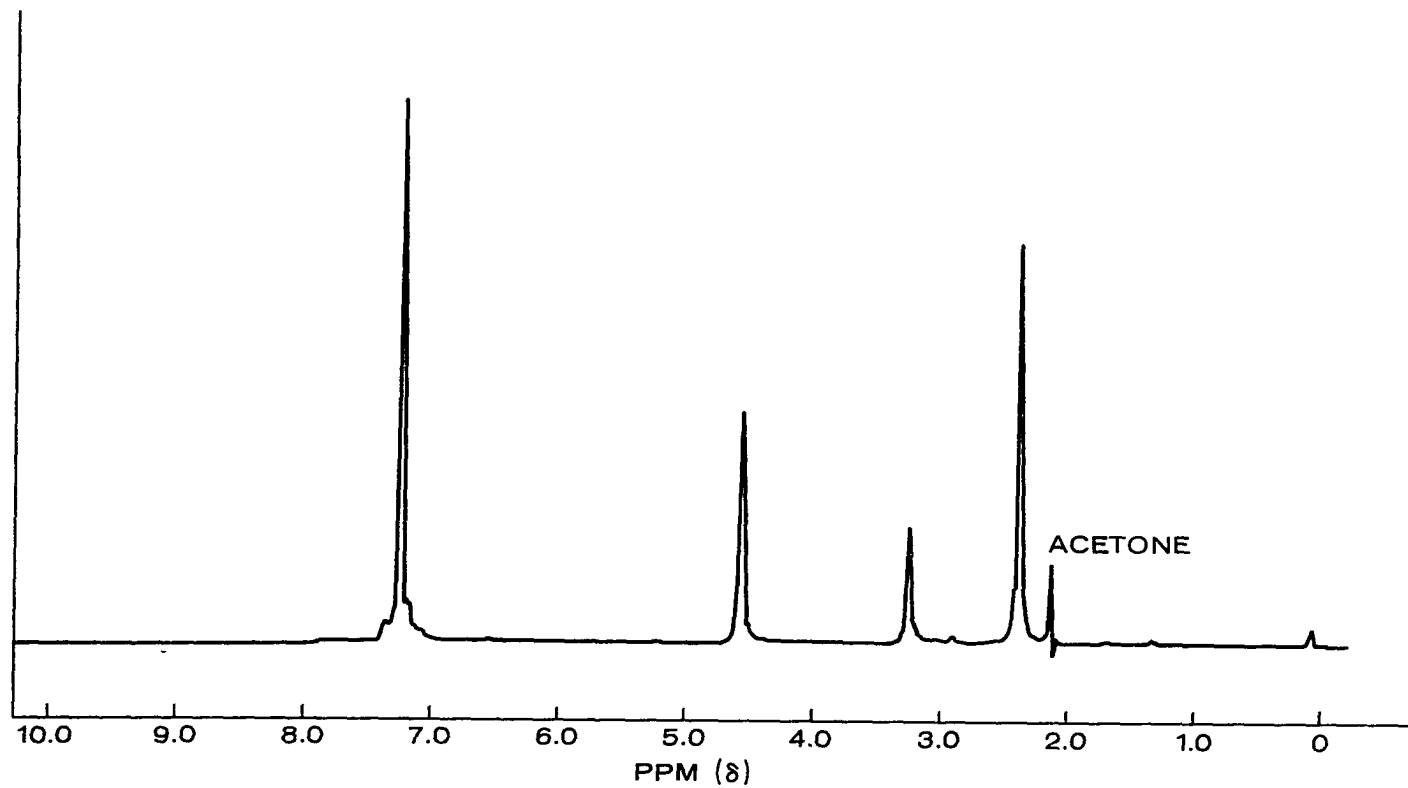
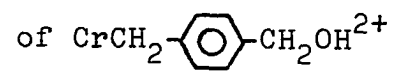


Figure 14. ^1H NMR spectrum of the base decomposition product



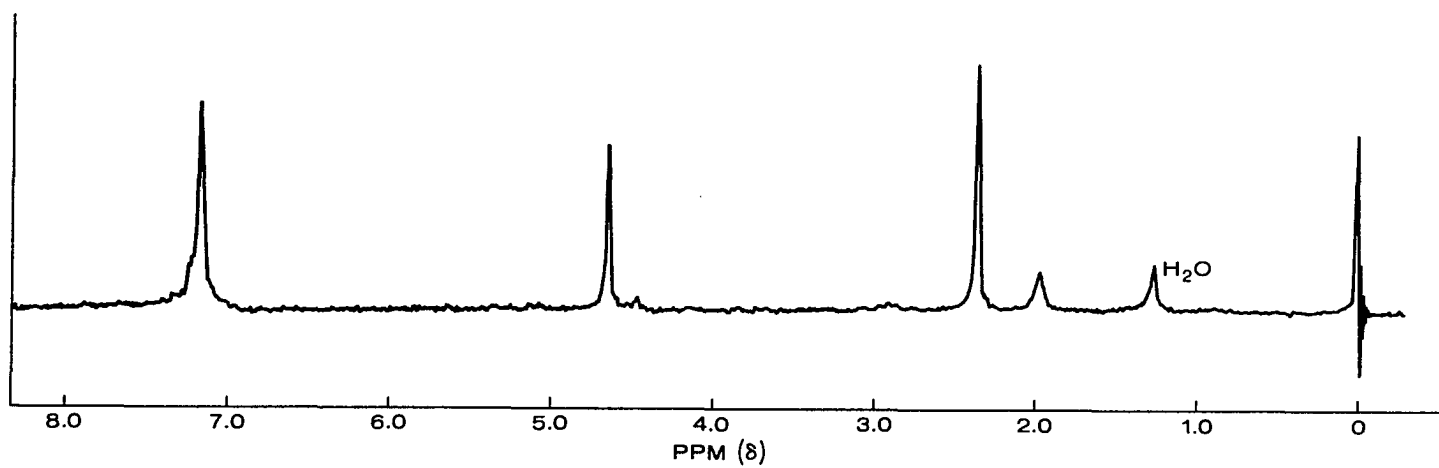


Figure 15. ^1H NMR spectrum of the base decomposition product

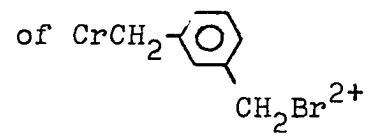


Table 4. Elemental analyses of poly-p-xylylene samples

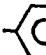
Sample #	Found		Theoretical	
	%C	%H	%C	%H
1 ^a	76.56 ^b	6.98	92.3	7.7
	76.39	6.91		
	79.71 ^c	7.22		
	79.48	7.24		
2 ^d	75.39	7.41		
	75.87	7.36		
3 ^e	71.61	5.75		
	71.75	5.91		
4 ^f	80.98	7.02		
	81.63	7.04		
	80.85	7.06		

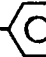
^aAuthentic sample from ICN Life Sciences.

^bAuthentic sample with normal combustion elemental analysis.

^cAuthentic sample with oxidation catalyst added.

^dPrepared by electrochemical procedure.

^ePrepared by H⁺ decomposition of CrCH₂--CH₂Cr⁴⁺.

^fPrepared by Fe³⁺ decomposition of CrCH₂--CH₂OH²⁺.

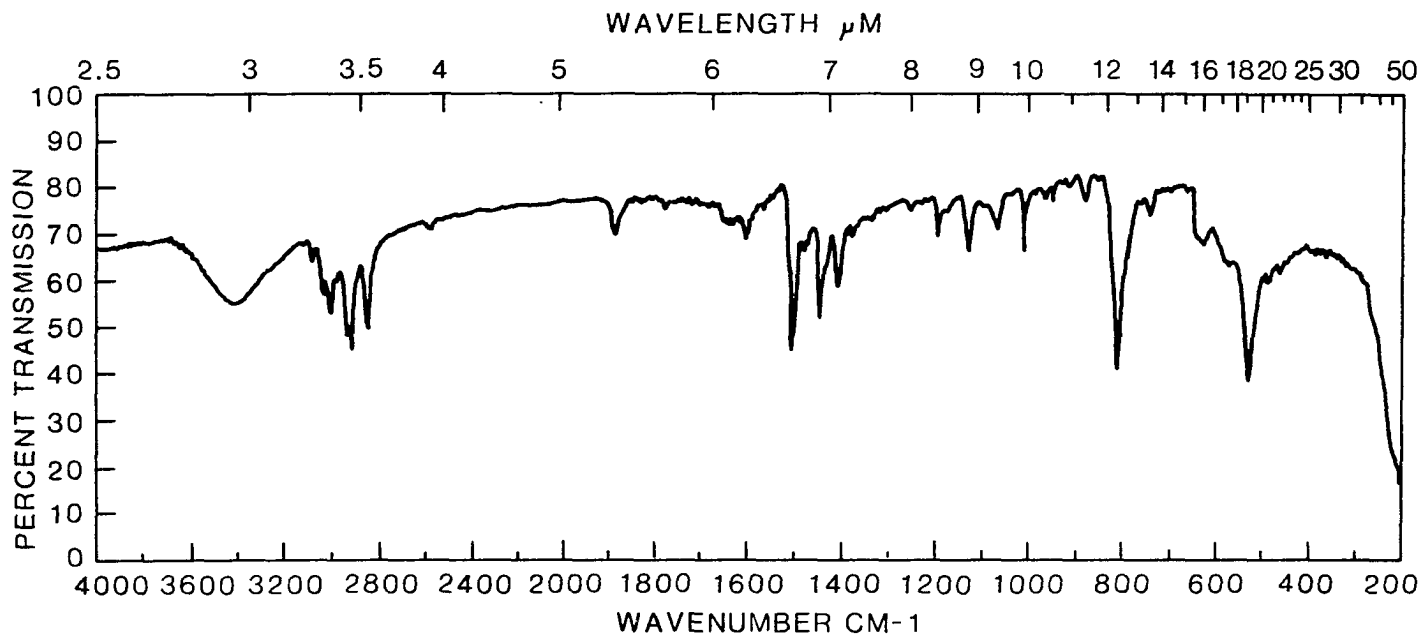


Figure 16. IR spectrum of authentic poly-p-xylylene

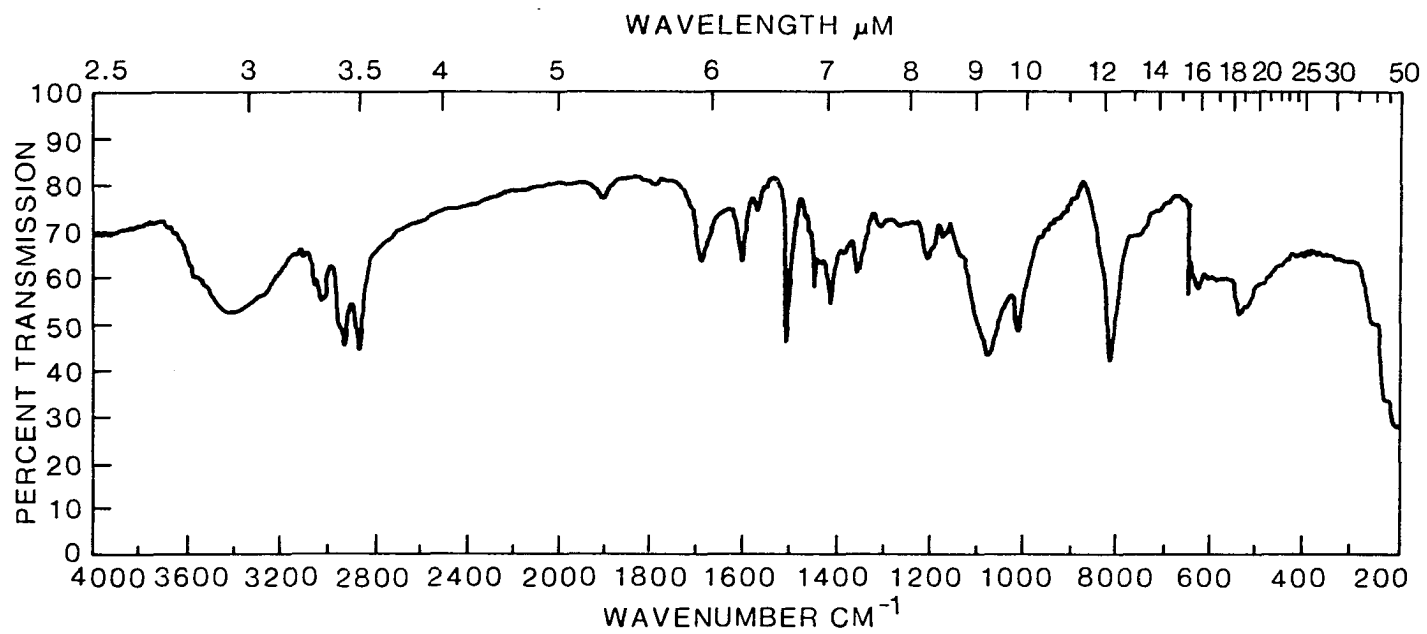


Figure 17. IR spectrum of poly-p-xylylene from the electrochemical preparation

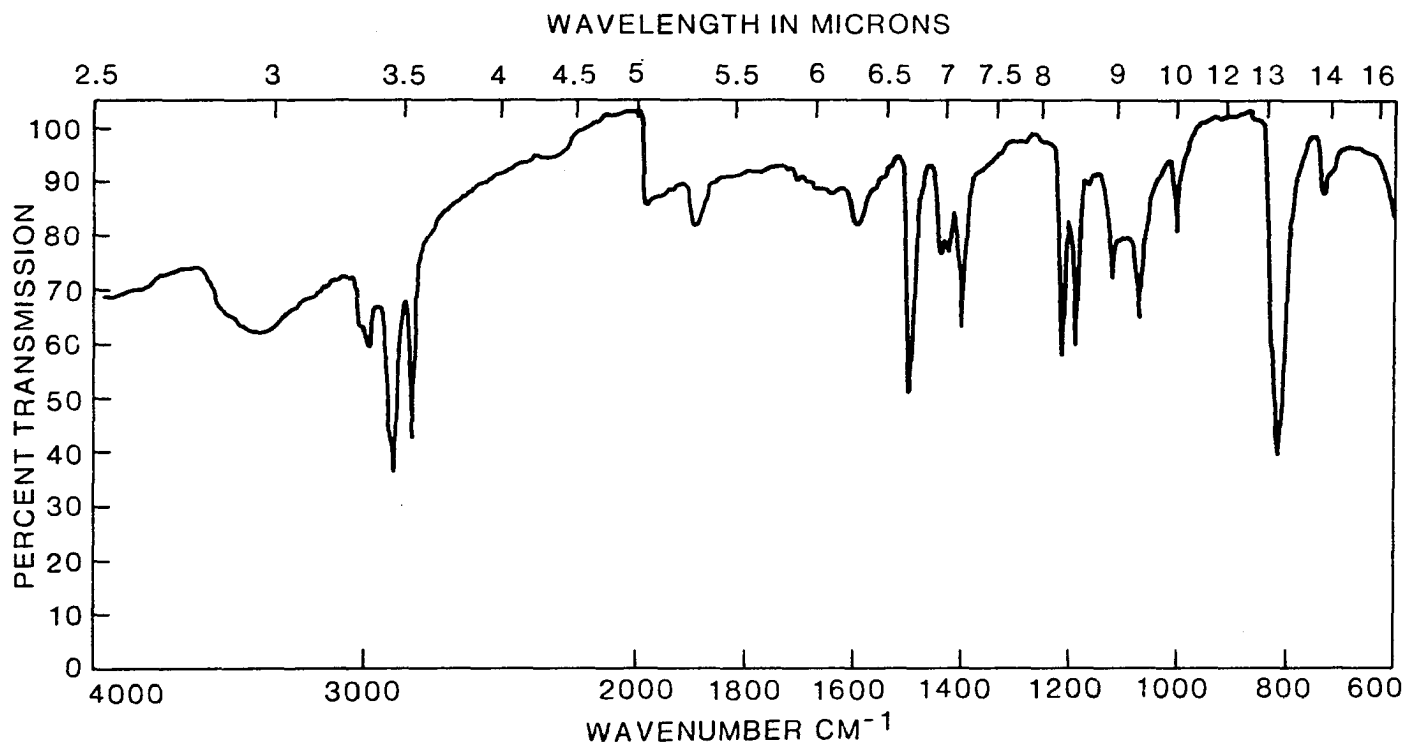


Figure 18. IR spectrum of polymer from Fe^{3+} decomposition of $\text{CrCH}_2\text{-C}_6\text{H}_4\text{-CH}_2\text{Cr}^{4+}$

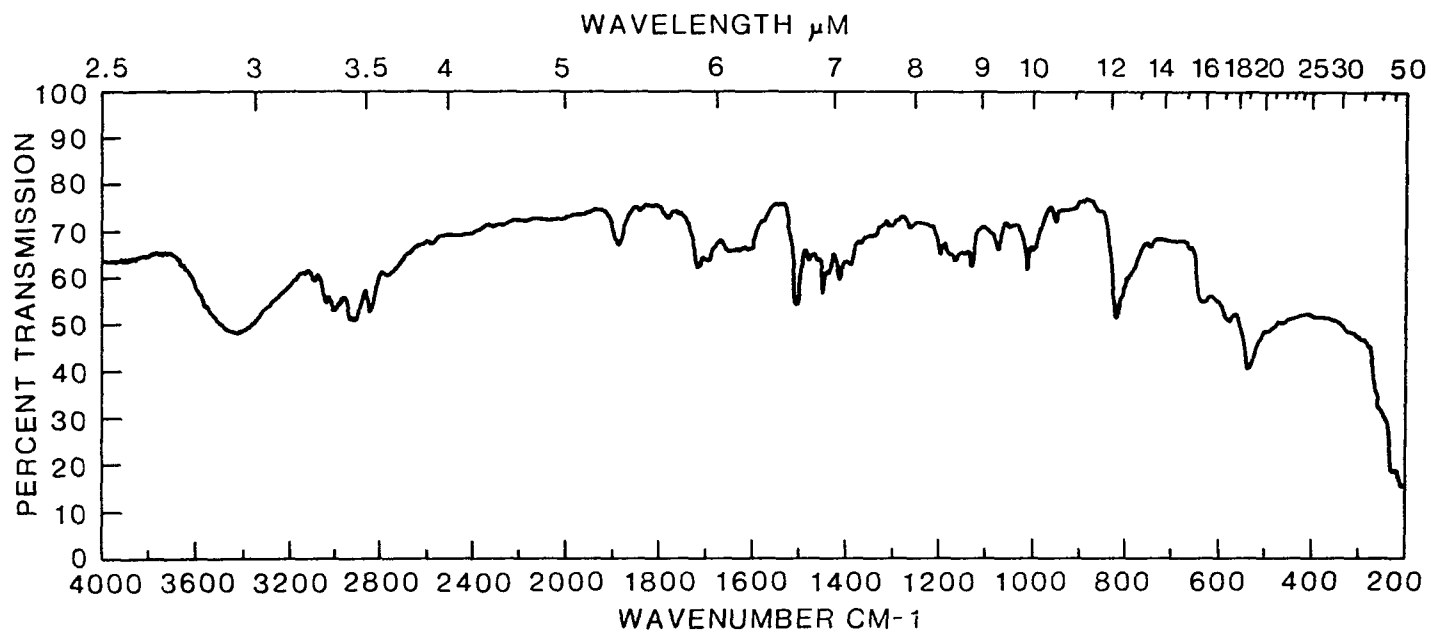


Figure 19. IR spectrum of polymer from Fe^{3+} decomposition of $\text{CrCH}_2\text{-CH}_2\text{OH}^{2+}$

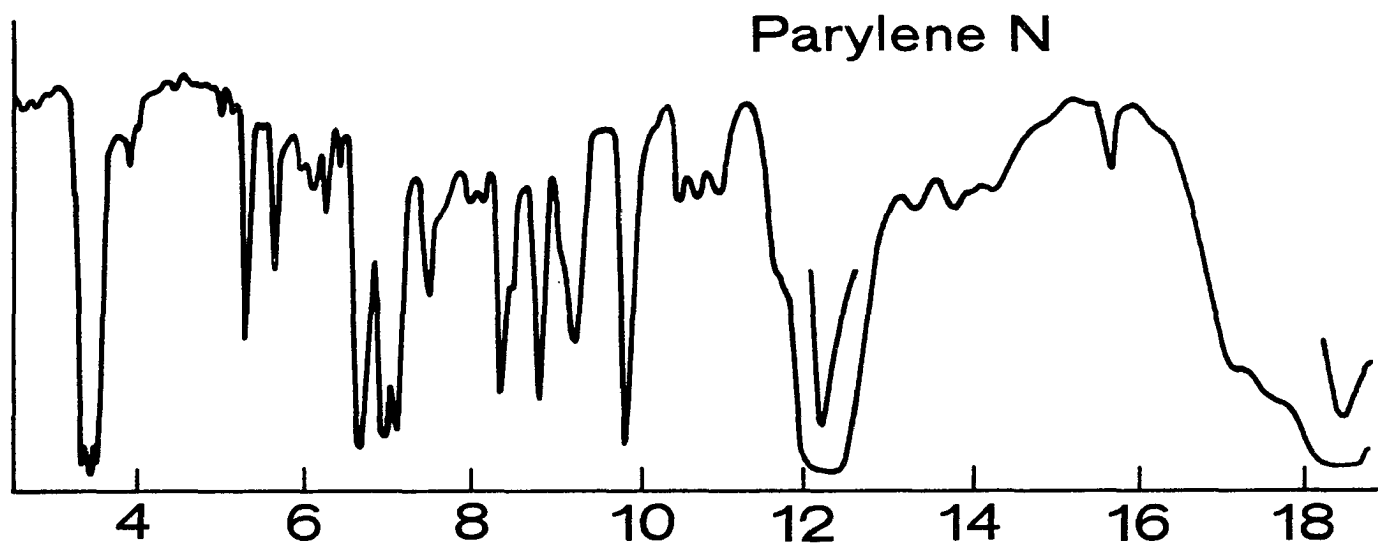
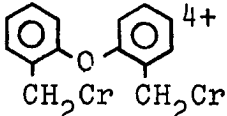
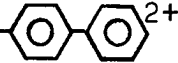
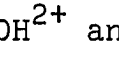
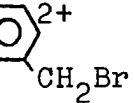
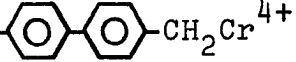
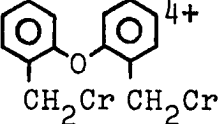


Figure 20. IR spectrum of a film of poly-*p*-xylylene

exception is the reaction of Fe^{3+} with Cr^{4+} with . This

reaction produced a mixture of CHCl_3 soluble organic products. There were at least three different products and so the reaction was not pursued further. The organochromium cations on the other hand generally produced simple organic compounds upon reaction with oxidizing agents. A prime example is that of the reaction of CrCH_2 - $^{2+}$ with Cu^{2+} or Fe^{3+} . The ^1H NMR spectra of the product is shown in Figure 21. It agrees well with the spectrum [δ 7.30 - 7.80 (Ar-H), δ 4.65 (s)] of a commercial sample (11) of *p*-phenylbenzyl alcohol. The additional peaks in the spectrum are assumed to come from a minor side reaction. The other two organochromium compounds, CrCH_2 - $^{2+}$ and CrCH_2 - $^{2+}$ produce poly-*p*-xylylene and presumably poly-*m*-xylylene, respectively. These surprising results formed the basis for much of the additional chemistry which was investigated.

The kinetics of the reaction of the organodichromium cations with oxidizing agents are given in Tables 5-8. Missing from these tables are the rate of reaction for CrCH_2 - $^{4+}$ and  $^{4+}$. In the first case the compound was too unstable to study. As soon as the cation was eluted from the ion-exchange resin, it began to

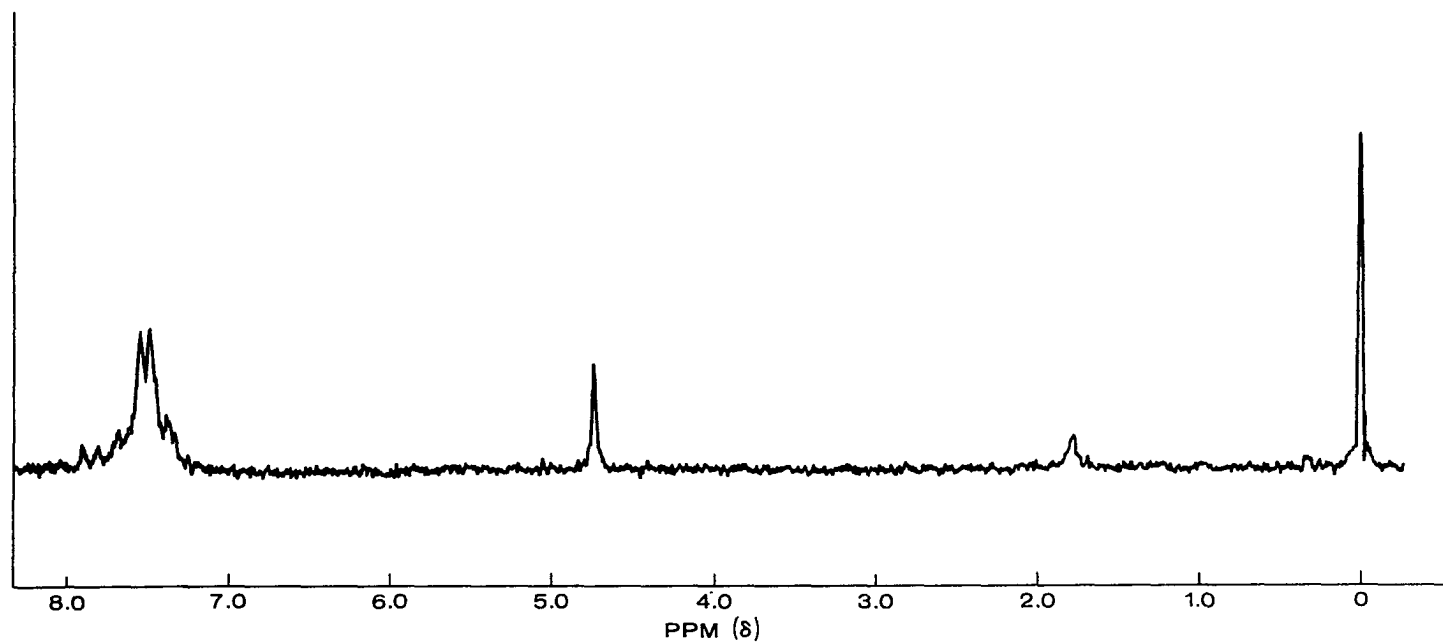


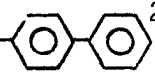
Figure 21. ¹H NMR spectrum of the product of reaction of CrCH_2 -²⁺ with Fe^{3+}

Table 5. The kinetics of the reaction of $\text{CrCH}_2\text{-C}_6\text{H}_4\text{-CH}_2\text{Cr}^{4+}$ with oxidizing agents^a

Copper(II)		Cobalt(III)	
$10^3 [\text{Cu}^{2+}] \text{ M}$	$10^3 k_1 (\text{s}^{-1})$	$10^3 [\text{Co}(\text{NH}_3)_5\text{Cl}^{2+}] \text{ M}$	$10^3 k_1 (\text{s}^{-1})$
6.75	2.47 (2)	4.5	2.51 (1)
13.5	2.48 (2)	9.0	2.58 (5)
27.0	2.56 (2)	18.0	2.45 (1)

^aIn aqueous perchlorate solution at 25.0°C with $[\text{H}^+] = 0.1 \text{ M}$ and the ionic strength (maintained with sodium perchlorate) = 1.0 M. The number in parentheses following each rate constant is the number of replicate determinations. The initial concentration of the chromium complex was usually 0.9 - 2.0 mM.

^bThe rate showed a slight dependence on $[\text{Fe}^{3+}]$, as described in the text; the value given is the rate constant extrapolated to zero concentration, representing the oxidant-independent pathway.

Iron(III)		H_2O_2	
$10^3 [\text{Fe}^{3+}] \text{ M}$	$10^3 k_1 (\text{s}^{-1})$	$10^3 [\text{H}_2\text{O}_2] \text{ M}$	$10^3 k_1 (\text{s}^{-1})$
(0)	(2.50) ^b	18.0	3.43 (5)
9.0	2.56 (1)		
18.0	2.65 (7)		
36.0	2.75 (1)		

Table 6. The kinetics of the reaction of $\text{CrCH}_2\text{-C}_6\text{H}_4\text{-CH}_2\text{Cr}^{4+}$ with oxidizing agents^a

Copper(II)		Cobalt(III)		Iron(III)	
$10^3 [\text{Cu}^{2+}] \text{ M}$	$10^3 k_1 (\text{s}^{-1})$	$10^3 [\text{Co}(\text{NH}_3)_5\text{Cl}^{2+}] \text{ M}$	$10^3 k_1 (\text{s}^{-1})$	$10^3 [\text{Fe}^{3+}] \text{ M}$	$10^3 k_1 (\text{s}^{-1})$
16.5	2.09 (1)	5.0	2.09 (1)	2.20	2.16 (2)
33.0	2.15 (5)	10.0	2.11 (4)	3.30	2.10 (2)
66.0	2.20 (1)	20.0	2.01 (1)	6.60	2.19 (1)

^aIn aqueous perchlorate solution at 25.0°C with $\text{H}^+ = 0.1 \text{ M}$ and the ionic strength (maintained with sodium perchlorate) = 1.0 M. The number in parentheses following each rate constant is the number of replicate determinations. The initial concentration of the chromium complex was usually 0.4 - 0.7 mM.

Table 7. The kinetics of the reaction of $\text{CrCH}_2\text{-C}_6\text{H}_4\text{-CH}_2\text{-CH}_2\text{-C}_6\text{H}_4\text{-CH}_2\text{Cr}^{4+}$ with oxidizing agents^a

Copper(II)		Cobalt(III)		Iron(III)	
$10^3 [\text{Cu}^{2+}] \text{ M}$	$10^3 k_1 (\text{s}^{-1})$	$10^3 [\text{Co}(\text{NH}_3)_5\text{Cl}^{2+}] \text{ M}$	$10^3 k_1 (\text{s}^{-1})$	$10^3 [\text{Fe}^{3+}] \text{ M}$	$10^3 k_1 (\text{s}^{-1})$
16.5	3.18 (1)	5.0	3.17 (1)	0	3.05 ^b
33.0	3.12 (8)	10.0	3.11 (6)	3.20	3.19(2)
66.0	3.17 (1)	20.0	3.07 (1)	4.10 6.60	3.25(6) 3.36(3)

^aIn aqueous perchlorate solution at 25.0°C with $[\text{H}^+] = 0.1 \text{ M}$ and the ionic strength (maintained with sodium perchlorate) = 1.0 M. The number in parentheses following each rate constant is the number of replicate determinations. The initial concentration of the chromium complex was usually 0.4 - 0.6 mM.

^bThe rate showed a slight dependence on $[\text{Fe}^{3+}]$, as described in the text; the value given is the rate constant extrapolated to zero concentration, representing the oxidant-independent pathway.

Table 8. The kinetics of the reaction of $\text{CrCH}_2\text{-C}_6\text{H}_4\text{-CH}_2\text{-C}_6\text{H}_4\text{-CH}_2\text{Cr}^{4+}$ with oxidizing agents^a

Copper(II)		Cobalt(III)		Iron(III)	
$10^3 [\text{Cu}^{2+}] \text{ M}$	$10^3 k_1 (\text{s}^{-1})$	$10^3 [\text{Co}(\text{NH}_3)_5\text{Cl}^{2+}] \text{ M}$	$10^3 k_1 (\text{s}^{-1})$	$10^3 [\text{Fe}^{3+}] \text{ M}$	$10^3 k_1 (\text{s}^{-1})$
10.0	2.63 (2)	---	---	0.0	2.55 ^b
20.00	2.61 (11)	---	---	9.0	2.56 (1)
40.0	2.71 (1)	---	---	18.0	2.67 (4)
---	---	---	---	36.0	2.80 (1)

^aIn aqueous perchlorate solution at 25.0°C with $[\text{H}^+] = 0.1 \text{ M}$ and the ionic strength (maintained with sodium perchlorate) = 1.0 M. The number in parentheses following each rate constant is the number of replicate determinations. The initial concentration of the chromium complex was usually 0.4 - 0.5 mM.

^bThe rate showed a slight dependence on $[\text{Fe}^{3+}]$, as described in the text; the value given is the rate constant extrapolated to zero concentration, representing the oxidant-independent pathway.

decompose to polymer and Cr^{3+} . The only way that this cation could be studied was to keep it in the presence of small amounts of Cr^{2+} to inhibit the homolysis reaction. Initially, it was thought that the reaction in the presence of small amounts of Cr^{2+} could be studied because the oxidizing agent in excess would quickly scavenge the Cr^{2+} and then react with the organodichromium cation in the usual fashion. The reactions were run, but irreproducible two-stage kinetics were seen. In addition when small amounts of Cr^{2+} were added to $\text{CrCH}_2\text{-C}_6\text{H}_5^{2+}$, the rate constant for homolysis increased by 30-35%. These two factors led us to conclude that the method had some problems, and so the rate for $\text{CrCH}_2\text{-C}_6\text{H}_4\text{-C}_6\text{H}_4\text{-CH}_2\text{Cr}^{4+}$ will simply be given as $\gg 3.0 \times 10^{-3} \text{ s}^{-1}$. In the second case the problem with the kinetics was that the organic products of the reaction are terribly insoluble in water. This caused the cell to cloud during the course of the reaction, and since the turbidity does not obey Beer's Law, it ruined the kinetic runs. Initially, the nonpolymeric nature of the products was thought to be an advantage. It was felt that this would keep the cell cleaner, and so the kinetics would be easier to obtain. Quite to the contrary, the polymer formed and fell to the bottom of the cell out of the light path while the organic material clouded the entire solution.

In most of the reactions of organodichromium cations with Fe^{3+} there was a slight dependence upon $[\text{Fe}^{3+}]$. A

typical example is shown in Figure 22 for the reaction of $\text{CrCH}_2\text{-C}_6\text{H}_4\text{-CH}_2\text{-CH}_2\text{-C}_6\text{H}_4\text{-CH}_2\text{Cr}^{4+}$. There is only a very slight dependence, and the effect totally disappeared when the ionic strength was lowered to 0.1 M or the $[\text{H}^+]$ was increased to 0.2 M. Since it played such a minor role in these reactions, it was not investigated in any great detail, but Table 9 shows how the situation can be handled (46). (Figure 23).

The kinetics of the reaction of the organochromium compounds with oxidizing agents are given in Tables 10-12. In all cases the reaction with Fe^{3+} showed either a small or moderate dependence upon $[\text{Fe}^{3+}]$. In the case of $\text{CrCH}_2\text{-C}_6\text{H}_4\text{-C}_6\text{H}_4^{2+}$ there was a pronounced effect; but due to a lack of reliable rate constants, this effect could not be quantified. In the case of $\text{CrCH}_2\text{-C}_6\text{H}_4\text{-CH}_2\text{Br}^{2+}$ at 0.1 H^+ , the effect could barely be seen as is illustrated in Figure 24. Figure 25 shows the same effect at 0.1 M H^+ /0.3 M NaClO_4 . In the case of $\text{CrCH}_2\text{-C}_6\text{H}_4\text{-CH}_2\text{OH}^{2+}$ the effect was again small and was quantified in the same manner.

A representative sample of the kinetic data from the analog computer experiments are presented in two sets. The first set encompassing Figures 26-35 represent a study of the effect of the ratio ϵ_A/ϵ_B upon the plot of $\ln|A_t - A_\infty|$ versus time. These figures exhibit certain important trends. All of the cases except the statistical case, $k_1/k_2 = 2$ and

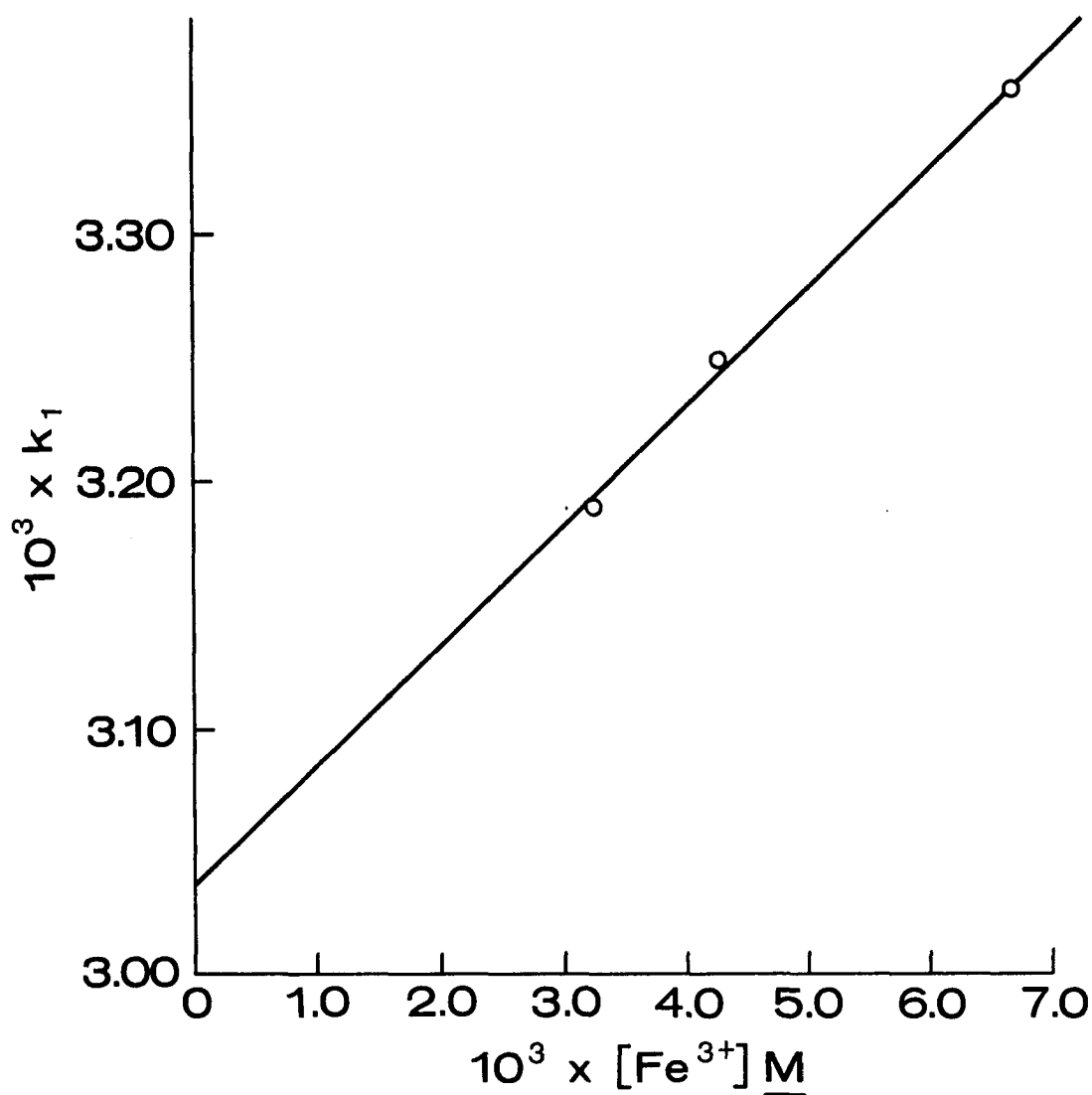




Figure 22. A plot of k_{obs} versus $[\text{Fe}^{3+}]$ for the reaction of CrCH_2 -- CH_2 - CH_2 -- $\text{CH}_2\text{Cr}^{4+}$

Table 9. The treatment of data for the rate law $k_{app} = k_1 + k_2 [X]$

The rate law $k_{app} = k_1 + k_2 [X]$ is one commonly encountered in acid studies. This serves as a trial function which is then tested by a graphical procedure. The linearity of the plot of k_{app} versus $[X]$ affirms this relationship. The slope corresponds to k_2 and the intercept k_1

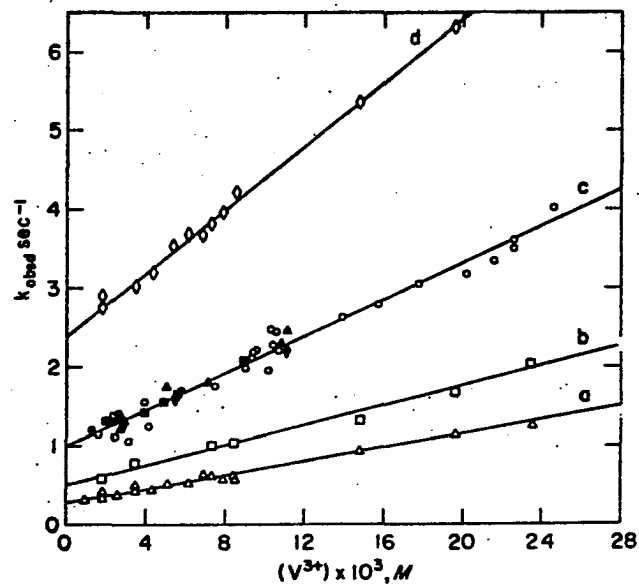


Figure 23. Plots of k_{obsd} versus (V^{3+}) (37)

Table 10. The kinetics of the reaction of $\text{CrCH}_2\text{-C}_6\text{H}_4\text{-CH}_2\text{OH}^{2+}$ with oxidizing agents^a

Copper(II)		Cobalt(III)	
$10^3 [\text{Cu}^{2+}] \text{ M}$	$10^3 k_1 (\text{s}^{-1})$	$10^3 [\text{Co}(\text{NH}_3)_5\text{Cl}^{2+}] \text{ M}$	$10^3 k_1 (\text{s}^{-1})$
2.50	1.66 (1)	1.0	1.69 (1)
5.00	1.65 (7)	2.0	1.68 (5)
10.00	1.69 (2)	4.0	1.71 (1)

^aIn aqueous perchlorate solution with $[\text{H}^+] = 0.1 \text{ M}$. The number in parentheses following each rate constant is the number of replicate determinations. The initial concentration of the chromium complex was usually 0.4 - 0.7 mM. Other than the magnitude of the iron(III)-dependent contribution, the rate constant is invariant from $\mu = 0.1 \text{ M}$.

^bThe rate shows a slight dependence on $[\text{Fe}^{3+}]$, as described in the text; the value given is the rate constant extrapolated to zero concentration, representing the oxidant-independent pathway.

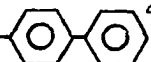
Cobalt(III)		Iron(III)	
$10^3 [\text{Co}(\text{NH}_3)_5\text{Br}^{2+}] \underline{\text{M}}$	$10^3 k_1 (\text{s}^{-1})$	$10^3 [\text{Fe}^{3+}] \underline{\text{M}}$	$10^3 k_1 (\text{s}^{-1})$
0.7	1.65 (1)	0.0	1.65 ^b
1.3	1.67 (3)	9.0	1.90 (4)
2.6	1.64 (1)	18.0	2.14 (5)

Table 11. The kinetics of the reaction of $\text{CrCH}_2\text{-C}_6\text{H}_4\text{-CH}_2\text{Br}^{2+}$ with oxidizing agents^a

Copper(II)		Cobalt(III)		Iron(III)	
$10^3 [\text{Cu}^{2+}] \text{ M}$	$10^3 k_1 (\text{s}^{-1})$	$10^3 [\text{Co}(\text{NH}_3)_5\text{Cl}^{2+}] \text{ M}$	$10^3 k_1 (\text{s}^{-1})$	$10^3 [\text{Fe}^{3+}] \text{ M}$	$10^3 k_1 (\text{s}^{-1})$
16.5	1.22 (1)	5.0	1.21 (1)	0.0	1.21 ^b
33.0	1.24 (6)	10.0	1.22 (4)	1.60	1.32(3)
66.0	1.27 (1)	20.0	1.25 (1)	3.30	1.48(5)
---	---	---	---	6.60	1.70(4)

^aIn aqueous perchlorate solution at 25.0°C with $[\text{H}^+] = 0.1 \text{ M}$ and ionic strength (maintained with sodium perchlorate) = 0.4 M. The number in parentheses following each rate constant is the number of replicate determinations. The initial concentration of the chromium complex was usually 0.5 - 0.7 mM.

^bThe rate shows a slight dependence on $[\text{Fe}^{3+}]$, as described in the text; the value given is the rate constant extrapolated to zero concentration, representing the oxidant-independent pathway.

Table 12. The kinetics of the reaction of $\text{CrCH}_2\text{-}$  $^{2+}$ with oxidizing agents^a

Copper(II)		Cobalt(III)		Iron(III)	
$10^3 [\text{Cu}^{2+}] \text{ M}$	$10^3 k_1 (\text{s}^{-1})$	$10^3 [\text{Co}(\text{NH}_3)_5\text{Cl}^{2+}] \text{ M}$	$10^3 k_1 (\text{s}^{-1})$	$10^3 [\text{Fe}^{3+}] \text{ M}$	$10^3 k_1 (\text{s}^{-1})$
8.3	3.19 (2)	--- ^b	---	0.0	3.20 ^c
16.6	3.28 (6)	---	---	13.0	4.50(3)
33.2	3.19 (2)	---	---	31.7	5.50(3)
---	---	---	---	63.3	9.20(3)

^aIn aqueous perchlorate solution at 25.0°C with $[\text{H}^+] = 0.1 \text{ M}$ and ionic strength (maintained with sodium perchlorate) = 0.4 M . The number in parentheses following each rate constant is the number of replicate determinations. The initial concentration of the chromium complex was usually 0.4 - 0.7 mM.

^bThe rate constants for this complex should be regarded as approximate owing to the precipitation of organic products during the runs. The cobalt runs were impossible to analyze.

^cThe rate shows a slight dependence on $[\text{Fe}^{3+}]$, as described in the text; the value given is the rate constant extrapolated to zero concentration, representing the oxidant-independent pathway.

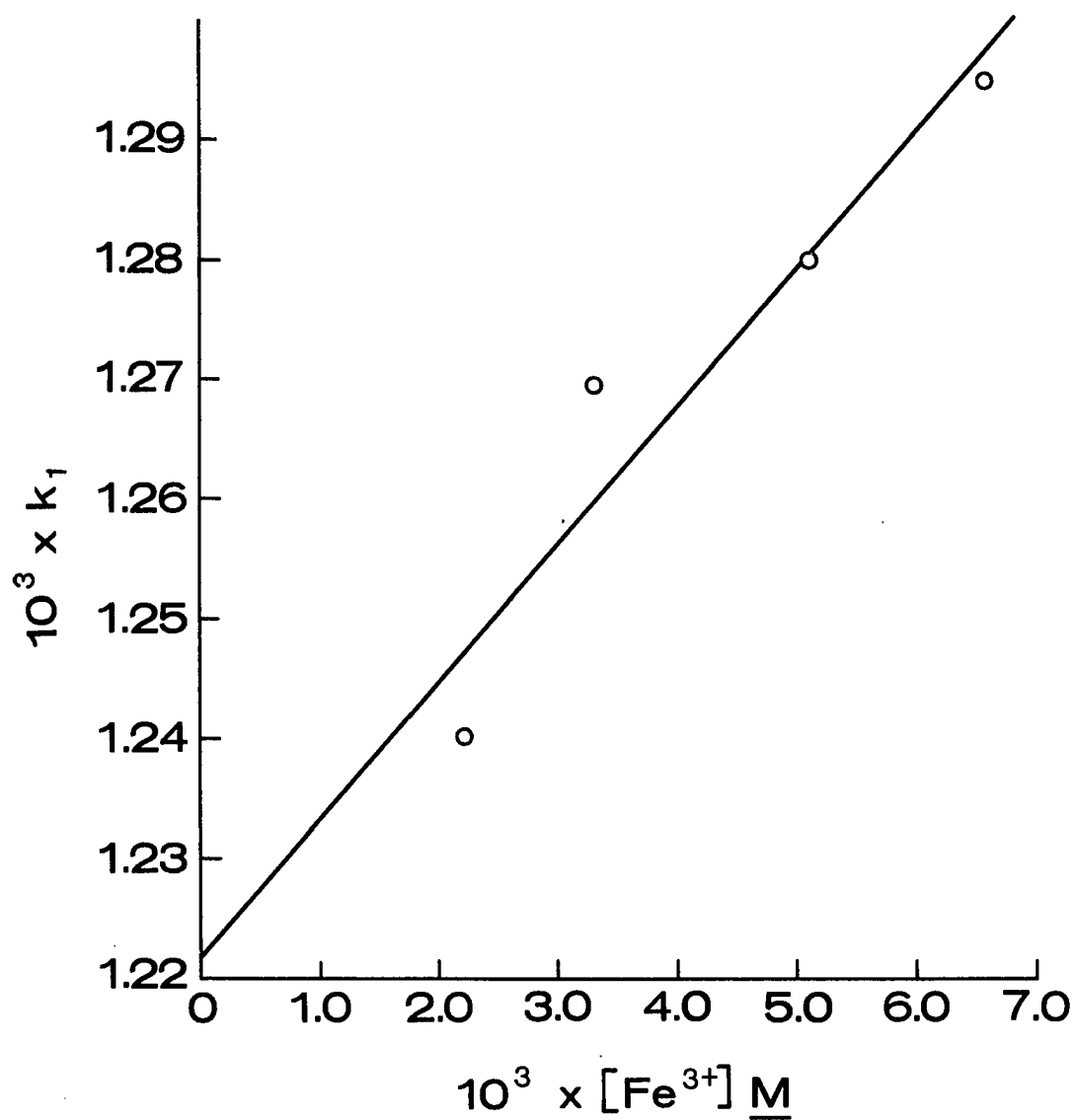
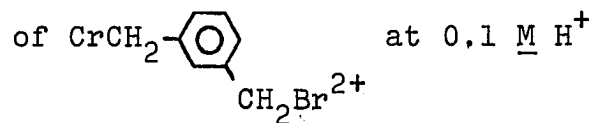


Figure 24. A plot of k_{obs} versus $[\text{Fe}^{3+}]$ for the reaction



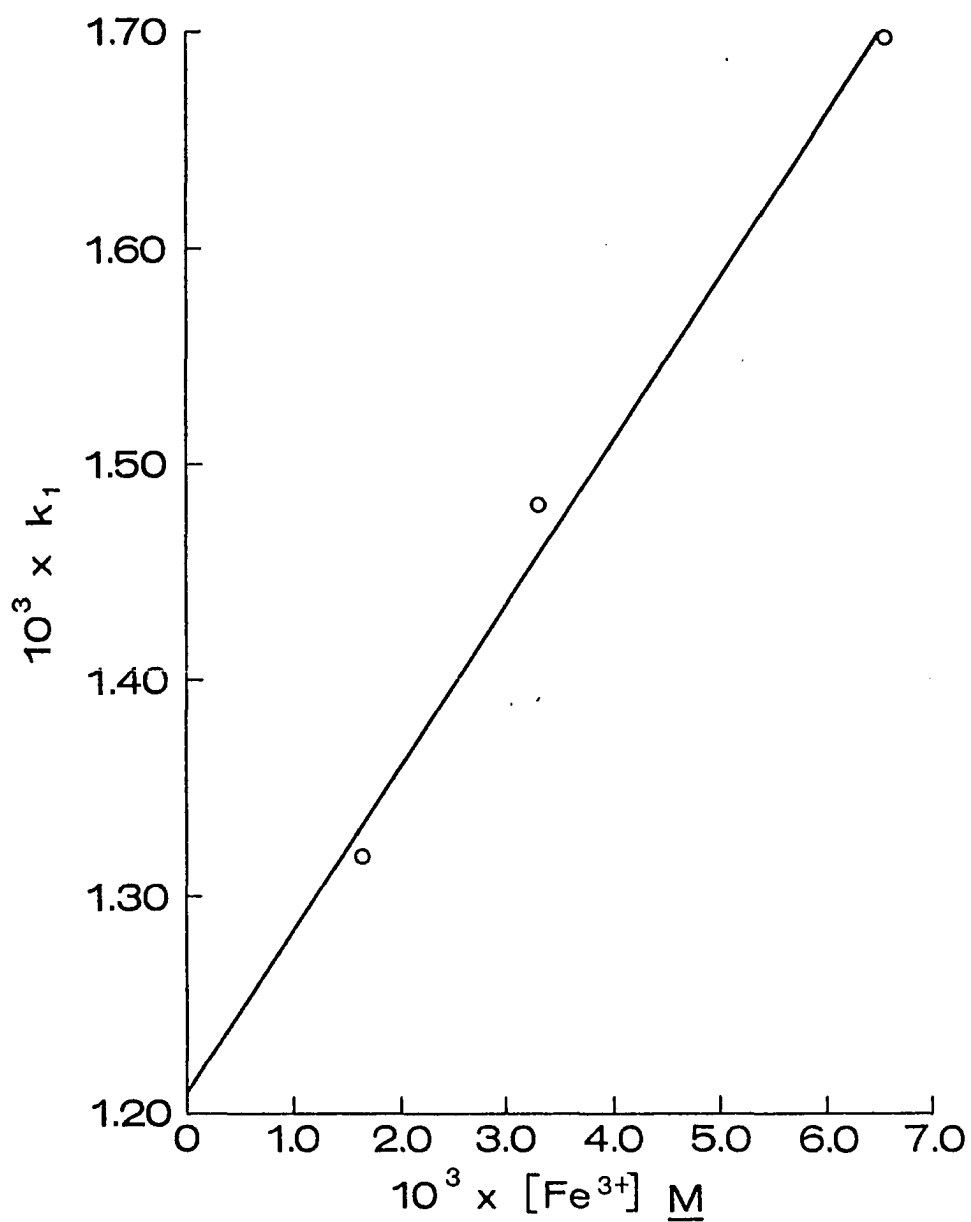
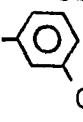


Figure 25. A plot of k_{obs} versus $[\text{Fe}^{3+}]$ for the reaction of CrCH_2 - at 0.1 M HClO_4 /0.3 M NaClO_4

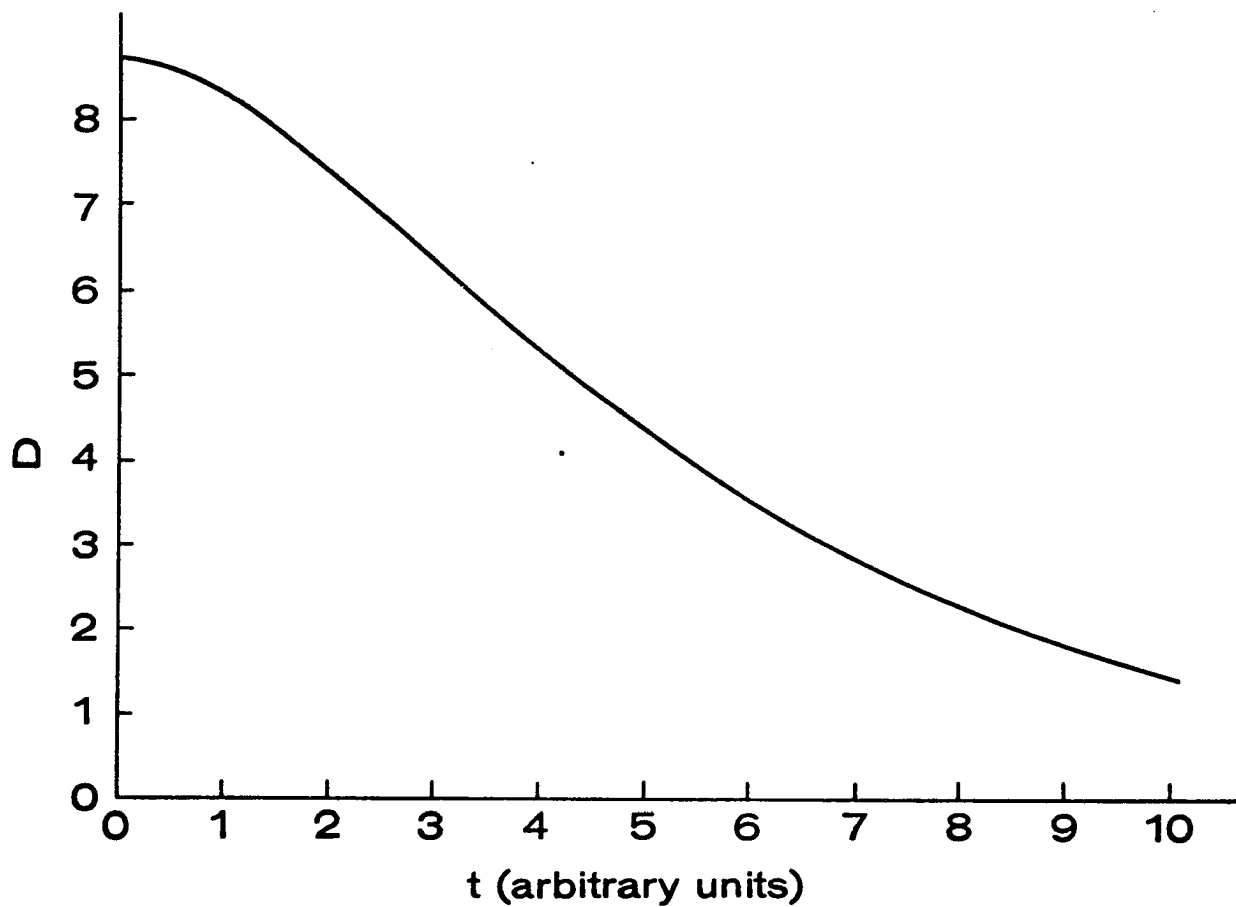


Figure 26. A plot of absorbance versus time for $A \xrightarrow{k_1} B \xrightarrow{k_2} C$ with $[A]_0 = 1.0$, $[B]_0 = [C]_0 = 0$, $k_1 = 0.50$, $k_2 = 0.25$, $\epsilon_A = 1.0$, $\epsilon_B = 1.0$, $\epsilon_C = 0$

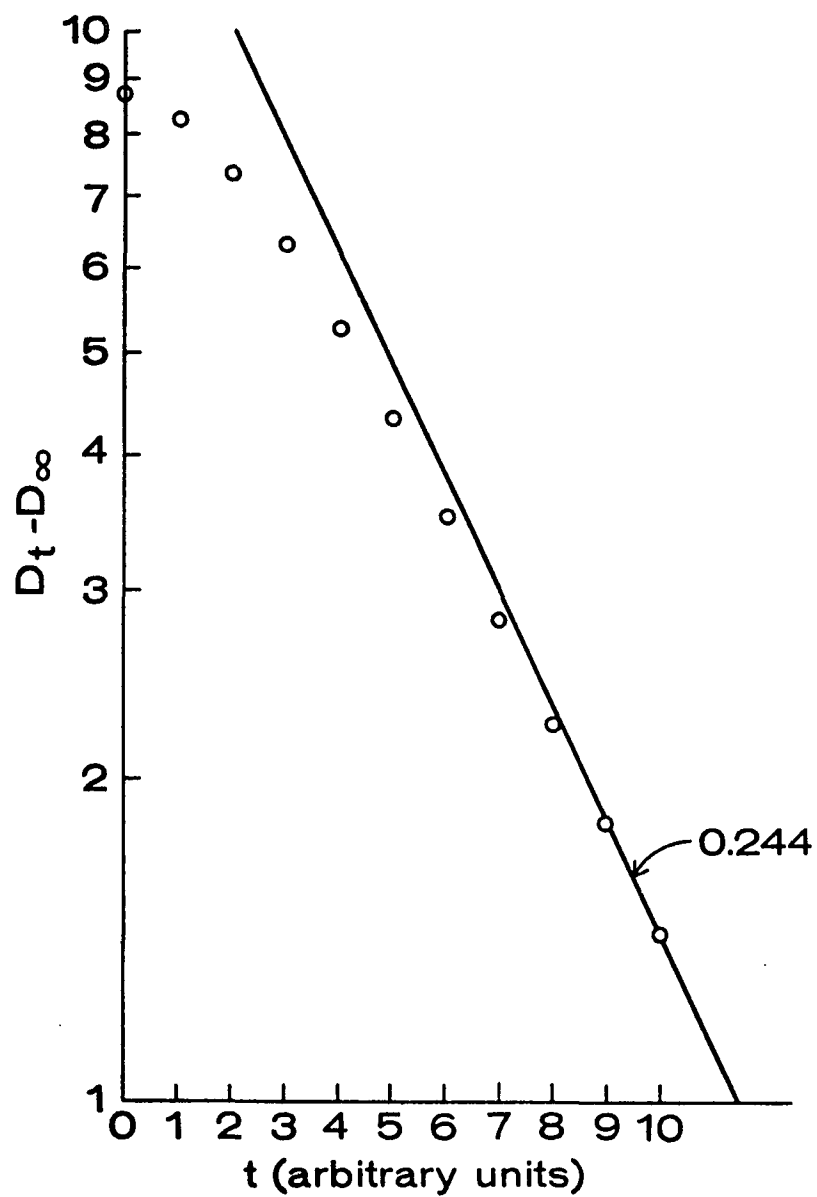


Figure 27. A plot of $\ln|D_t - D_\infty|$ versus time for $A \xrightleftharpoons[k_2]{k_1} B \xrightarrow{k_2} C$ with $[A]_0 = 1.0$, $[B]_0 = [C]_0 = 0$, $k_1 = 0.50$, $k_2 = 0.25$, $\epsilon_A = 1.0$, $\epsilon_B = 1.0$, $\epsilon_C = 0$

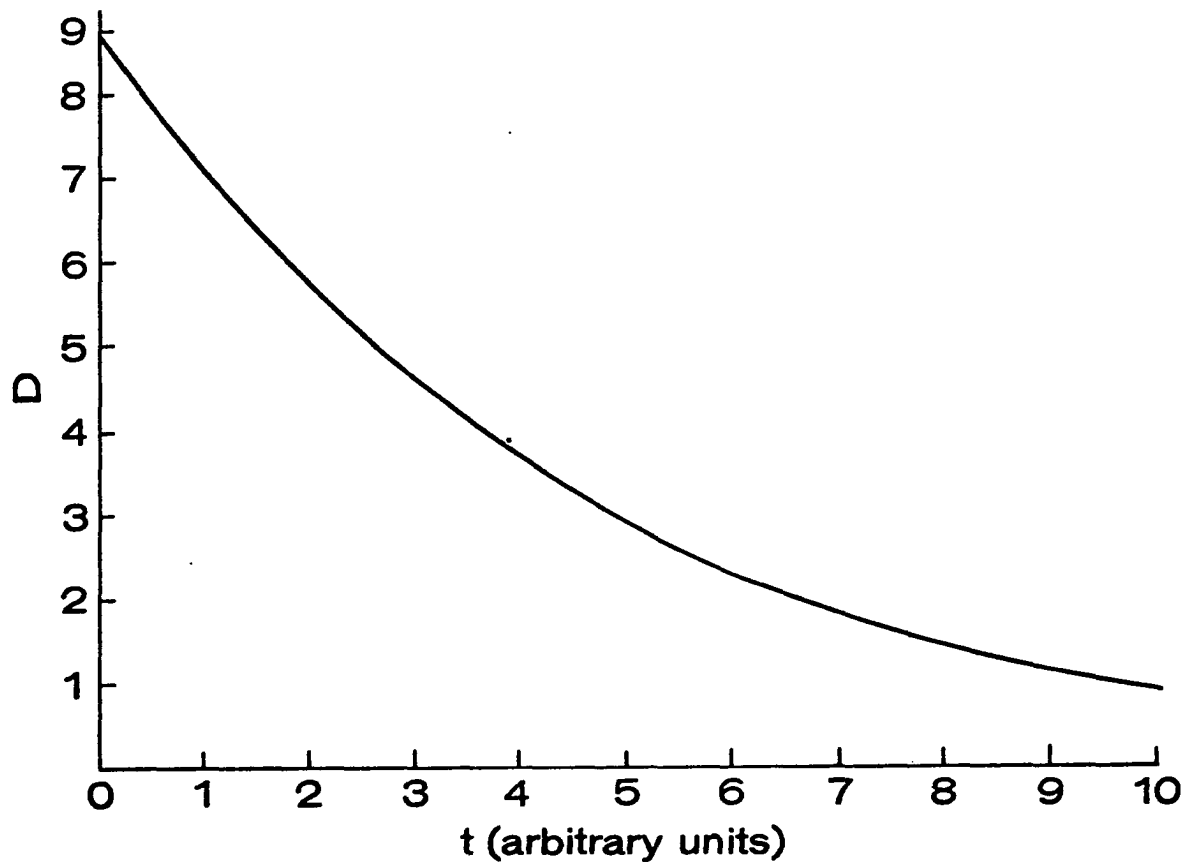


Figure 28. A plot of absorbance versus time for $A \xrightarrow{k_1} B \xrightarrow{k_2} C$ with $[A]_0 = 1.0$, $[B]_0 = [C]_0 = 0$, $k_1 = 0.50$, $k_2 = 0.25$, $\epsilon_A = 1.0$, $\epsilon_B = 0.6$, $\epsilon_C = 0$

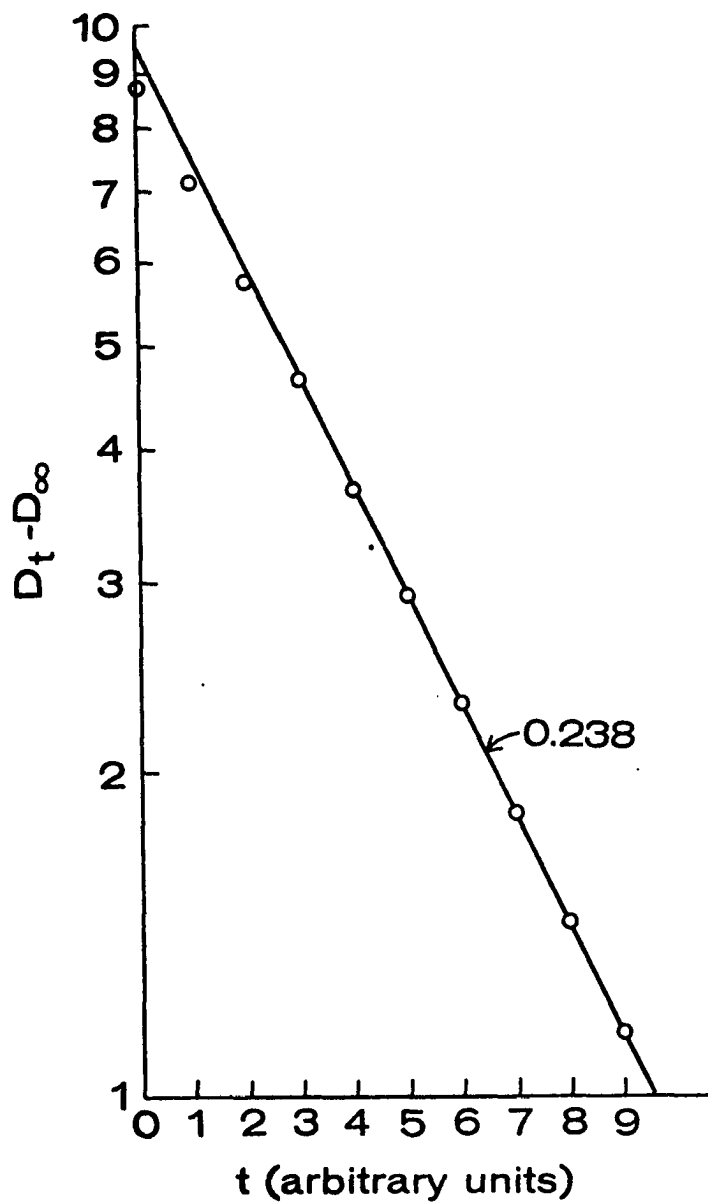


Figure 29. A plot of $\ln|D_t - D_\infty|$ versus time for
 $A \xrightarrow{k_1} B \xrightarrow{k_2} C$ with $[A]_0 = 1.0$, $[B]_0 = [C]_0 = 0$,
 $k_1 = 0.50$, $k_2 = 0.25$, $\epsilon_A = 1.0$, $\epsilon_B = 0.6$, $\epsilon_C = 0$

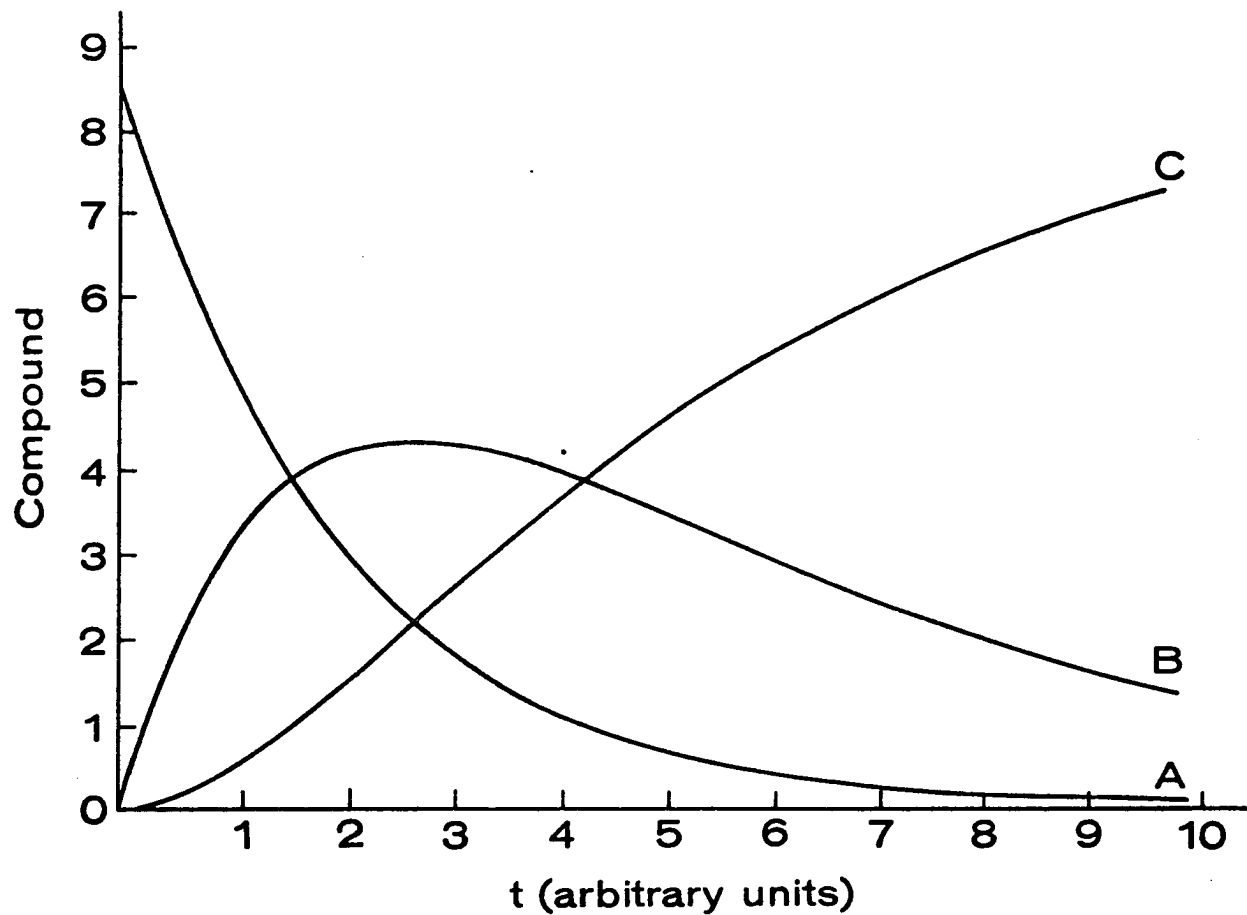


Figure 30. A plot of [A], [B] and [C] versus time for $A \xrightarrow{k_1} B \xrightarrow{k_2} C$ with $[A]_0 = 1.0$, $[B]_0 = [C]_0 = 0$, $k_1 = 0.50$, $k_2 = 0.25$, $\epsilon_A = 1.0$, $\epsilon_B = 0.5$, $\epsilon_C = 0$

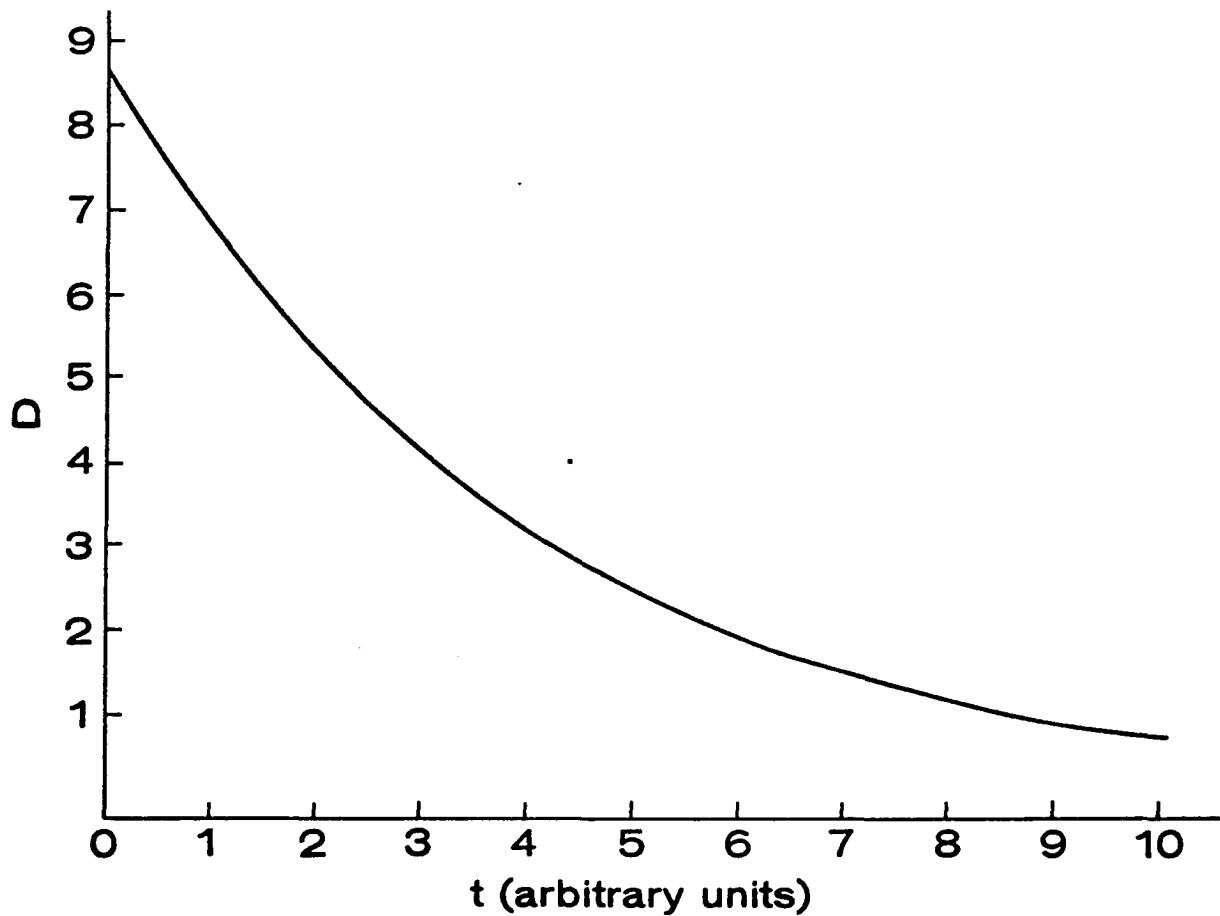


Figure 31. A plot of absorbance versus time for $A \xrightarrow{k_1} B \xrightarrow{k_2} C$ with $[A]_0 = 1.0$, $[B]_0 = [C]_0 = 0$, $k_1 = 0.50$, $k_2 = 0.25$, $\epsilon_A = 1.0$, $\epsilon_B = 0.5$, $\epsilon_C = 0$

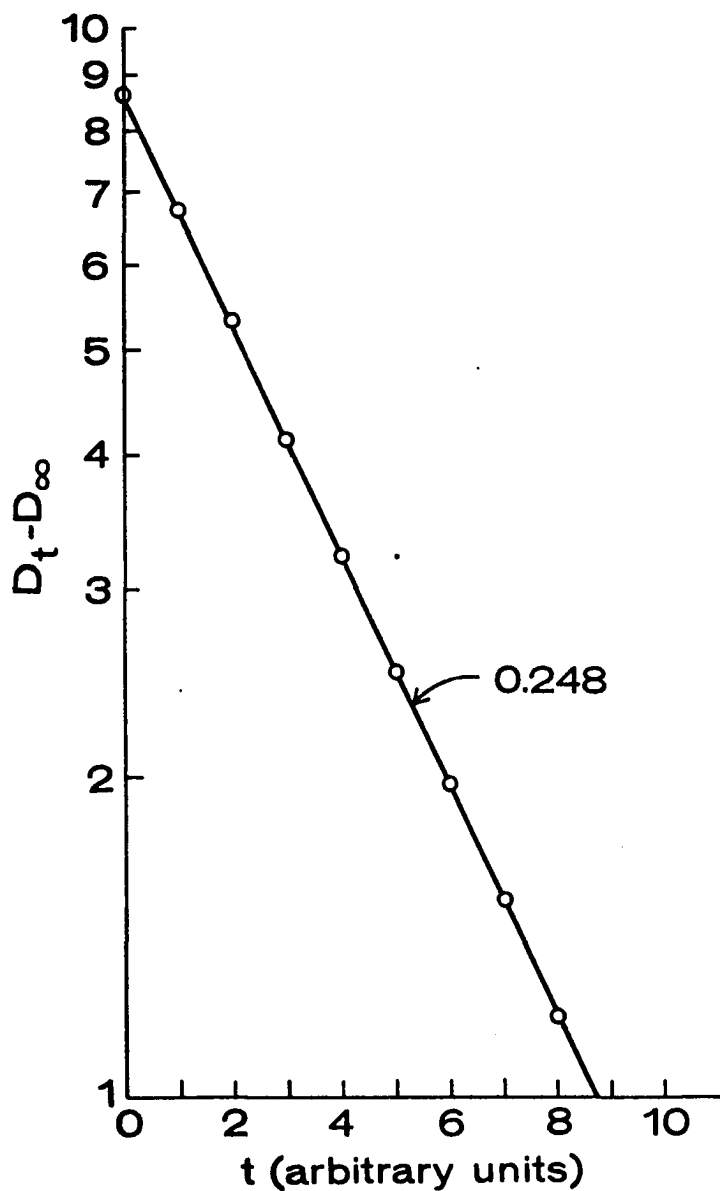


Figure 32. A plot of $\ln|D_t - D_\infty|$ versus time for $A \xrightarrow{k_1} B \xrightarrow{k_2} C$ with $[A]_0 = 1.0$, $[B]_0 = [C]_0 = 0$, $k_1 = 0.50$, $k_2 = 0.25$, $\epsilon_A = 1.0$, $\epsilon_B = 0.5$, $\epsilon_C = 0$

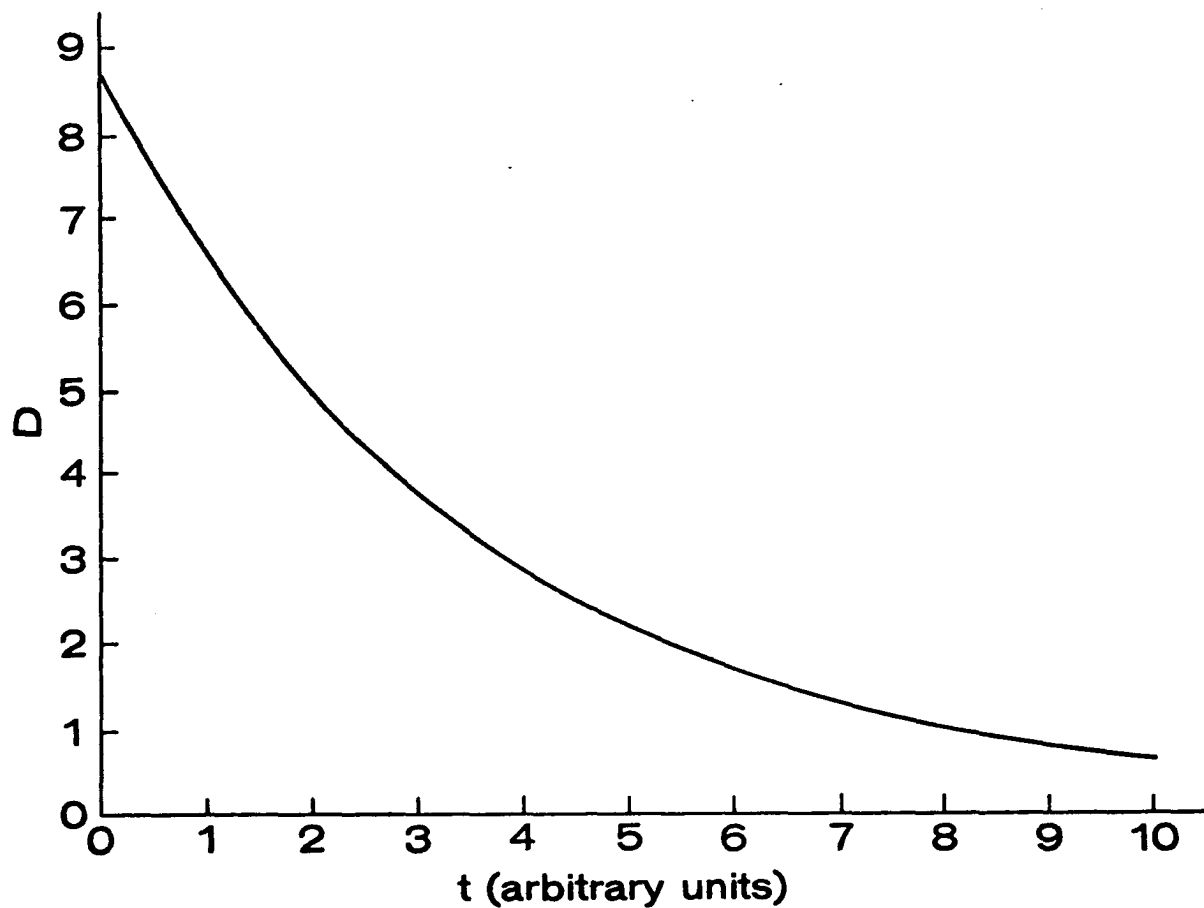


Figure 33. A plot of absorbance versus time for $A \xrightarrow{k_1} B \xrightarrow{k_2} C$ with $[A]_0 = 1.0$, $[B]_0 = [C]_0 = 0$, $k_1 = 0.50$, $k_2 = 0.25$, $\epsilon_A = 1.0$, $\epsilon_B = 0.4$, $\epsilon_C = 0$

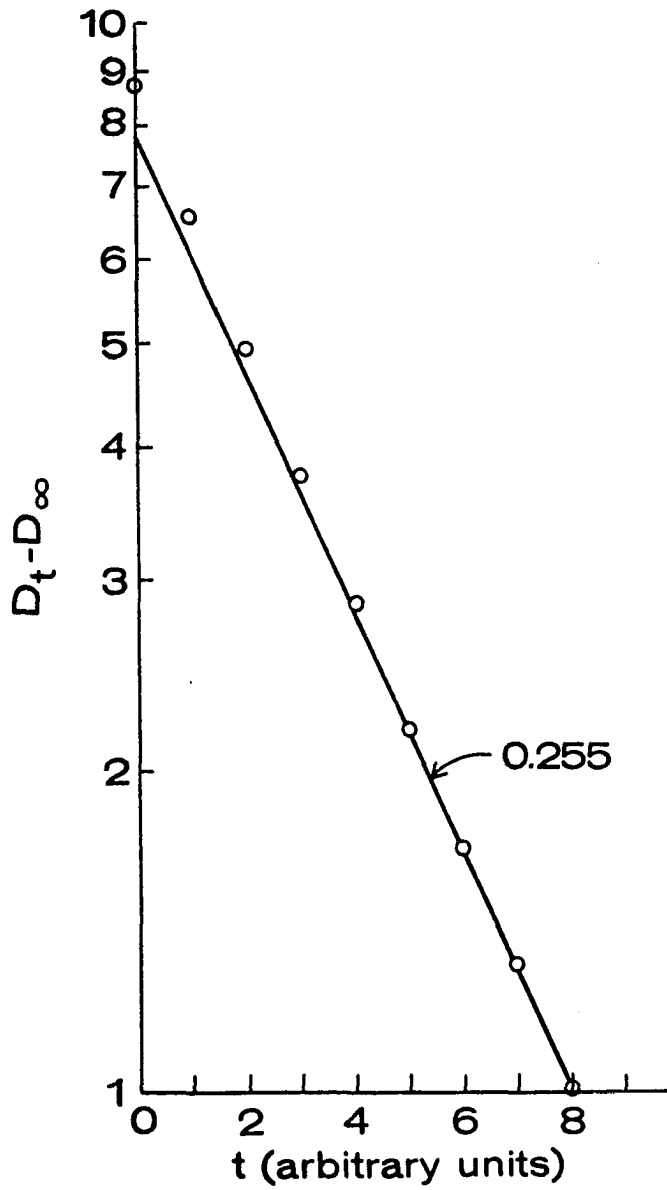


Figure 34. A plot of $\ln|D_t - D_\infty|$ versus time for $A \xrightarrow{k_1} B \xrightarrow{k_2} C$ with $[A]_0 = 1.0$, $[B]_0 = [C]_0 = 0$, $k_1 = 0.50$, $k_2 = 0.25$, $\epsilon_A = 1.0$, $\epsilon_B = 0.4$, $\epsilon_C = 0$

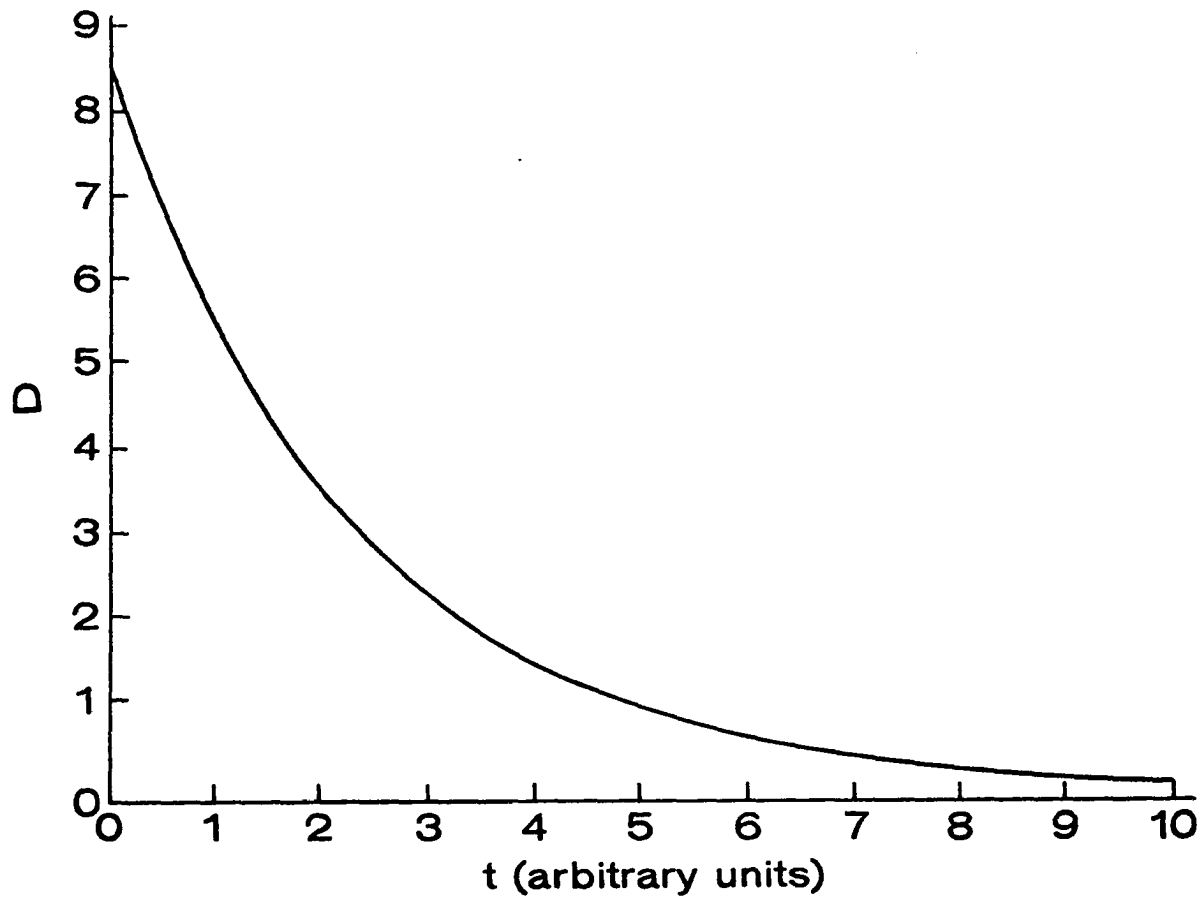


Figure 35. A plot of absorbance versus time for $A \xrightarrow{k_1} B \xrightarrow{k_2} C$ with $[A]_0 = 1.0$,
 $[B]_0 = [C]_0 = 0$, $k_1 = 0.50$, $k_2 = 0.25$, $\epsilon_A = 1.0$, $\epsilon_B = 0.1$, $\epsilon_C = 0$

$\epsilon_A/\epsilon_B = 2$, exhibited two-stage kinetics exactly as anticipated. The statistical case, although unanticipated, can be predicted based upon a complete kinetic derivation. The equations for either the formation or decomposition reaction are presented in Table 13. Another trend was the variation in the number of points available for determining the value for k_2 . At the extremes, $\epsilon_A/\epsilon_B = 1.0$ or $\epsilon_A/\epsilon_B = 10.0$, there were few points available for the determination of k_2 . Put in another way, the reactions had to be allowed to proceed for long periods of time to see only the reaction $B \rightarrow C$. Near the statistical case, $\epsilon_A/\epsilon_B = 2$, both stages were clearly visible and the rate constants easy to determine. Another trend was the position of the points early in the reaction relative to the line corresponding to k_2 . For the cases where $\epsilon_A/\epsilon_B < 2.0$ the early points were below the line corresponding to k_2 . For the case where $\epsilon_A/\epsilon_B > 2.0$, the early points were above the line corresponding to k_2 . The final general observation was that the two stages could be resolved as long as ϵ_B was at least 20% different from half the value of ϵ_A .

The second set of kinetic data, including Figures 36-43, represent a study of the effect of the ratio k_1/k_2 upon the plot of $\ln|D_t - D_\infty|$ versus time. In this case, several trends were observed, and they were quite different from those of the first set. In this set the values of k_1/k_2 were restricted to values ≥ 4.0 . As a result, the statistical

Table 13. Rate law derivation for statistical kinetics^a

$D_t - D_\infty^b = \alpha e^{-k_1 t} + \beta e^{-k_2 t}$	
$\alpha = \frac{(\epsilon_A - \epsilon_C)k_2 + (\epsilon_B - \epsilon_A)k_1}{k_2 - k_1} [A]_0$	$\beta = \frac{(\epsilon_C - \epsilon_B)k_1}{k_2 - k_1} [A]_0$
Formation kinetics	Decomposition kinetics
$\epsilon_C = 2\epsilon_B \quad \epsilon_A = 0 \quad k_1 = 2k_2$	$\epsilon_C = 0 \quad \epsilon_A = 2\epsilon_B \quad k_1 = 2k_2$
$\alpha = \frac{-2\epsilon_B k_2 + \epsilon_B 2k_2}{-k_2} [A]_0$	$\alpha = \frac{2\epsilon_B k_2 - \epsilon_B 2k_2}{-k_2} [A]_0$
$\alpha = 0$	$\alpha = 0$
$\beta = \frac{2\epsilon_B k_2}{-k_2} [A]_0$	$\beta = \frac{-2\epsilon_B k_2}{-k_2} [A]_0$
$D_t - D_\infty = -2\epsilon_B [A]_0 e^{-k_2 t}$	$D_t - D_\infty = +2\epsilon_B [A]_0 e^{-k_2 t}$
$\ln D_\infty - D_t = \ln 2\epsilon_B [A]_0 - k_2 t$	$\ln D_t - D_\infty = \ln 2\epsilon_B [A]_0 - k_2 t$

^aFor a complete derivation of the general equations, see reference 46.

^bD represents absorbance.

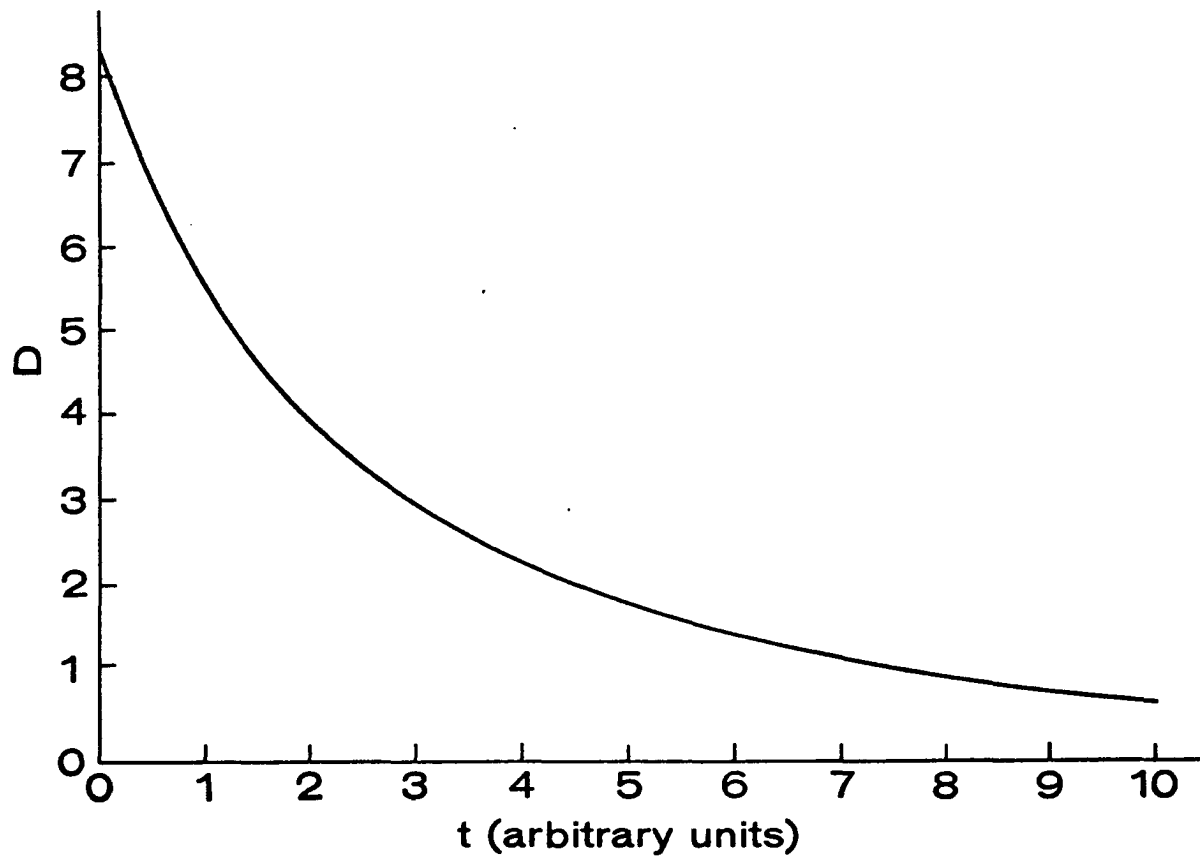


Figure 36. A plot of absorbance versus time for $A \xrightarrow{k_1} B \xrightarrow{k_2} C$ with $[A]_0 = 1.0$, $[B]_0 = [C]_0 = 0$, $k_1 = 1.00$, $k_2 = 0.25$, $\epsilon_A = 1.0$, $\epsilon_B = 0.5$, $\epsilon_C = 0$

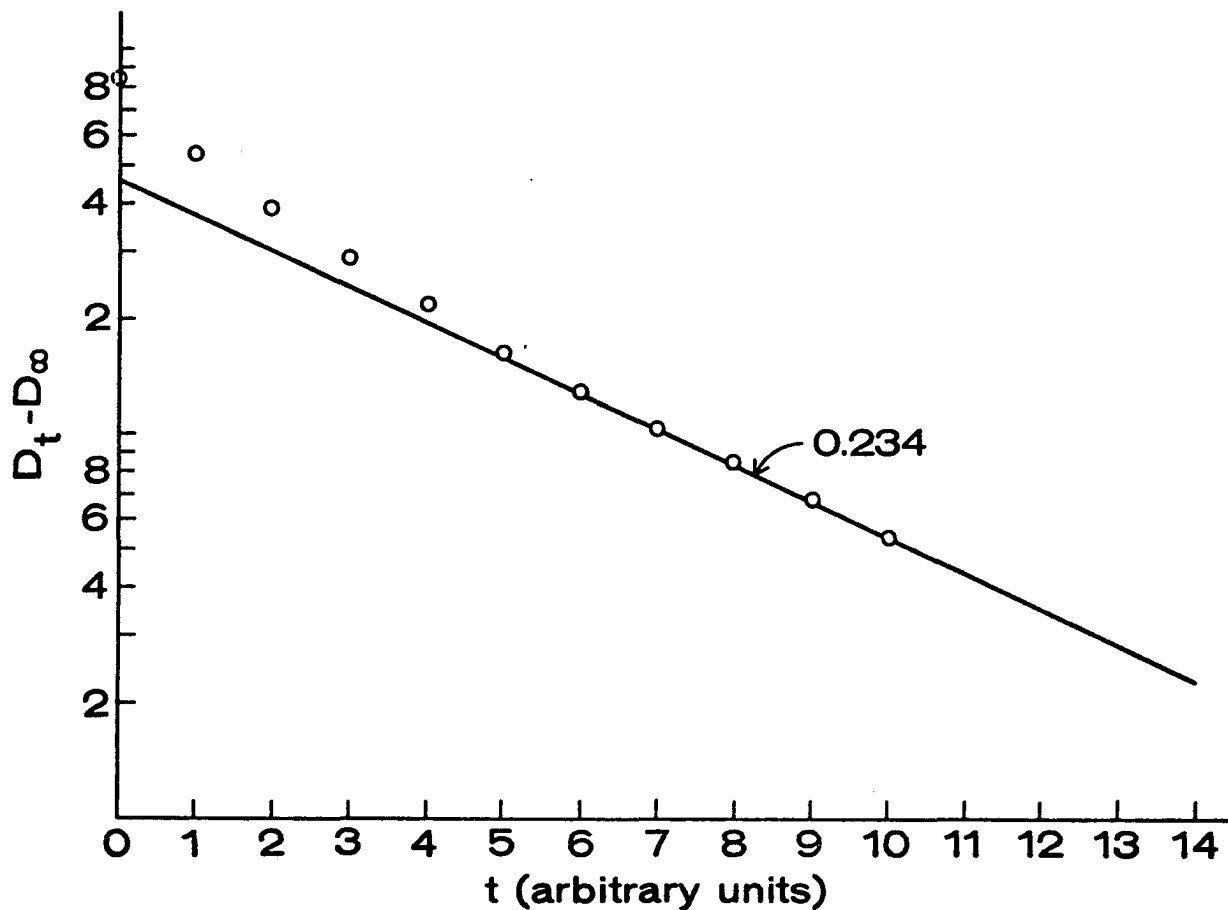


Figure 37. A plot of $\ln|D_t - D_\infty|$ versus time for $A \xrightarrow{k_1} B \xrightarrow{k_2} C$ with $[A]_0 = 1.0$, $[B]_0 = [C]_0 = 0$, $k_1 = 1.00$, $k_2 = 0.25$, $\epsilon_A = 1.0$, $\epsilon_B = 0.5$, $\epsilon_C = 0$

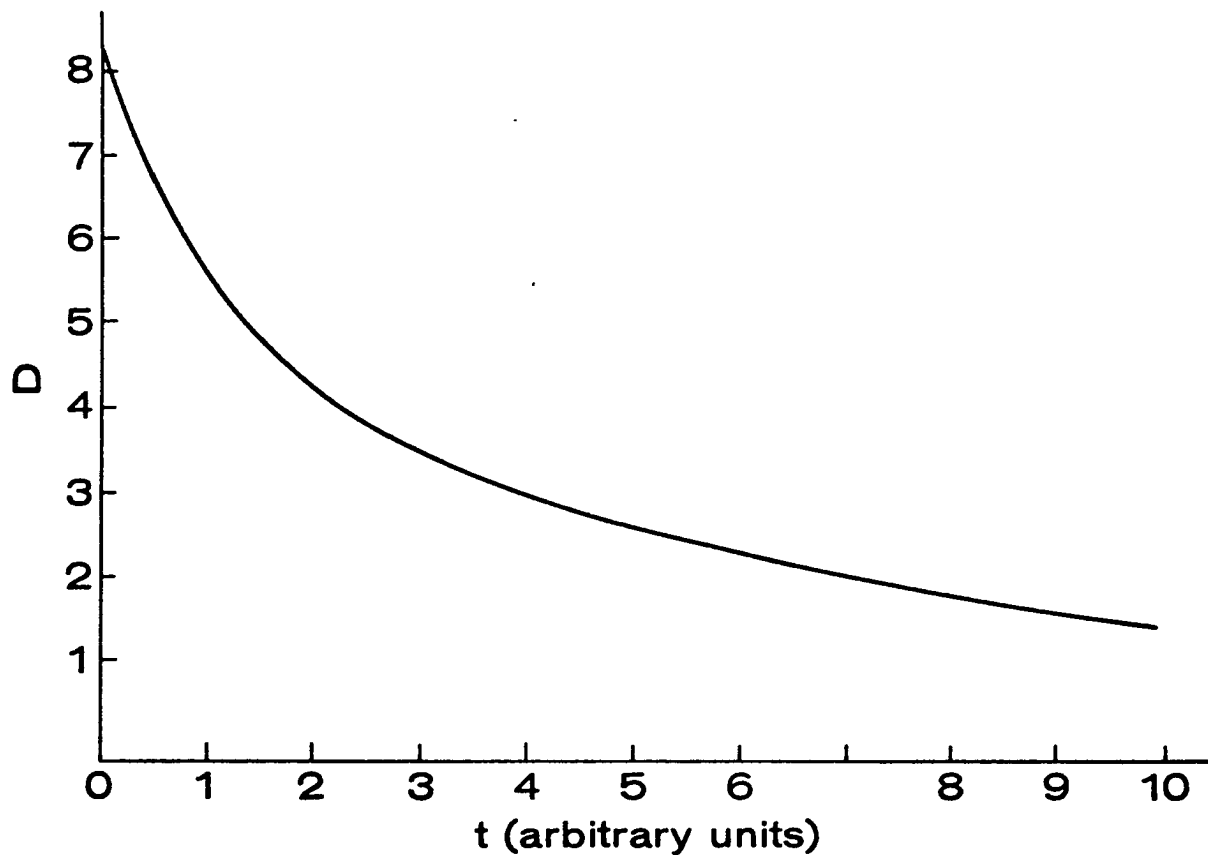


Figure 38. A plot of absorbance versus time for $A \xrightarrow{k_1} B \xrightarrow{k_2} C$ with $[A]_0 = 1.0$, $[B]_0 = [C]_0 = 0$, $k_1 = 1.00$, $k_2 = 0.125$, $\epsilon_A = 1.0$, $\epsilon_B = 0.5$, $\epsilon_C = 0$

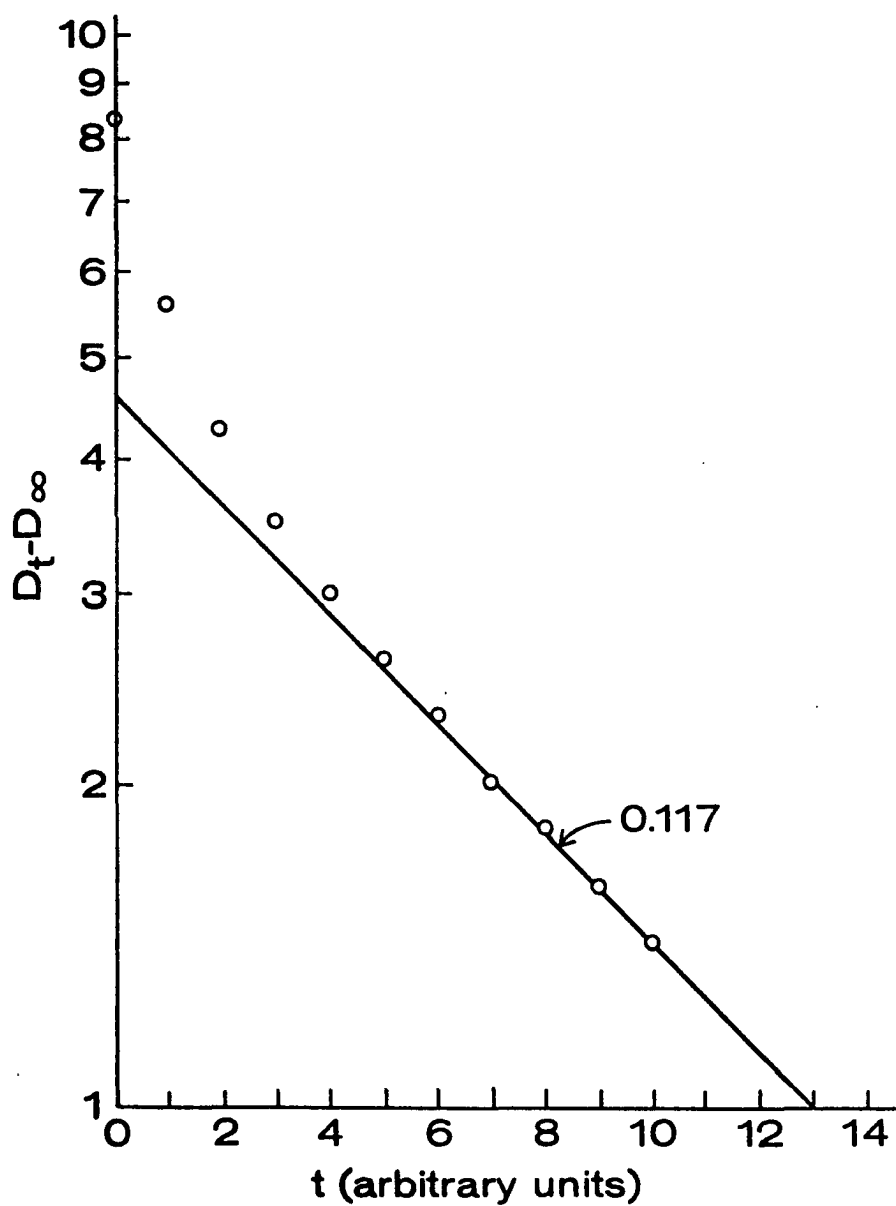


Figure 39. A plot of $\ln|D_t - D_\infty|$ versus time for $A \xrightarrow{k_1} B \xrightarrow{k_2} C$ with $[A]_0 = 1.0$, $[B]_0 = [C]_0 = 0$, $k_1 = 1.00$, $k_2 = 0.125$, $\epsilon_A = 1.0$, $\epsilon_B = 0.5$, $\epsilon_C = 0$

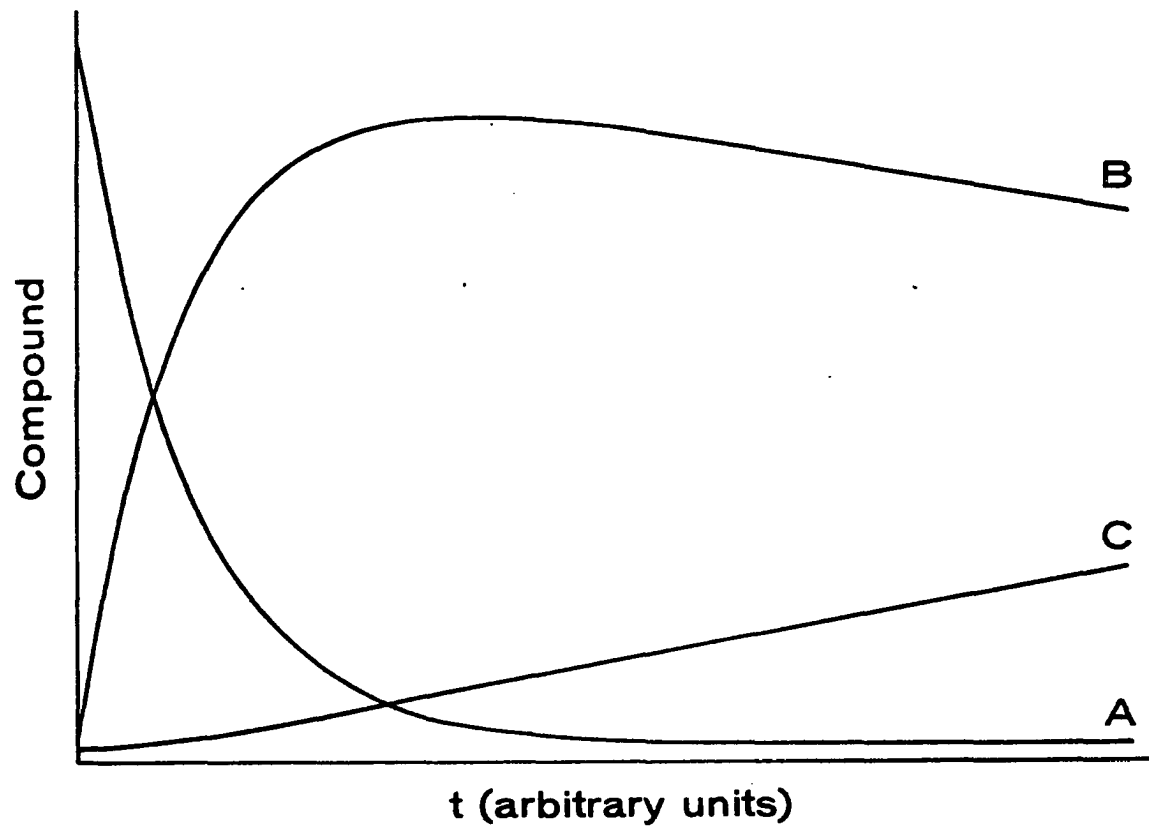


Figure 40. A plot of [A], [B] and [C] versus time for $A \xrightarrow{k_1} B \xrightarrow{k_2} C$ with $[A]_0 = 1.0$, $[B]_0 = [C]_0 = 0$, $k_1 = 1.00$, $k_2 = 0.033$, $\epsilon_A = 1.0$, $\epsilon_B = 0.5$, $\epsilon_C = 0$

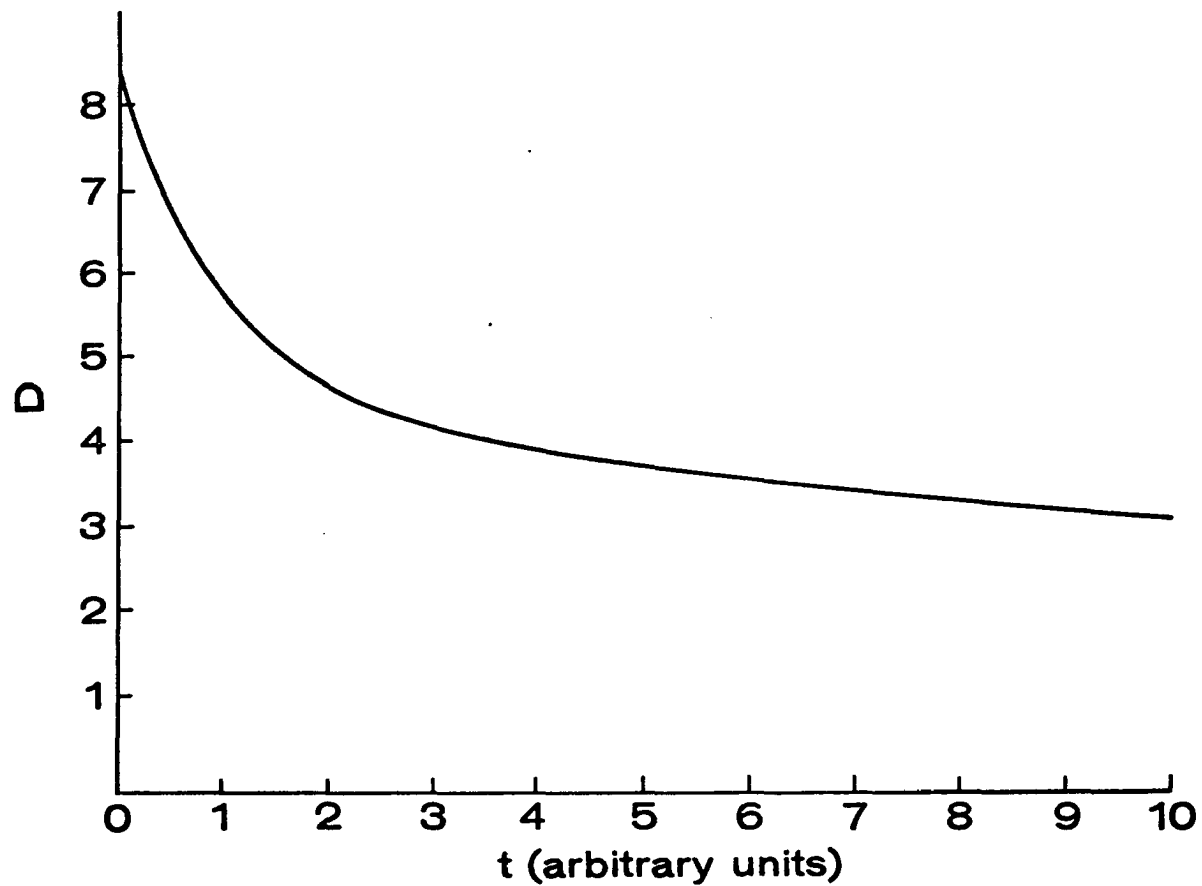


Figure 41. A plot of absorbance versus time for $A \xrightarrow{k_1} B \xrightarrow{k_2} C$ with $[A]_0 = 1.0$, $[B]_0 = [C]_0 = 0$, $k_1 = 1.00$, $k_2 = 0.033$, $\epsilon_A = 1.0$, $\epsilon_B = 0.5$, $\epsilon_C = 0$

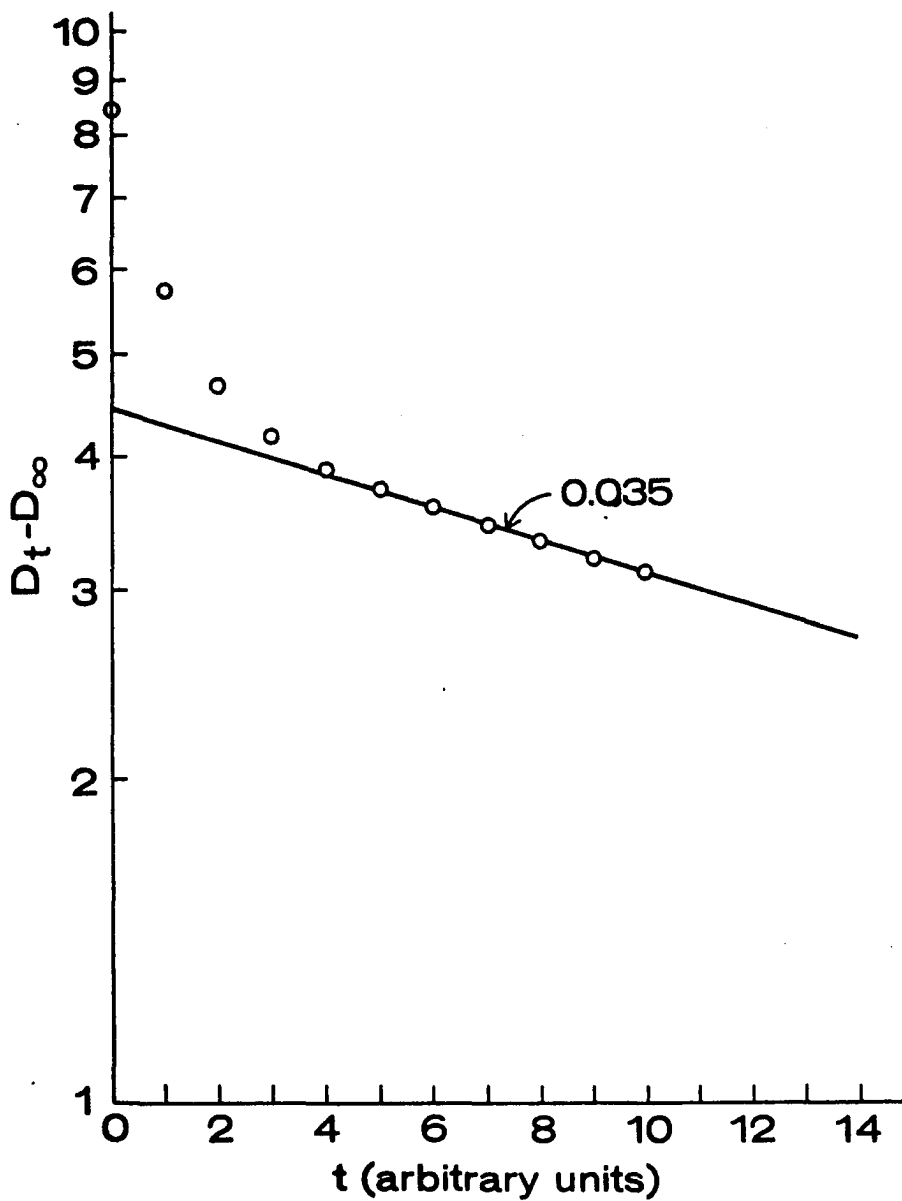


Figure 42. A plot of $\ln|D_t - D_\infty|$ versus time for $A \xrightarrow{k_1} B \xrightarrow{k_2} C$ with $[A]_0 = 1.0$, $[B]_0 = [C]_0 = 0$, $k_1 = 1.00$, $k_2 = 0.033$, $\epsilon_A = 1.0$, $\epsilon_B = 0.5$, $\epsilon_C = 0$

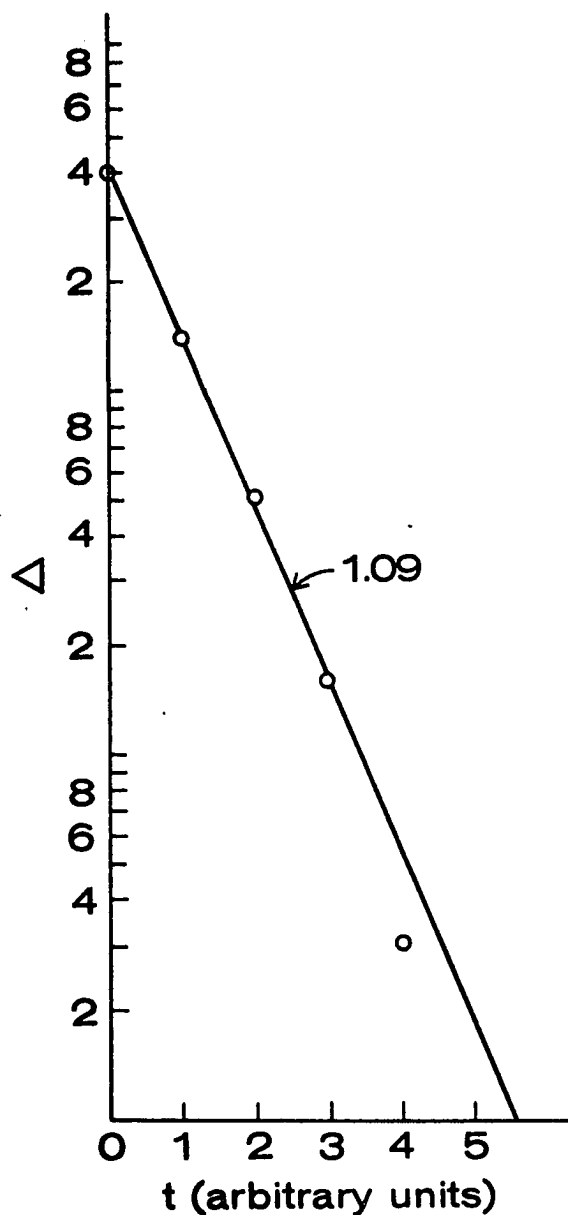


Figure 43. A plot of Δ versus time for $A \xrightarrow{k_1} B \xrightarrow{k_2} C$ with $[A]_0 = 1.0$, $[B]_0 = [C]_0 = 0$, $k_1 = 1.00$, $k_2 = 0.033$, $\epsilon_A = 1.0$, $\epsilon_B = 0.5$, $\epsilon_C = 0$

case was not encountered, and so all traces exhibited two-stage kinetics. Furthermore, one continued to see two-stage kinetics at the extremes of the ratio of k_1/k_2 with no difficulty. Also, as a result of the large value of the ratio of k_1/k_2 , all of the early points were above the line which corresponded to k_2 .

The results of the experiments to determine ϵ for several of the organodichromium cations as well as the substituted benzyl-chromium cations are presented in Table 14. The values were obtained on solutions which were fresh from the ion-exchange column, and so the samples should have experienced little decomposition prior to reaction. On the other hand, the organic products were polymers, and they may have effected the absorbance readings used to determine the value of ϵ . The runs were repeated several times and were shown to be reproducible. Therefore, the numbers are precise even though not necessarily accurate.

The results of the stoichiometry experiments are presented in Table 15. The numbers in the table represent the best numbers obtained after many runs under various conditions. The final results were obtained on samples that were totally prevented from contact with any metal needles. This precaution was necessary because the solutions proved to be capable of reacting with the needles to produce excess quantities of Fe^{2+} .

Table 14. The determination of ϵ for organochromium and organodichromium compounds

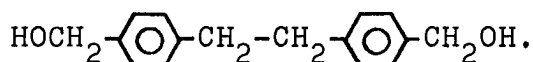
Compound	$A_{\lambda 360 \text{ nm}}$	[Co(III)] reduced \underline{M}	$\epsilon/\text{Cr-C}$ ($\text{cm}^{-1}\text{m}^{-1}$)	$\epsilon/\text{molecule}$ ($\text{cm}^{-1}\text{m}^{-1}$)
$\text{CrCH}_2\text{-C}_6\text{H}_4\text{-CH}_2\text{Cr}^{4+}$	3.294	1.32×10^{-3}	2490	4980
$\text{CrCH}_2\text{-C}_6\text{H}_3(\text{CH}_2\text{Cr}^{4+})$	19.01	8.59×10^{-3}	2213	4426
$\text{CrCH}_2\text{-C}_6\text{H}_4\text{-CH}_2\text{-CH}_2\text{-C}_6\text{H}_4\text{-CH}_2\text{Cr}^{4+}$	12.74	5.32×10^{-3}	2394	4788
$\text{CrCH}_2\text{-C}_6\text{H}_3(\text{CH}_2\text{Br}^{2+})$	6.10	2.79×10^{-3}	2186	2186
$\text{CrCH}_2\text{-C}_6\text{H}_4\text{-CH}_2\text{OH}^{2+}$	8.85	3.87×10^{-3}	2287	2287

Table 15. The stoichiometry of the reaction of Fe^{3+} and organodichromium compounds

Compound	[Cr-C] $\underline{\text{M}}$	[Fe^{2+}] found $\underline{\text{M}}$	[Fe^{2+}]/[Cr-C]	Fe^{2+} /molecule
$\text{CrCH}_2\text{-C}_6\text{H}_4^{2+ \text{a}}$	2.09×10^{-3}	4.50×10^{-3}	2.15/1	2.15/1
$\text{CrCH}_2\text{-C}_6\text{H}_4\text{-CH}_2\text{Cr}^{4+}$	9.01×10^{-4}	9.50×10^{-4}	1.05/1	2.10/1
$\text{CrCH}_2\text{-C}_6\text{H}_3(\text{CH}_2\text{Cr}^{4+})$	3.80×10^{-4}	3.82×10^{-4}	1.00/1	2.00/1

^aPerformed for comparison to 2.00/1 result in reference 9.

The electrolysis of α,α' -dibromo-p-xylene proceeded exactly as described by Covitz (42) to produce poly-p-xylylene. The material was collected and found to be of approximately the same purity as commercial samples. Primitive attempts to improve its purity by recrystallization failed. There are more exotic methods of purifying the polymer (45), but since the goal was not synthesis of polymer, these were not pursued further. The electrolysis of p-(bromomethyl)benzyl alcohol and $\text{CrCH}_2\text{-C}_6\text{H}_4\text{-CH}_2\text{OH}^{2+}$ proceeded smoothly, but failed to produce any polymer. The solutions reacted with approximately one electron per molecule of substrate, but the solutions remained homogeneous throughout the electrolysis. The organic products were not identified, but must have been simple organic molecules, such as



The photolysis of $(\text{Co})\text{-CH}_2\text{-C}_6\text{H}_4\text{-CH}_2\text{-}(\text{Co})$ produced poly-p-xylylene

in 20-30 minutes. In this case the dicobaloxime is so unstable that it can be photolyzed by room light. The

photolysis of $\text{Cr}\text{-CH}_2\text{-C}_6\text{H}_4\text{-CH}_2\text{-Cr}^{4+}$ also produced poly-p-xylylene, but it required 1-2 hours for the reaction to be completed. On the other hand, $(\text{Co})\text{-CH}_2\text{-C}_6\text{H}_4\text{-CH}_2\text{OH}$ and $\text{CrCH}_2\text{-C}_6\text{H}_4\text{-CH}_2\text{OH}^{2+}$

produced no polymer upon photolysis. The cobaloxime did

indeed decompose in the period of 30-60 minutes, but the product was a methanol-soluble product and not polymer. The organochromium cation, however, decomposed only slightly over four hours of photolysis. The decomposition product was polymer, but blank experiments showed that the same amount of polymer was produced in unphotolyzed solutions.

The products of decomposition of organodichromium cations in the presence of oxidizing agents or acid are given in Table 16. Most all of the materials were polymeric and the structure of their backbones were not significantly different. Poly-p-xylylene was very definitely identified by comparing its properties to that of an authentic sample of the polymer. The prime proof for the structure was the infrared spectra. In all cases the spectrum were run as KBr pellets which did not produce nice detailed spectra. Subtle changes such as removing every fourth methylene group could not be detected by this technique. Elemental analysis was attempted in the hope of finding a lower percent carbon. However, the elemental analysis of poly-p-xylylene was so low (80% as opposed to theoretical 92.3%) that a lowering of the % carbon could be attributed to several factors. These problems led to the structures which are assumed based on logical chemistry rather than rigorous chemical proof. In addition, copolymers could be produced by mixing the appropriate dichromium cations together and allowing

Table 16. The decomposition products of organodichromium cations

Organodichromium	Attacking Species	Nature of Product	Product
$\text{CrCH}_2\text{-C}_6\text{H}_4\text{-CH}_2\text{Cr}^{4+}$	$\text{Fe}^{3+}/\text{Cu}^{2+}/\text{Co}(\text{NH}_3)_5\text{Cl}^{2+}/\text{H}^+$	Polymeric	$\text{-(CH}_2\text{-C}_6\text{H}_4\text{-CH}_2\text{)}_n$
$\text{CrCH}_2\text{-C}_6\text{H}_3(\text{CH}_2\text{Cr}^{4+})$	$\text{Fe}^{3+}/\text{H}^+$	Polymeric	$\text{-(CH}_2\text{-C}_6\text{H}_3(\text{CH}_2\text{)}_n \text{ (?) }^a$
$\text{CrCH}_2\text{-C}_6\text{H}_4\text{-CH}_2\text{-CH}_2\text{-C}_6\text{H}_4\text{-CH}_2\text{Cr}^{4+}$	$\text{Fe}^{3+}/\text{Cu}^{2+}/\text{H}^+$	Polymeric	$\text{-(CH}_2\text{-C}_6\text{H}_4\text{-CH}_2\text{)}_n$
$\text{CrCH}_2\text{-C}_6\text{H}_4\text{-CH}_2\text{-C}_6\text{H}_4\text{-CH}_2\text{Cr}^{4+}$	$\text{Fe}^{3+}/\text{Cu}^{2+}/\text{H}^+$	Polymeric	$\text{-(CH}_2\text{-C}_6\text{H}_4\text{-CH}_2\text{-C}_6\text{H}_4\text{-CH}_2\text{)}_n \text{ (?)}$
$\text{CrCH}_2\text{-C}_6\text{H}_4\text{-C}_6\text{H}_4\text{-CH}_2\text{Cr}^{4+}$	$\text{Fe}^{3+}/\text{Cu}^{2+}/\text{H}^+$	Polymeric	$\text{-(CH}_2\text{-C}_6\text{H}_4\text{-C}_6\text{H}_4\text{-CH}_2\text{)}_n \text{ (?)}$
$\text{C}_6\text{H}_4(\text{CH}_2\text{Cr}^{4+})_2$	$\text{Fe}^{3+}/\text{Cu}^{2+}/\text{H}^+$	Monomeric	Several ^b

^aThe ? signifies that the material was isolated but could not be differentiated from other polymers.

^bThere were at least three products produced. They were produced in such small quantities that their identification was not attempted.

them to decompose. These results are exactly analogous to those reported by Lunk and Youngman (10),

The results of the decomposition of organochromium cations in the presence of acid or oxidizing agents are given in Table 17. The reactions which produced the polymeric product were totally unexpected. The reactions of $\text{CrCH}_2\text{-C}_6\text{H}_4\text{-CH}_2\text{OH}^{2+}$ may represent genuine chemistry, but the rapid decomposition of the precursor bromide may indicate that the decomposition is due to impurities. In the case of $\text{CrCH}_2\text{-C}_6\text{H}_4\text{-CH}_2\text{Br}^{2+}$, the compound was isolated in pure form and so its decomposition represents new chemistry. The $\text{CrCH}_2\text{-C}_6\text{H}_4\text{-C}_6\text{H}_4^{2+}$ reacted very much as a normal organochromium cation, and so exhibited no new chemistry.

Table 17. The decomposition products of organochromium cations

Organochromium	Attacking Species	Nature of Product	Product
$\text{CrCH}_2\text{-C}_6\text{H}_4\text{-CH}_2\text{OH}^{2+}$	$\text{Fe}^{3+}/\text{Cu}^{2+}/\text{H}^+$	Polymeric	$\text{-(CH}_2\text{-C}_6\text{H}_4\text{-CH}_2\text{)}_n$
$\text{CrCH}_2\text{-C}_6\text{H}_4\text{-C}_6\text{H}_4^{2+}$	$\text{Fe}^{3+}/\text{Cu}^{2+}$	Monomeric	$\text{HOCH}_2\text{-C}_6\text{H}_4\text{-C}_6\text{H}_4^{\text{a}}$
$\text{CrCH}_2\text{-C}_6\text{H}_3(\text{CH}_2\text{Br})^{2+}$	$\text{Fe}^{3+}/\text{Cu}^{2+}$	Polymeric	$\text{-(CH}_2\text{-C}_6\text{H}_3(\text{CH}_2)\text{)}_n \text{ (?) }^{\text{b}}$

^aSee section on isolation of organic products.

^bAssumed to be this material, but not conclusively proved.

DISCUSSION

The synthesis of the organodichromium cations proceeded much the same as the organochromium cations. The cations were all yellow colored and highly charged. The high charge on the cations necessitated the use of weakly binding ion-exchange resin. Sephadex SP-C25 resin allowed these species to be eluted with 0.1 M HClO_4 /0.9 M NaClO_4 which proved to be reasonable conditions. The organodichromium cations were eluted after Cr^{3+} and before any Cr(III) dimer, $[\text{Cr}(\text{OH})_2\text{Cr}]^{4+}$ (47). This is certainly very consistent with the organodichromium compounds having a 4+ charge. The resin proved ideal for separating unreacted Cr^{2+} and oxidation product Cr^{3+} from organodichromium cations as well as Cr(III) dimers. Cr^{2+} and Cr^{3+} were eluted with 0.1-0.2 M NaClO_4 under which condition the 4+ species of interest did not move. When the ionic strength was increased by eluting with 0.1 M HClO_4 /0.9 M NaClO_4 , the organodichromium cations were removed from the column. When the ionic strength was again increased to 2.0-2.5 M NaClO_4 , finally the Cr(III) dimer came off the column. In addition to the resin separating the cations of interest, it also protected these cations from decomposition. Significant decomposition of these organodichromium cations occurred within 1-2 hours in septum-covered bottles in the absence of excess Cr^{2+} . The resin protected these cations so that they were stable for 1-2 days. This proved extremely

helpful when trying to store the cations for use in successive, slow decomposition kinetic runs.

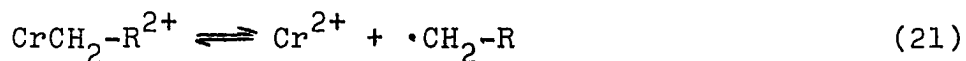
The one product which appears in the balanced equation but has not yet been mentioned is CrBr^{2+} . This was the first product, but from our work did not appear to survive the reaction conditions. Adin, Doyle, and Sykes have thoroughly studied this reaction and shown the rate law to follow equation 20 (48). In this rate law the values of the k 's are

$$\frac{-d[\text{CrBr}^{2+}]}{dt} = (k_1 + k_2/[\text{H}^+] + \frac{k'[\text{Cr}^{2+}]}{[\text{H}^+]})[\text{CrBr}^{2+}] \quad (20)$$

given as $k_1 = 9.0 \times 10^{-6} \text{ s}^{-1}$ and $k_2 = 1.14 \times 10^{-6} \text{ M}^{-1} \text{ s}^{-1}$ ($30^\circ\text{C } \mu = 2.0 \text{ M}$) and $k' = 1.74 \times 10^{-3} \text{ s}^{-1}$ ($25^\circ\text{C } \mu = 1.0 \text{ M}$) (48). This clearly points to the fact that the Cr^{2+} catalyzed path is the most important one under most conditions. In order to prevent this aquation reaction, it is necessary to perform the reaction at high $[\text{H}^+]$ and low $[\text{Cr}^{2+}]$. When runs were performed at $1.0 \text{ M } \text{H}^+$ and with exactly stoichiometric amounts of Cr^{2+} , the solution turned green instead of yellow. The CrBr^{2+} was separated by ion-exchange chromatography and analyzed by its visible spectrum [λ 622 nm ($\epsilon = 19.9$), λ 432 nm ($\epsilon = 22.4$)]. Under the conditions given, it was possible to isolate 75-80% of the theoretical CrBr^{2+} . This again lends proof that the reaction proceeds as indicated in the balanced equation.

Most all of the yellow organodichromium cations had strong absorption maxima between 355-360 nm. The sole exception was $\text{CrCH}_2\text{-}\langle\text{C}_6\text{H}_4\text{-C}_6\text{H}_4\text{-CH}_2\text{Cr}^{4+}$ which exhibited a maximum at λ 330 nm. The normal organodichromium compounds also exhibited two additional peaks in the ultraviolet region around 300 nm and 265 nm. These values compare very favorably with the values for benzyl-chromium [λ 356 nm ($\epsilon = 2200$), λ 295 nm ($\epsilon = 6970$), and λ 273 nm ($\epsilon = 7670$)] (9). Based on the spectra, it is concluded that the normal organodichromium cations should be very similar to organochromium cations such as benzyl-chromium.

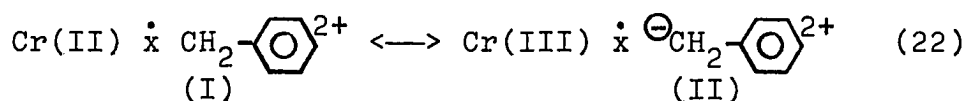
The unusual organodichromium cation had different chemistry as well as a unique spectrum. It was the only highly unstable organodichromium cation which was studied. It was so unstable that it totally decomposed within two minutes after eluting it from the ion-exchange column. The only means available to study it was by adding small amounts of Cr^{2+} to the solution. This presumably helped stabilize the cation by forcing the homolysis seen in equation 21 far



to the left and thereby suppressing the decomposition of the radicals. This stabilizing effect of Cr^{2+} is general to all organodichromium compounds studied as well as benzyl-chromium. When $\text{CrCH}_2\text{-}\langle\text{C}_6\text{H}_4\text{-C}_6\text{H}_4\text{-CH}_2\text{Cr}^{4+}$ and small amounts of Cr^{2+} were

decomposed by excess Fe^{3+} or $\text{Co}(\text{NH}_3)_5\text{Cl}^{2+}$, the rate of the decomposition was almost an order of magnitude faster than the other organodichromium cations. The fast reaction plus the copious quantities of polymer made it impossible to exactly quantify the results.

The kinetic and spectral observations can be rationalized by viewing the two resonance structures shown in equation 22.



The structures are drawn to stress the importance of the location of the charge within the structure. For the sake of simplicity, the structures and explanation are given for the case of a mono-organochromium cation, but the same arguments can be applied to each of the two sites in the case of organodichromium cations. The majority of the known chemistry of benzyl-chromium is by the homolysis pathway (9) and so proceeds by reaction of I. Thus, groups which tend to stabilize I relative to II lead to compounds which decompose readily by homolytic pathways. Precisely this effect is seen in Figure 44 which is a reproduction of work by Nohr and Espenson (9). Electron-withdrawing substituents stabilize structure II relative to I and so undergo homolysis at a slower rate than electron-donating substituents.

This same sort of argument can be applied to the spectral data. Kochi and Davis (2) have pointed out the

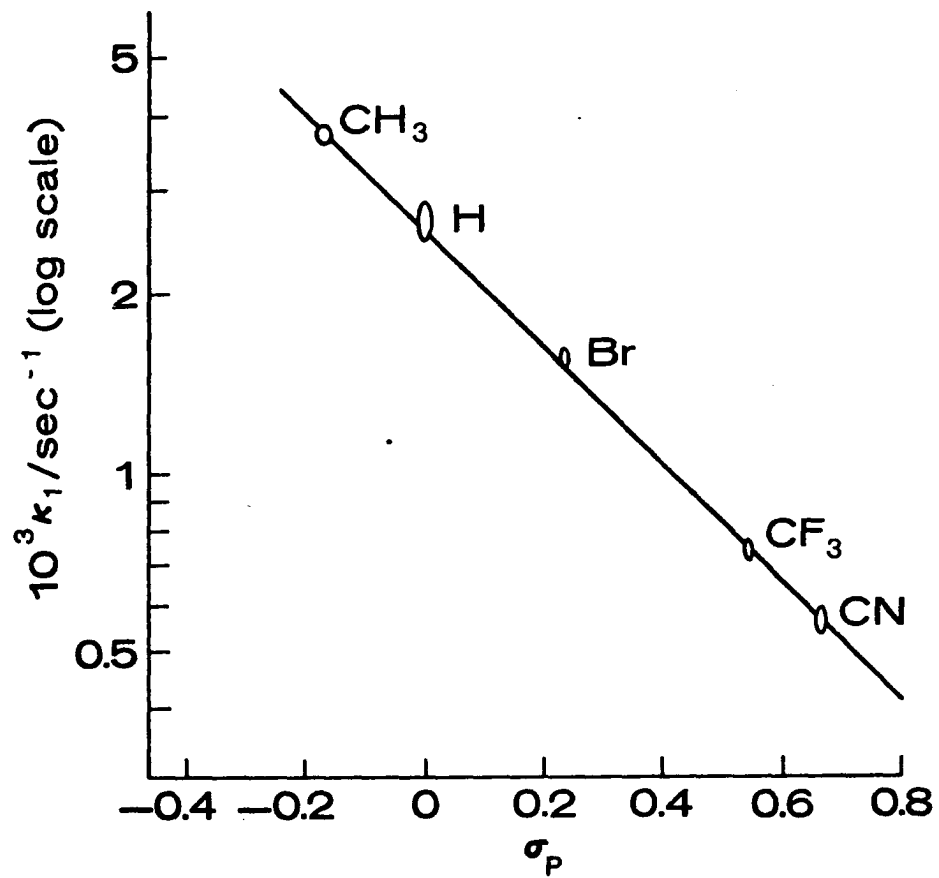
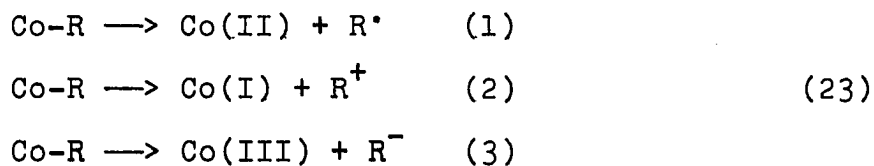


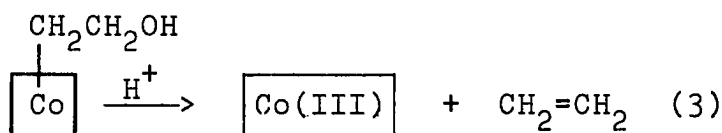
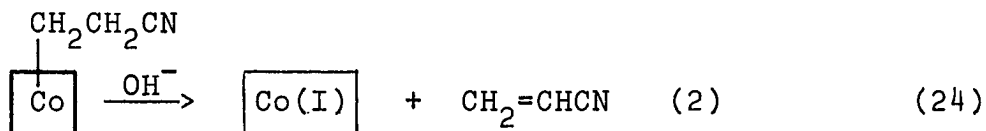
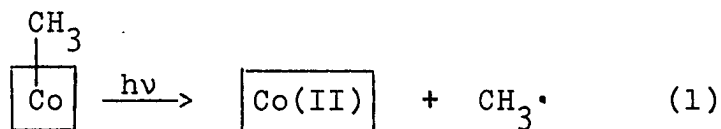
Figure 44. A plot of k_1 versus σ_p for the decomposition of substituted benzyl-chromium cation and oxidizing agents

close resemblance of the spectra of benzyl radicals in rigid glass to those of benzyl-chromium cations. This again shows the importance of structure I to the chemistry of the cation. In addition, they attributed the bands at 360-270 nm to charge transfer transitions. Since the carbon has no π electrons to donate to the metal, it appears logical to call these metal-to-ligand charge transfer bands. This assignment would closely parallel the change in going from structure I to II. Since the absorbance for most organodichromium compounds was at lower energy (longer wavelength) than that for $\text{CrCH}_2\text{-}\langle\text{C}_6\text{H}_4\text{-}\langle\text{C}_6\text{H}_4\text{-}\text{CH}_2\text{Cr}^{4+}$, this implies a greater ease of electron transfer to the ligand. This corresponds to a greater contribution by structure II which is the stable form. As a result, the "normal" organodichromium cations exhibited greater stability to homolysis (49,50).

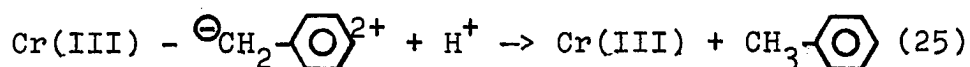
This explanation fits the observed data, but support for these proposed structures is required. A close analogy to this is the work done on alkylcobalamines. Abeles and Dolphin (51) explained the various reactivity patterns of these compounds by use of the scheme shown as equation 23.



They lend support for such mechanisms through the reactions outlined in equation 24. These authors propose these simply

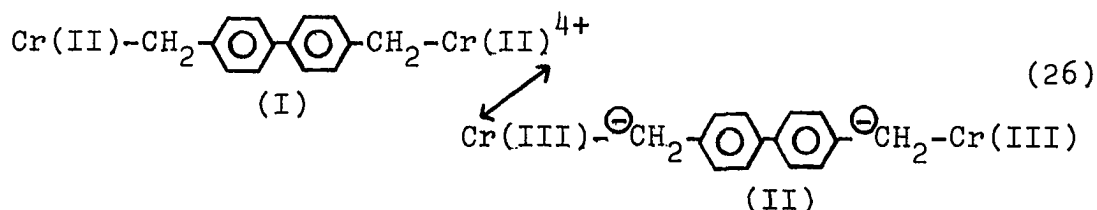


as routes of reaction for the alkylcobalamines, but they can also be used to describe resonance structures for the compounds themselves. In the case of benzyl-chromium cations, pathway (2) can be eliminated due to the low probability of forming Cr(I). Thus, paths (1) and (3) should be able to explain all of the observed chemistry of benzyl-chromium. From known results (9), it appears that the largest part of the chemistry is by path (1). One case which has not been clearly explained by the homolysis pathway is the acidolysis. The kinetics of this reaction have proved elusive (8) as well as a satisfactory explanation for the preponderance of the product toluene over bibenzyl (9). Both of these results can be explained by a path exactly like (3). This is seen in equation 25. The explanation for the observed products is



that since H^+ does not react rapidly with either Cr^{2+} or $\text{C}_6\text{H}_5\text{-CH}_2^{\cdot}$, the homolysis path (1) is shut off and so the majority of the reaction is through pathway (3). The lack of simple kinetics is explained by the competition between pathways which is very sensitive to conditions such as $[H^+]$, buffer used, and temperature.

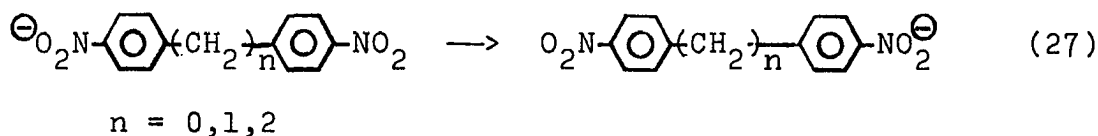
All results for benzyl-chromium seem consistent with the proposed explanation, but it still remains to apply it to the case of organodichromium cations. The simplest way of analyzing this is to examine the series which contain $n = 0,1,2$ methylene groups. For the case $n = 0$, the two benzene rings should be very close to coplanar if biphenyl itself serves as a good model (52,53). This implies good resonance communication between the two extreme ends of the rings. The applicable resonance structures are shown in equation 26. This represents the effects of both chromium



atoms attempting to donate electron density to the organic portion of the molecule. As one chromium donates electron density to the methylene carbon, the increase in density is felt at the opposite end of the other ring. This forces electron density onto the second chromium which produces

Cr(I). This is extremely unstable and so it donates electron density back to chromium number one. This sort of a synergistic effect makes it difficult for either site to donate very much electron density. As a result, structure I predominates and so homolytic cleavage is a rapid process.

In the cases of $n = 1$ and $n = 2$, there are methylene groups between the two benzene rings preventing them from being in conjugation. This acts to isolate the sites from one another's influence, and so they behave like benzylchromium. This same effect was investigated by Harriman and Maki (54) for slightly different reactions. They studied the movement of an electron from one end of the molecule to the other as illustrated in equation 27. They prepared the



anion by electrochemical procedures and then studied the movement by ESR. Their results indicated most rapid movement for $n = 0$ and least for the case of $n = 2$. This again indicates maximum communication between ends for $n = 0$ just as we see in our case. This all fits the scheme until the case $\text{CrCH}_2-\text{C}_6\text{H}_4-\text{CH}_2\text{Cr}^{4+}$ is examined. This example is well suited to resonance communication between sites, but yet it behaves just like the "normal" organodichromium cations. It has a normal electronic spectrum and reacts with oxidizing

agents at the usual rate. There is clearly no sign of communication and so it behaves as do most other organodichromium carbons.

Additional evidence supporting the formulation of the organodichromium cations as two isolated benzyl-chromium sites comes from the determination of ϵ values. These values are seen in Table 14 and are typically 4500-5000. These values are very close to twice the value for benzyl-chromium (2400). The comparison is even more strongly supported when

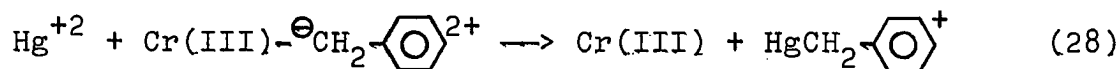
comparing $\text{CrCH}_2\text{-C}_6\text{H}_4\text{-CH}_2\text{Cr}^{4+}$ with $\text{CrCH}_2\text{-C}_6\text{H}_4\text{-CH}_2\text{Br}^{2+}$. The

respective values (4426 and 2186) are within experimental error in a ratio of 2:1. These facts strongly support the effect of two carbon-chromium bonds to be the sum of the effect of two benzyl-chromium cations. In other words, the two sites are independent of each other.

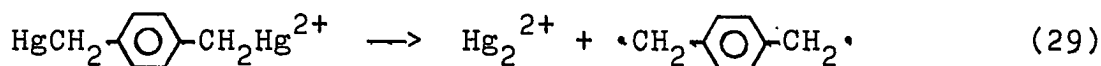
All of the data presented are consistent with the formulations of the structures, but do not prove them. The most conclusive evidence would be a structural determination of a single crystal by X-ray diffraction techniques. This approach proved futile for benzyl-chromium due to decomposition (55), and so it was not attempted for the organodichromium cations. The next most obvious method of proving the structure is to compare the products of reaction for benzyl-chromium with those observed for the organodichromium

cations. As Coombes, Johnson and Winterton have demonstrated (56), similar products imply similar starting materials. This approach has been adopted for several different reagents, and the results will be presented in detail.

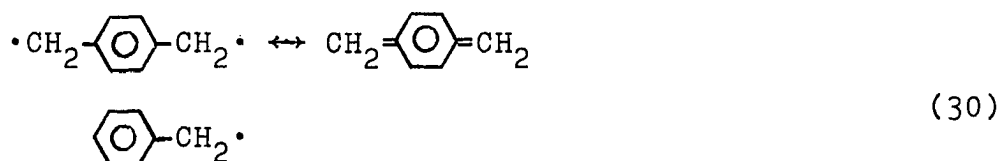
The first reaction is that of Hg^{+2} with the carbon-chromium bonds. This reaction has been extensively studied (26,57) and shown to proceed via an SE2 mechanism. The rate of the reaction is generally fast and the isolated products are alkyl- Hg^+ and Cr^{3+} . This reaction is well-described by pathway (3) as shown below in equation 28. In the case of



the organodichromium cations, the reaction proceeded instantly and produced Cr^{3+} and a white precipitate. Isolation and purification of the white material indicated it to be a mixture of compounds. The first is a white Hg_2^{+2} salt and the other a polymeric type of material. Evidently the organodimercurials were formed initially, but decomposed prior to isolation. The decomposition obviously represents a homolysis of the mercury-carbon bond in much the same manner as the SH1 homolysis of the chromium-carbon bond. This is represented schematically in equation 29. This sort

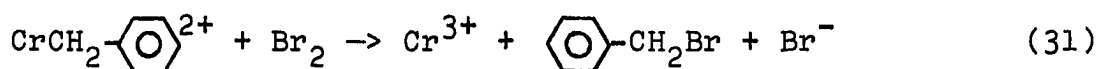


of the reaction is not surprising in light of the weak mercury-carbon bond (50-200 kJ/mole) (58) which exists in these types of compounds. This homolytic type of reaction has been seen in the case of dibenzyl-mercury (59), but either thermolysis or photolysis are required to allow the reaction to proceed at a measurable rate. In the present examples a biradical will be produced which would promote stability relative to the case where the benzyl radical is produced. The added stability shown in equation 30 will

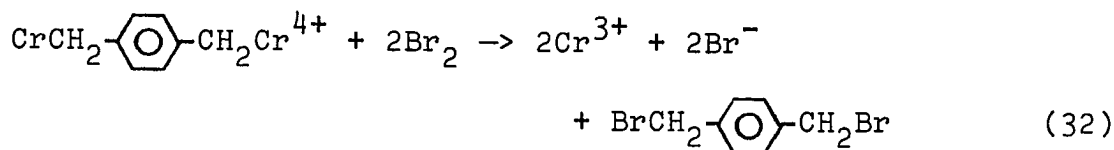


lead to greater ease of homolysis. In the example where substitution is meta instead of para, $\text{CrCH}_2-\text{C}_6\text{H}_3(\text{CH}_2\text{Cr}^{4+})$, the desired organodimercurial was stable and could be isolated and analyzed. The isolation of this dimercurial provides strong proof for the proposed structure of the precursor organodichromium cation.

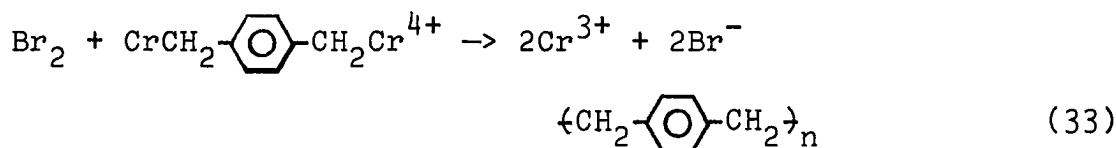
The reaction with other electrophiles (60) was attempted but only polymeric products were obtained. The most interesting was the reaction of bromine with the organochromium cations. This reaction proceeded according to equation 31



for benzyl-chromium (61). If this reaction proceeded via a similar mechanism for the organodichromium cations, the reaction would follow equation 32. This represents production of

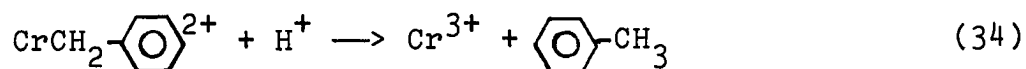


the dibromide which was originally reacted with Cr^{2+} . The experiments have shown that the actual product is polymeric, presumably poly-p-xylylene in this case. This obviously implies a different type of reaction in these cases. A balanced equation which describes the products is shown in equation 33. Since the reaction did not proceed in a manner



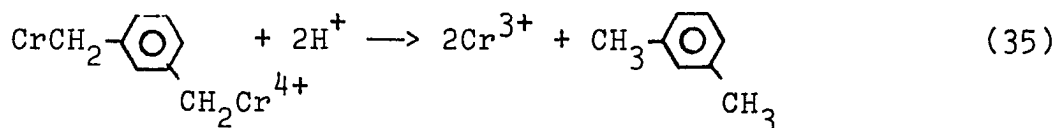
analogous to benzyl-chromium, the reaction was not studied in any detail. The reaction did not produce any simple organic products and so did not support the proposed structures.

Another potential electrophile, H^+ , was also investigated. In the case of benzyl-chromium, the reaction is represented in equation 34. The product is a simple organic

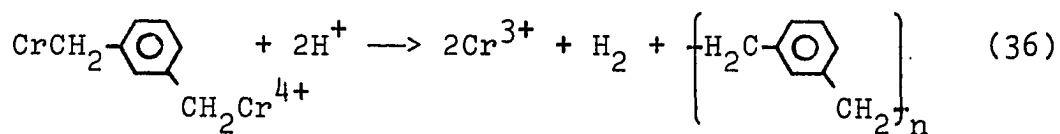


compound which can be easily isolated and identified. In the case of the organodichromium cations, the anticipated

product is presented in equation 35. The anticipated product, m-xylene, was never detected, but instead poly-m



xylylene was isolated (Table 16). In these cases, a balanced equation is presented in equation 36. It is difficult to



envision the proton simply undergoing one electron reduction, but this seems the best way to explain the observed products. This is another case where there is a substantial difference in the chemistry of the organodichromium cations relative to benzyl-chromium. The results with the weaker electrophiles suggest very little contribution of structure I to the structure of the organodichromium cations.

Another series of reactions which were investigated was the reaction with oxidizing agents. The products of the reaction with benzyl-chromium are given in Table 18 (9). An analogous table of the anticipated products of the reaction of $\text{CrCH}_2\text{-}\langle\text{O}\rangle\text{-CH}_2\text{Cr}^{4+}$ is listed as Table 19. The observed products in the case of the organodichromium cations were polymer, in this case poly-p-xylylene. This result agrees very well with the chemistry expected for $\text{Co}(\text{NH}_3)_5\text{Cl}^{2+}$. This

Table 18. The organic products of the reaction of benzyl-chromium and oxidizing agents

Organochromium	Oxidant	Observed organic Product
$\text{CrCH}_2\text{-C}_6\text{H}_5^{2+}$	$\text{Cu}^{2+}/\text{Fe}^{3+}$	$\text{C}_6\text{H}_5\text{-CH}_2\text{OH}$
$\text{CrCH}_2\text{-C}_6\text{H}_5^{2+}$	O_2	$\text{C}_6\text{H}_5\text{-C(=O)H}$
$\text{CrCH}_2\text{-C}_6\text{H}_5^{2+}$	$\text{Co}(\text{NH}_3)_5\text{Cl}^{2+}$	$\text{C}_6\text{H}_5\text{-CH}_2\text{-CH}_2\text{-C}_6\text{H}_5$

Table 19. The anticipated organic products of the reaction of $\text{CrCH}_2\text{-C}_6\text{H}_4\text{-CH}_2\text{Cr}^{4+}$ and oxidizing agents

Organodichromium	Oxidant	Anticipated Organic Product
$\text{CrCH}_2\text{-C}_6\text{H}_4\text{-CH}_2\text{Cr}^{4+}$	$\text{Cu}^{2+}/\text{Fe}^{3+}$	$\text{HOCH}_2\text{-C}_6\text{H}_4\text{-CH}_2\text{OH}$
$\text{CrCH}_2\text{-C}_6\text{H}_4\text{-CH}_2\text{Cr}^{4+}$	O_2	$\text{HC(=O)-C}_6\text{H}_4\text{-C(=O)-H}$
$\text{CrCH}_2\text{-C}_6\text{H}_4\text{-CH}_2\text{Cr}^{4+}$	$\text{Co(NH}_3)_5\text{Cl}^{2+}$	$\text{(CH}_2\text{-C}_6\text{H}_4\text{-CH}_2\text{)}_n$

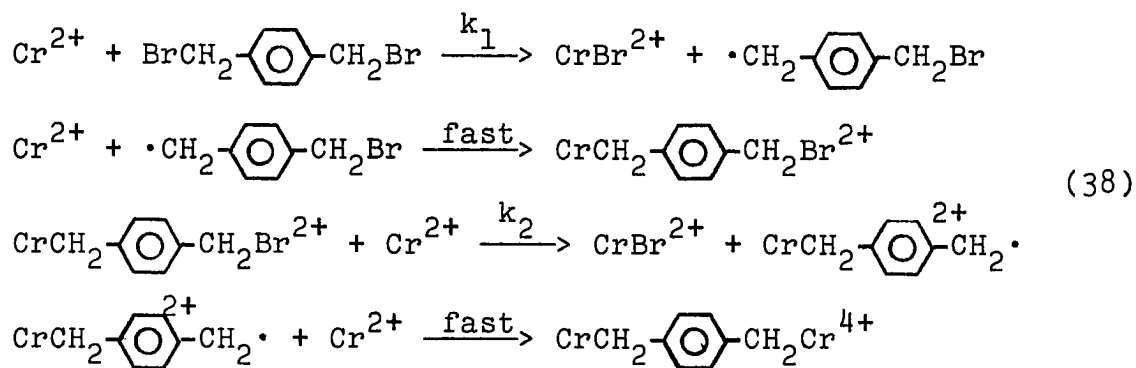
The proposed mechanism can also be attacked from the point of view of reasonable chemistry. The first step which is rate limiting is the homolysis of a carbon-chromium bond. This chemistry is precisely analogous to that seen in benzyl-chromium (9) and the kinetics are comparable to those for benzyl-chromium. The rapid reaction of Cr^{2+} with the oxidants is well known from the literature (62) and is essential to the kinetics arguments presented for benzyl-chromium (9). The last step is the homolysis of a second carbon-chromium bond. This may again be compared to the case of benzyl-chromium except for the fact that there is also a radical center in the same molecule. In the case cited, the diradical product formed is known to be stable at low temperatures (63). Thus, it does not seem unrealistic to call the step rapid and claim that the diradical can survive in the presence of oxidizing agents long enough to encounter another molecule of itself and thus begin polymerization. In the general case, however, the diradical is not stabilized and so further explanation is required. The reaction can be viewed as replacing a chromium-carbon σ bond with a carbon-carbon π bond (each radical end contributes 1/2 of a π bond). Since the carbon-chromium bond is not very stable, it does not seem unreasonable to assume that the carbon-carbon π bond is more stable. This again falls into the pitfall of using thermodynamics to explain

kinetic results, but at least it makes it seem reasonable. More on the mechanism will be mentioned under the kinetics section.

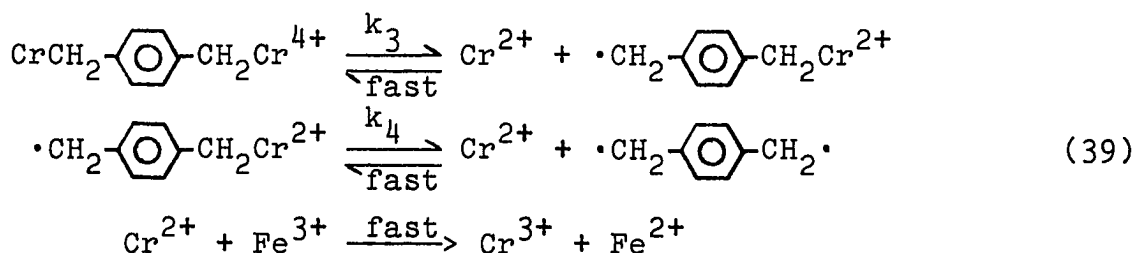
None of the reactions mentioned thus far lend much support for the proposed structures of the organodichromium cations. The base decomposition with Na_2CO_3 proved to be the one area where the chemistry of the organodichromium cations paralleled that of benzyl-chromium. As is seen in Table 3, most of the organodichromium cations decomposed to the corresponding hydrocarbons in high yield. The same was also true for the substituted benzyl-chromium cations. The two which did not produce hydrocarbons were $\text{CrCH}_2\text{-C}_6\text{H}_4\text{-CH}_2\text{Cr}^{4+}$ and $\text{CrCH}_2\text{-C}_6\text{H}_3(\text{CH}_2\text{Cr}^{4+})$. They both produced the corresponding polymer. In the latter case this was not disappointing because the organodimercurial proved its structure without a doubt. In the former case, however, it was the last attempt at obtaining an identifiable derivative. All the evidence for its structure rests upon its favorable comparison with these other well-characterized organodichromium cations.

The kinetics of the formation and decomposition reaction of the organodichromium cations were investigated. Initial work on both types of reaction indicated single-stage kinetics. This observations was surprising in light of the

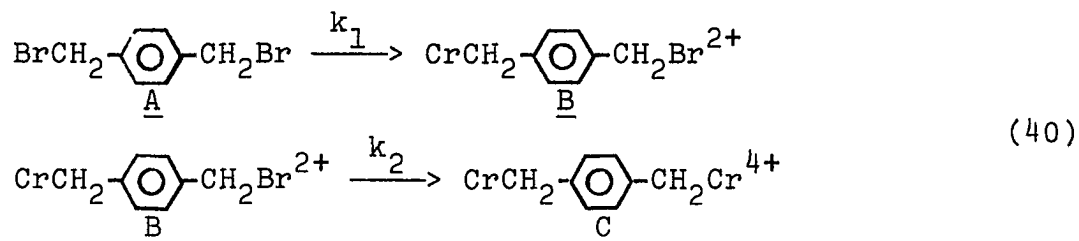
fact that both molecules had two sites at which to react (two bromides for the formation reaction and two chromiums for the decomposition reaction). This led us to further investigate both reactions. The formation scheme is shown as equation 38. The decomposition scheme is presented in



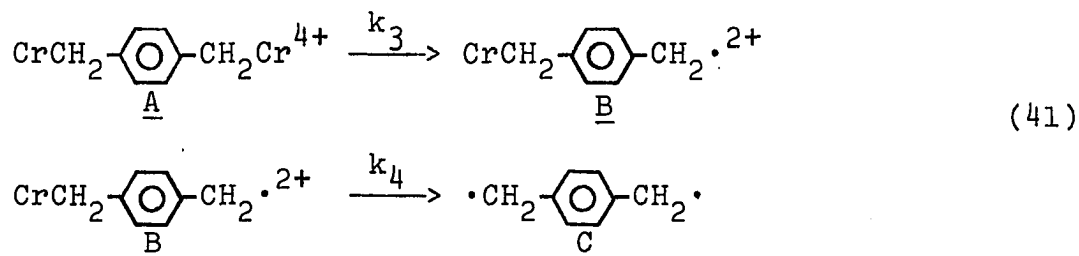
equation 39. Both of these schemes can be simplified to A→B→C when certain factors are taken into consideration.



In the case of the formation kinetics, Cr^{2+} is added in large excess and the kinetics simplify to the pseudo-first-order case. In addition, kinetics studies only slow steps and so the fast steps can be combined to form the scheme shown in equation 40. In the case of the decomposition reaction,



Fe^{3+} is used in large excess so that the back reaction of the two equilibria are effectively stopped. In addition, Fe^{3+} is in such large excess that its concentration does not change during the course of the reaction. Finally, Cr^{3+} has such a low extinction coefficient that it does not effect the absorbance. The final reaction scheme is shown in equation 41. These two equations will serve as the basis for the kinetics analysis which follows.



Chipperfield (64) in the process of following up on work by Buckingham, Francis and Sargeson (65) has done a thorough study of $A \rightarrow B \rightarrow C$. The author has shown that there are four distinct cases when $A \rightarrow B \rightarrow C$ will produce single-stage kinetics. These correspond to the four different ways one of the terms of the general equation shown as equation 42

$$D_t - D_\infty = \alpha e^{-k_1 t} + \beta e^{-k_2 t}
 \tag{42}$$

can vanish. The conditions are (a) $k_1 \ll k_2$, (b) $k_2 \ll k_1$,

(c) $\epsilon_B = \epsilon_C$, or (d) $k_2/k_1 = \frac{\epsilon_B - \epsilon_A}{\epsilon_C - \epsilon_A}$. Conditions a and b can be

explained by looking at the general equation. As k_2 becomes very large, $e^{-k_2 t}$ becomes very small and so $\beta e^{-k_2 t}$ disappears. The opposite is true if k_1 becomes very large.

Thus, (a) or (b) produce single-stage kinetics. Condition (c) can only be understood by examining the complete equation shown as equation 43. Under condition (c), $\epsilon_C = \epsilon_B$

$$D_t - D_\infty = \alpha e^{-k_1 t} + \beta e^{-k_2 t} \quad (43)$$

$$\alpha = \frac{(\epsilon_A - \epsilon_C)k_2 + (\epsilon_B - \epsilon_A)k_1}{k_2 - k_1} [A]_0 \quad \beta = \frac{(\epsilon_C - \epsilon_B)k_1}{k_2 - k_1} [A]_0$$

and this makes $\beta=0$ which means the second term disappears. This is intuitively correct because if a reaction proceeds without a change in absorbance ($\epsilon_C = \epsilon_B$) you cannot determine it spectrophotometrically. This is the case here because you can follow k_1 but not k_2 . The last case, (d), is easily derived by setting $\alpha=0$ and solving for k_2/k_1 . This case will correspond to the situation where the k which is determined will correspond to k_2 . There are obviously many situations which can meet the conditions of case (d). These will be addressed separately.

Two of the most interesting cases fall under the heading of statistical kinetics. The first case is the situation

beginning with a nonabsorbing reactant. This case has been adequately covered by Chipperfield (64) and corresponds to $k_1 = 2k_2$ and $\epsilon_C = 2\epsilon_B$, $\epsilon_A = 0$. The substitution of $\epsilon_A = 0$ causes case (d) to break down to $k_2/k_1 = \epsilon_B/\epsilon_C$. Multiplication and rearrangement of the symbols as shown in equation 44 leads

$$\begin{aligned} k_1 &= 2k_2 & \epsilon_C &= 2\epsilon_B \\ 2k_2\epsilon_C &= 2k_1\epsilon_B & & \\ k_2/k_1 &= \epsilon_B/\epsilon_C & & \end{aligned} \quad (44)$$

to the same conditions. As a result, the statistical formation kinetics are a sub-set of condition (d). This case will be satisfied if the two sites available for attack in A do not interact. If this condition is met, then A has twice as many reactive sites as B and so due to statistics, $k_1 = 2k_2$. Since the sites cannot interact, C has twice as many absorbing sites and so $\epsilon_C = 2\epsilon_B$. Thus, this case may have chemical significance in certain cases.

The second case, the decomposition kinetics under statistical conditions, is new and will be covered in detail. This case corresponds to the case $\epsilon_A = 2\epsilon_B$, $\epsilon_C = 0$, and $k_1 = 2k_2$. The expression of case (d) when $\epsilon_C = 0$ is $k_2/k_1 = \epsilon_A - \epsilon_B / \epsilon_A$. Applying the statistical conditions and using the appropriate mathematical operations, it can be shown that this is the correct equation. This is done in equation 45. This again shows that this is a sub-set of

$$\begin{aligned}
\varepsilon_C &= 2\varepsilon_B & k_1 &= 2k_2 \\
2\varepsilon_B k_1 &= 2\varepsilon_A k_2 \\
\frac{k_1 \varepsilon_A}{2} &= k_2 \varepsilon_A & & (45) \\
\frac{k_1}{2} (\varepsilon_A - \varepsilon_B) &= k_2 \varepsilon_A - \frac{k_2 \varepsilon_A}{2} \\
k_1 (\varepsilon_A - \varepsilon_B) &= k_2 \varepsilon_A \\
\frac{k_2}{k_1} &= \frac{\varepsilon_A - \varepsilon_B}{\varepsilon_A}
\end{aligned}$$

case (d). The chemistry would again correspond to an example of 2 noninteracting sites. In this situation, A has two and B one site, so $k_1 = 2k_2$ and $\varepsilon_A = 2\varepsilon_B$. Thus, this may also be a chemically significant example.

Chipperfield (64) has taken case (d) and thoroughly developed all of the possible situations for the formation reaction. Since the kinetics of the formation reaction were not particularly useful, the kinetic analysis will be limited to decomposition cases. Chipperfield presents his data in the form of a graph which is shown in Figure 45. There are several aspects of this which require explanation before presenting new results. The primary focus of interest is the dotted line of slope one. This represents the case where $k_2/k_1 = \varepsilon_B/\varepsilon_C$. The hatched lines represent the boundaries beyond which one should begin to see two-stage kinetics. The first point is that the dotted line goes through the

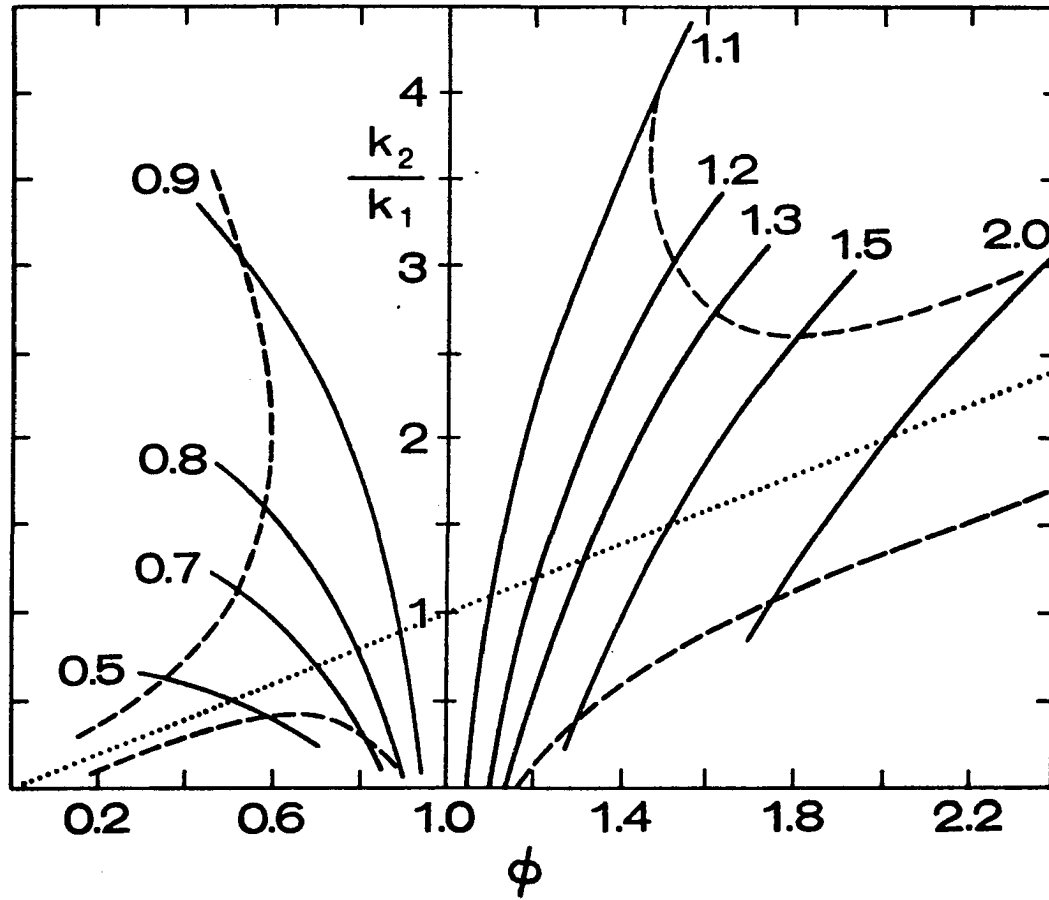


Figure 45. A plot of k_2/k_1 versus ϕ where $\phi = \epsilon_B/\epsilon_C$

statistical point ($k_2/k_1 = 2$, $\epsilon_B/\epsilon_C = 2$) as it must. Next is that the hatched lines open up near $\epsilon_B/\epsilon_C = 1$. This is caused by case (c) which says that if $\epsilon_B = \epsilon_C$ single-stage kinetics will be seen regardless of the value of k_1 and k_2 . Finally, as the extremes in the values of ϵ_B/ϵ_C are reached, there are extremely tightly defined values of k_2/k_1 which produce single stage kinetics.

This analysis can be applied to the decomposition kinetics simply by setting $\phi = \epsilon_B/\epsilon_A$. For the case of statistical kinetics with A being the most strongly absorbing species, the only area of concern is the left half of the graph. As the analog computer results showed, the dotted line must contain the point $k_2/k_1 = 0.5$, $\epsilon_B/\epsilon_A = 0.5$ and it does. The second point is the variations permitted in k_2/k_1 and ϵ_B/ϵ_A while maintaining single stage kinetics. The analog computer results suggested that small variations of k_2/k_1 from 0.5 quickly exhibited two-stage kinetics while larger variations in ϵ_A/ϵ_B were permitted before two-stage kinetics were seen. This is exhibited in the graph by beginning at the point 0.5, 0.5 and moving vertically up or down. One crosses the hatched lines quickly indicating that small variations in k_2/k_1 quickly lead to two-stage kinetics. On the other hand in moving horizontally from left to right there is a considerable distance to be covered before the hatched lines are crossed. This points to a

great deal of flexibility in the values of ϵ_B/ϵ_A which produce single-stage kinetics. Thus, the theoretical analysis and the analog computer point to the same conclusions. Both methods indicate a large number of cases near the statistical cases of general case (d) which do not meet the strict conditions of case (d) but will in practice produce single-stage kinetics. These conclusions will be important to remember when considering actual kinetic data.

The kinetics of the formation reaction was studied with very little success. Runs done on the same solution were not at all reproducible. Some runs showed single-stage kinetics while others showed two-stage kinetics. In addition, runs at different wavelengths produced very different values for the rate constant. The source of the problem appeared to be erratic D_∞ values. These varied by as much as 0.2-0.3 absorbance units from run to run with the same solutions. Due to these drastic problems, no specific comments can be made, but several general conclusions can be reached. First, most of the organodichromium cations were formed at nearly the same rate as benzyl-chromium. There were two exceptions $\text{CrCH}_2\text{-C}_6\text{H}_4\text{-CH}_2\text{Cr}^{4+}$ and $\text{CrCH}_2\text{-C}_6\text{H}_3(\text{CH}_2\text{Cr}^{4+})$.

They were formed at significantly slower rates than the other examples. In the former case, no intermediate could be isolated implying that either $k_2 \gg k_1$ or that the

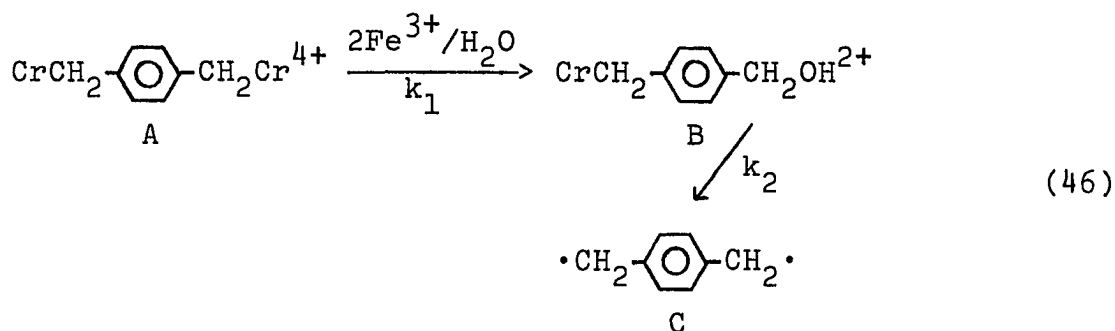
intermediate $\text{CrCH}_2\text{-}\langle\bigcirc\rangle\text{-CH}_2\text{Br}^{2+}$ decomposed by an alternative route so that it could not be isolated. In the latter case, $\text{CrCH}_2\text{-}\langle\bigcirc\rangle\text{-CH}_2\text{Br}^{2+}$ could be isolated thereby showing that

this case must have two-stage kinetics. These varying results, with two very similar organodichromium cations, made data interpretation even more suspect, and so the formation reactions were not further studied.

The kinetics of the decomposition reactions with oxidizing agents proved to be much more straightforward. In all cases single-stage kinetics were observed. Since the reactions studied could be broken down into $A \rightarrow B \rightarrow C$, there were only four kinetic possibilities (64). These were (a) $k_2 \gg k_1$, (b) $k_1 \gg k_2$, (c) $\epsilon_B = \epsilon_C$, (d) $\epsilon_A/\epsilon_B = 2.0$ and $k_1/k_2 = 2.0$. Case (b) does not seem reasonable for a rate constant of $\sim 10^{-3} \text{ s}^{-1}$. Case (b) would imply that organodichromium cations could not be studied because one of the chromium-carbon bonds would quickly break. When the oxidizing agent was added, there should have been a sudden decrease in absorbance due to the loss of one of the carbon-chromium bonds. In reality this sort of effect was never seen, and so this possibility was eliminated. Case (c) corresponds to the case where $\epsilon_B = \epsilon_C$, and since all products are known not to absorb ($\epsilon_C = 0$), $\epsilon_B = 0$. Any intermediate designed as B will contain one carbon-chromium bond. This

type of bond always absorbs around 360 nm, and so it does not seem reasonable to consider $\epsilon_B = 0$.

This leaves case (d) and (a) to be considered, and since they are very different they will be discussed separately. Case (d), the statistical case, can be represented as shown in equation 46. In this case, B is



a stable compound which should be stable and thus easy to study. For case (d) to hold $k_1 = 2k_2$ and $\epsilon_A = 2\epsilon_B$. It does not seem unreasonable that the two sites in A react twice as fast as B. In addition, Table 14 clearly shows that ϵ for organodichromium cations is twice that for organochromium cations. With this in mind $\text{CrCH}_2\text{-}\langle\bigcirc\rangle\text{-CH}_2\text{OH}^{2+}$ was synthesized and studied. From Table 14 $\epsilon_B/\epsilon_A = 0.46$, and from Tables 5 and 10 $k_2/k_1 = 0.67$. If these figures are inserted into Figure 44, it can clearly be seen that it falls well within the hatched line indicating single-stage kinetics. These results are all in accord with the statistical case. The mechanism does, however, predict that the intermediate should be stable and isolable. Experiments were

done with less than stoichiometric quantities of the oxidizing agent, but no 2+ species were separated. The only material seen on the ion-exchange resin was $\text{CrCH}_2\text{-C}_6\text{H}_4\text{-CH}_2\text{Cr}^{4+}$. This strongly suggests that no intermediate of any lifetime was produced. Thus, a stable species ($k_1 = 1.67 \times 10^{-3} \text{ s}^{-1}$) such as $\text{CrCH}_2\text{-C}_6\text{H}_4\text{-CH}_2\text{OH}^{2+}$ is not produced, and so case (d) is eliminated.

The final case is case (a) where $k_2 \gg k_1$. In this case the intermediate B is identified as $\text{CrCH}_2\text{-C}_6\text{H}_4\text{-CH}_2^{2+}$. This in fact has one carbon-chromium bond, but it is in reality also a radical. If it behaves as most radicals, it will rapidly react to produce products (see for example the formation reaction for benzyl-chromium). It would decompose rapidly so that no intermediate could be isolated and also so that $k_2 \gg k_1$. Thus, the kinetics seem to be most consistent with case (a) and so all discussion will center around this sort of mechanism.

The first reaction studied was that of $\text{CrCH}_2\text{-C}_6\text{H}_4\text{-CH}_2\text{Cr}^{4+}$ and the oxidizing agents seen in Table 5. All of the oxidizing agents examined with the exception of H_2O_2 reacted at the same rate within experimental error. This same observation had been made in the case of benzyl-chromium. As a matter of fact, the average for the three similar oxidants, $2.51 \times 10^{-3} \text{ s}^{-1}$, is essentially the same as the value $2.63 \times 10^{-3} \text{ s}^{-1}$ reported for benzyl-chromium (9). The

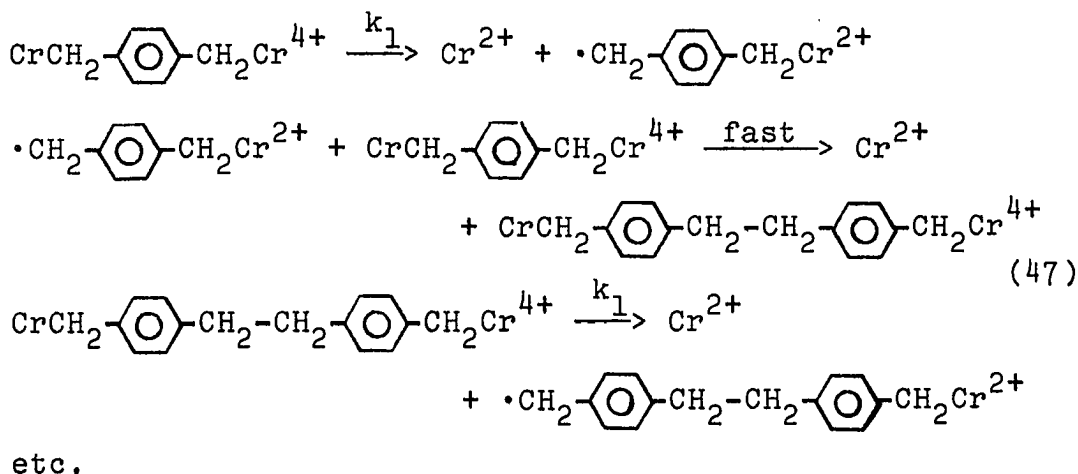
high potential for H_2O_2 , 1.776 volts, suggests that it may exhibit different chemistry than the other oxidants.

Perhaps it is strong enough to attack the chromium-carbon bond directly instead of waiting for homolysis. Whatever the chemistry involved, it is different from the other oxidants and so will not be further investigated.

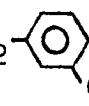
The analysis of this rate constant relative to the value $2.63 \times 10^{-3} \text{ s}^{-1}$ for benzyl-chromium will be broken into two distinct parts. The first involves the resonance and inductive effect of one $\text{CH}_2\text{-Cr}(\text{OH}_2)_5$ group para to the other. Obviously, the metal center is electropositive relative to carbon and there should be electron donation by the inductive effect. The resonance effect should involve interaction between the metal d orbitals, basically empty, and the filled π orbitals on the benzene ring. There is an intervening methylene group which should make this electron withdrawing effect only weakly felt. As a result, the inductive effect should dominate and produce a net electron-donating effect or enhancement of the rate of homolysis. The second analysis involves the effect of the two groups from a statistical point of view. Evidence has already been shown to argue for two totally independent sites. Thus, the organodichromium cations should react twice as fast as benzyl-chromium simply due to statistics. Thus, all effects considered point to the homolysis of this organodichromium

cation undergoing homolysis at a significantly higher rate than benzyl-chromium. The observed results show that the rates were essentially the same.

These results suggest the possibility of a mechanism different from the one already proposed. This explanation centers around the idea that all benzyl-chromium bonds break essentially at the same rate. Once the bond breaks, the organic radical produced then attacks a different carbon-chromium bond to liberate a second mole of Cr^{2+} . This longer organometallic can then suffer homolysis to continue the process. As the process is repeated, the organic fragment increases in length. Finally, homolysis followed by destruction of the radical by something besides the organodichromium cation would lead to the organic polymer. This sort of scheme is shown in equation 47. It is a logical way around proposing diradicals in solution, but it also has

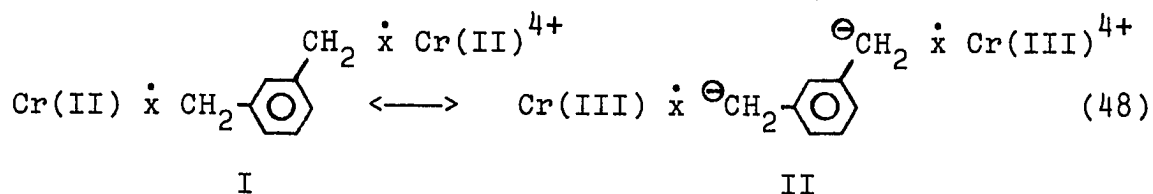


some major drawbacks. The second dichromium is a known compound which was studied. Its rate of homolysis was $\sim 3.12 \times 10^{-3} \text{ s}^{-1}$ and not 2.57×10^{-3} . While this might be rationalized as being within experimental error, it points to the fact that not all Cr-C bonds undergo homolysis at the same rate. This fact is displayed even more vividly in Figure 44. There is a factor of seven in the rate of reaction between p-methyl and p-cyano benzyl-chromium. On these grounds, this sort of mechanism seems impossible and so will be dismissed from further discussion. The explanation is that $\text{CH}_2\text{Cr}(\text{OH}_2)_5$ must be an electron-withdrawing group in the para position. Extrapolation from Figure 44 suggests a σ_p of approximately +0.31 which is very close to the value for a bromine group. The source of this effect eludes explanation, but it can be shown to exist for all the "normal" organodichromium cations. It will, therefore, be treated as an experimental observation of a poorly defined property.

The next compound studied was CrCH_2 -. The

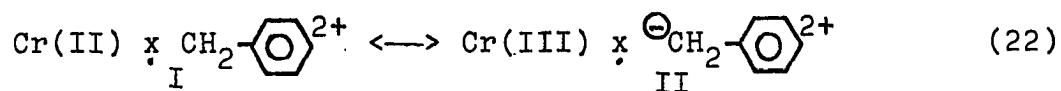
rate of decomposition was again independent of the concentration and nature of the oxidant and was equal to $2.13 \times 10^{-3} \text{ s}^{-1}$. This number is significantly lower than the value for the corresponding para isomer. An analysis of the factors effecting the kinetics again indicates a large

decelerating effect for the $\text{CH}_2\text{Cr}(\text{OH}_2)_5$ group in the meta position. This observation can be explained two different ways. One is that the effect of $\text{CH}_2\text{Cr}(\text{OH}_2)_5$ is largely inductive in nature. In the meta position, it is closer to the reactive site and so its effect is more strongly felt. This obviously requires the group to inductively remove electron density, a notion which is contrary to chemical intuition. The other explanation is that electrons are being withdrawn by the inductive effect, but being donated by resonance. In the para position, there is a strong competition between these two effects with neither dominating. In the meta position, the resonance has little effect (0.33 times the para position (66)), and so the inductive effect is felt almost completely. A possible explanation which does not involve discussing the effect of the one group on the other is the competition between the two resonance structures previously mentioned. These are shown in the case of the organodichromium cation in equation 48. The high, overall $4+$ charge causes each chromium site




to absorb more of the positive charge. Since the two sites are not communicating, they cannot feel the effect which the other is causing. As a result, they both tend to absorb more positive charge than the chromium in benzyl-chromium. Thus, structure II contributes more to the actual structure and so homolysis is slower than that predicted by statistics, $2(2.63 \times 10^{-3} \text{ s}^{-1})$. Of course, the old problem of $\text{CrCH}_2\text{-C}_6\text{H}_4\text{-CH}_2\text{Cr}^{4+}$ is still around. This explanation says no communication between sites, but if that is so why communication for $\text{CrCH}_2\text{-C}_6\text{H}_4\text{-C}_6\text{H}_4\text{-CH}_2\text{Cr}^{4+}$. This is a problem which cannot be easily resolved.

A new effect which appeared in these kinetics is the dependence of the rate of reaction upon $[\text{Fe}^{3+}]$. All cases previously studied were independent of the concentration of the oxidizing agent. This new result was especially surprising because Fe^{3+} was the only oxidant studied which exhibited this behavior. The dependence was seen by the fact that the reaction rate increase slightly as $[\text{Fe}^{3+}]$ was increased. The proof came from the straight line plot for k_{obs} versus Fe^{3+} (Table 9). The increase in rate was small, perhaps 10%, for large increases, 10-fold, in $[\text{Fe}^{3+}]$. Thus, the effect was very small and could be easily overlooked in this case. The effect can again be explained by reference to the resonance structures reproduced in equation 22.



These structures suggest two possible modes of reaction. Structure I can homolytically cleave to produce Cr^{2+} and the benzyl radical. These fragments then react with Fe^{3+} in the usual fashion. The other possibility is that Fe^{3+} could attack structure II directly prior to homolysis. The first route would represent the normal, Fe^{3+} independent, homolysis pathway. The other path is the Fe^{3+} dependent, direct attack mode. For the organodichromium cation under discussion, the direct attack contributed only a small amount to the overall reaction, and so it may indicate some facets of the mechanism.

The initial concern was why Fe^{3+} exhibited this behavior while none of the other oxidants did. This can be explained by examining the potentials of the oxidizing agents. The values are $\text{Fe}^{3+} = +0.770$ volts, $\text{Co}^{2+} = +0.158$ volts, and $\text{Co}(\text{NH}_3)_5\text{Cl} < +0.34$ volts (67,68). Obviously, Fe^{3+} is a much stronger oxidizing agent than the other two. Therefore, it is not surprising that it can initiate direct attack while the others cannot. Exactly such an effect may explain the large rate enhancement seen in the reaction of CrGH_2 -- $\text{CH}_2\text{Cr}^{4+}$ with H_2O_2 ($E_o = +1.776$ volts). Thus, direct attack appears to occur only for the stronger oxidizing agents.

The proposed mechanism suggests certain tests to further validate its correctness. First, cations which tend to

stabilize structure II should undergo homolysis slower and also show a larger contribution from direct attack. The reaction outlined represents the reaction of a 4+ organodichromium cation with a 2+ or 3+ charged Fe^{3+} (69). Obviously, this sort of reaction should be sensitive to ionic strength effects. In addition, if the charge is reduced by studying benzyl-chromium or its derivatives instead of the organodichromium cations, the contribution from the direct attack pathway should increase. All of these ideas will be tested by examining $\text{CrCH}_2\text{-C}_6\text{H}_4\text{-CH}_2\text{Br}^{2+}$ relative to $\text{CrCH}_2\text{-C}_6\text{H}_4\text{-CH}_2\text{Cr}^{4+}$.

The next compound studied was the first member of the series with $n = 0,1,2$. The rate of reaction of $\text{CrCH}_2\text{-C}_6\text{H}_4\text{-CH}_2\text{-CH}_2\text{-C}_6\text{H}_4\text{-CH}_2\text{Cr}^{4+}$ was independent of the nature and concentration of the oxidizing agent (Fe^{3+} was again a slight bit faster). The average value, $3.12 \times 10^{-3} \text{ s}^{-1}$, was very similar to the other values obtained for organodichromium cations. This value also does not reflect the statistical value of two relative to benzyl-chromium. Thus, again, the second carbon-chromium bond must be demonstrating a retarding effect toward the other bond. The best explanation again appears to be the increased importance of structure II. The rate constants for this organodichromium cation, as well as the others in the series, are best compared

to $\text{CrCH}_2\text{-}\langle\text{O}\rangle\text{-CH}_2\text{Cr}^{4+}$ rather than the meta isomer. This point will be proved by examining the results for $\text{CrCH}_2\text{-}\langle\text{O}\rangle\text{-CH}_2\text{Br}^{2+}$

in a later section.

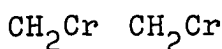
In the case of the homolysis with Fe^{3+} , the Fe^{3+} independent as well as Fe^{3+} dependent paths were again seen. In this case, the effect was studied quantitatively as seen in Figure 22. The intercept represents the $[\text{Fe}^{3+}]$ independent path which should correspond to pure homolysis. The value $3.04 \times 10^{-3} \text{ s}^{-1}$ is very close to the value $3.12 \times 10^{-3} \text{ s}^{-1}$ obtained for the other oxidizing agents, thus lending strong support to the proposed explanation. The slope of the line represents the $[\text{Fe}^{3+}]$ dependent portion of the reaction. The value is $6.29 \times 10^{-2} \text{ s}^{-1} \text{ m}^{-1}$ which represents a larger value than $k_1 = 3.04 \times 10^{-3} \text{ s}^{-1}$. However, this is a second order rate constant, and so the value $k_{\text{Fe}^{3+}}[\text{Fe}^{3+}]$ must be considered. When allowing for the low concentrations of Fe^{3+} used, it can be seen that the k_1 path makes a much larger contribution. As a matter of fact, the $[\text{Fe}^{3+}]$ dependent pathway never contributes more than 10% of the total reaction. In light of the experimental problems encountered (polymer production), the experimental uncertainties are at least $\pm 10\%$. As a result, the significance of these results may be challenged. The experimental points

presented represent the average of three very close runs. All runs were performed on samples of the same solution and all were run within hours of each other. As a result of all these precautions, the small effect is attributed to the chemistry described and not experimental error.

The next member of the series to be studied was $\text{CrCH}_2\text{-C}_6\text{H}_4\text{-CH}_2\text{-C}_6\text{H}_4\text{-CH}_2\text{Cr}^{4+}$. This organodichromium cation proved to be very similar to those already described. The homolytic cleavage proceeded with a rate constant $k_1 = 2.61 \times 10^{-3} \text{ s}^{-1}$. This number is very close to that for the case $n = 2$. This illustrates the small difference which is brought about by removing one of the methylene groups from between the benzene rings. Essentially one methylene group insulates the sites nearly as well as two methylene groups. Again, the homolysis with Fe^{3+} is a bit faster than the other oxidizing agents indicating direct Fe^{3+} attack in addition to homolysis. In this case, the effect of the $\text{CH}_2\text{Cr}(\text{OH}_2)_5$ group can be separated from the remainder of the organic group. The organic part, $\text{CH}_2\text{-C}_6\text{H}_4$, has a σ_p value of -0.09 (66) and so should enhance the homolysis above the 2:1 statistical value. Obviously, the second chromium-carbon site has a large enough effect to overcome both of these trends in the opposite direction. Again, more experimental evidence for the strong effect of the second chromium-carbon bond.

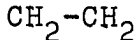
The last member of the series, $\text{CrCH}_2\text{-C}_6\text{H}_4\text{-C}_6\text{H}_4\text{-CH}_2\text{Cr}^{4+}$, has already been discussed in great detail. This organo-dichromium cation decomposed approximately ten times faster than any others studied. This has been attributed to excellent resonance communication between the two extremes of the organic molecule. Thus, the large contribution of structure I, and so rapid homolysis. The results of the series $n = 0, 1, 2$ showed a trend which was abrupt between $n = 1$ and $n = 0$, but was in general agreement with the work of Harriman and Maki (54).

In the course of searching for molecular coupling products, $\text{C}_6\text{H}_4\text{-O-C}_6\text{H}_4^{4+}$, was investigated. Molecular models



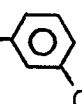
indicate that the diradical formed from cleavage of the two Cr-C bonds should be in an ideal position to close to produce a simple organic compound as a product instead of polymer.

The anticipated product, $\text{C}_6\text{H}_4\text{-O-C}_6\text{H}_4$, is a known compound (70-



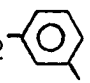
72) and should be easy to identify. In fact, the product of the decomposition with oxidizing agents was largely simple organic material. The problem is that it appeared to be a mixture of compounds from the ^1H NMR spectra. In addition, none of the peaks in the spectra corresponded to those anticipated for the desired product. Apparently, the bulky

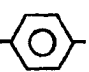
$\text{Cr}(\text{OH}_2)_5$ groups must change the chemistry to prevent the production of the desired compounds. The most logical explanation appears to be that they change the conformations of the two rings in order to keep the $\text{Cr}(\text{OH}_2)_5$ groups as far apart as possible. Thus, when homolysis occurs, the two methylene groups are far away from each other and so undergo separate chemistry. Thus, the internal coupling product was not formed, and so this aspect of the chemistry could not be studied. The observed organic product suggested that the kinetics of decomposition of this organodichromium cation might be easier to obtain. Quite to the contrary, the organic products tended to cloud the cell and so make the kinetics impossible to obtain. The effect will also be seen later in the case of a substituted benzyl-chromium cation.

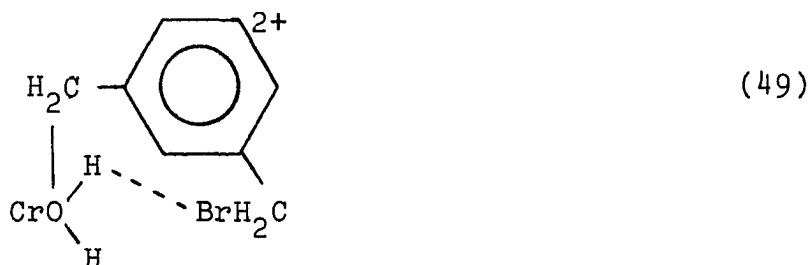
The most critical substituted benzyl-chromium cation studied was CrCH_2 -. The fact that it could be synthesized, isolated, and studied while the analogous para isomer could not indicated that the substitution pattern had a profound effect. These results suggested that the two sites in the meta isomer were more isolated from one another. This lack of communication is clearly seen in the results for the ϵ determination (Table 14). The fact that the ϵ for this organochromium cation is exactly one-half of that for the organodichromium cation strongly supported the

contention of noninteracting sites. The ϵ for $\text{CrCH}_2\text{-C}_6\text{H}_4\text{-CH}_2\text{Cr}^{4+}$ was also twice that of benzyl-chromium, and so the difference between these two systems must be very subtle.

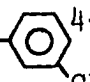
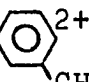
The homolysis of $\text{CrCH}_2\text{-C}_6\text{H}_3(\text{CH}_2\text{Br})\text{Cr}^{2+}$ also contains some very informative features. The first is that the rate of homolysis ($1.23 \times 10^{-3} \text{ s}^{-1}$) is relatively slow for benzyl-chromium cations. As a matter of fact, it is nearly as slow as the *p*- CF_3 substituted benzyl-chromium. This is very surprising because the values for CH_2Br are $\sigma_m = +0.12$ and $\sigma_p = +0.14$ (66). Obviously, this implies that the linear free-energy correlation for the meta substituted benzyl-chromiums must be quite a bit different from that for the para isomers. If a linear free-energy correlation does exist, the slope ρ must be substantially steeper than that seen in Figure 44. This suggests that a new type of mechanism may intervene when the substituents are in the meta position. The most logical explanation for this phenomenon would be some sort of through space interaction. This seems reasonable when the proximity of the bulky $\text{Cr}(\text{OH}_2)_5$ group to the large CH_2Y substituents is demonstrated with molecular models. Possible evidence for this effect can be seen by comparing the k_1 value for this with *p*-bromobenzyl-chromium. The bromine group is directly on the ring and has a σ_p value

of +0.23 (66) which should be reflected in a much slower rate of homolysis than a meta CH_2Br group. In fact, its value, $1.56 \times 10^{-3} \text{ s}^{-1}$, is significantly higher than that for the case CrCH_2 -- $\text{CH}_2\text{Br}^{2+}$ ($1.23 \times 10^{-3} \text{ s}^{-1}$). This enhanced

effect in the meta position also carries over to the organo-dichromium cations. CrCH_2 -- $\text{CH}_2\text{Cr}^{4+}$ should exhibit the greatest effect of the electron withdrawing $\text{Cr}(\text{OH}_2)_5$ group because it is in direct conjugation. Quite to the contrary, the rate for the meta isomer is retarded by a greater amount. A drawing to illustrate the effect is presented as equation 49. The work described here did not permit much comment

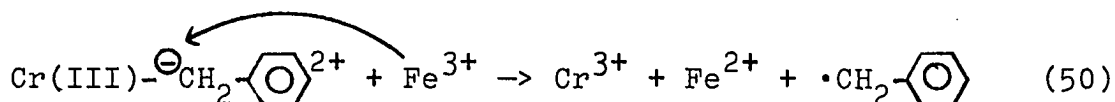


about the precise nature of this effect, and so it will be treated as an experimental observation that the meta position is less reactive.

Another interesting comparison can be made between CrCH_2 -- $\text{CH}_2\text{Cr}^{4+}$ and CrCH_2 -- $\text{CH}_2\text{Br}^{2+}$. These two comprise an ideal set with which to test the validity of the statistical kinetic relationship. These two groups are both relatively

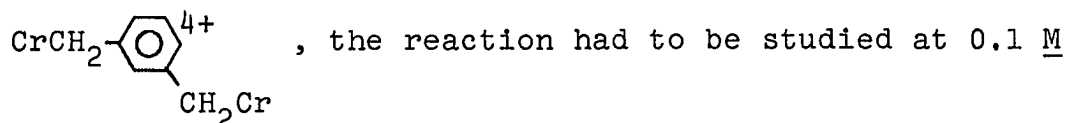
strongly electron withdrawing and so the only advantage the organodichromium cation should have is the two sites relative to one. The values $2.13 \times 10^{-3} \text{ s}^{-1}$ and $1.23 \times 10^{-3} \text{ s}^{-1}$ are very close to the statistical value of 2:1. From these results it appears that the $\text{Cr}(\text{OH}_2)_5$ group is a better electron withdrawing group than the Br. This effect has been seen many times over and in this case explains the value less than 2:1.

The final interesting fact is the rate of homolysis with Fe^{3+} . This reaction again has an Fe^{3+} dependent path as well as the independent path. This case is interesting because proper control of conditions allows the dependent path to comprise a large portion of the total reaction. The direct attack is shown schematically below in equation 50.



This reaction is between two positively charged species and so should exhibit an ionic strength dependence. For the case run at 0.1 M H^+ , the rate constants are $k_1 = 1.22 \times 10^{-3} \text{ s}^{-1}$ and $k_{\text{Fe}^{3+}} = 1.06 \times 10^{-2} \text{ m}^{-1} \text{ s}^{-1}$ (see Figure 23). Again, at the low Fe^{3+} concentrations used, the $k_{\text{Fe}^{3+}}[\text{Fe}^{3+}]$ pathway contributes no more than 10% to the overall reaction. However, when the ionic strength was increased to $0.1 \text{ M HClO}_4/0.3 \text{ M NaClO}_4$, the dependent pathway plays a more

important role (see Figure 24). In this case, $k_1 = 1.21 \times 10^{-3} \text{ s}^{-1}$ and $k_{\text{Fe}^{3+}} = 7.54 \times 10^{-2} \text{ m}^{-1} \text{ s}^{-1}$. This large increase in the value of $k_{\text{Fe}^{3+}}$ with increasing ionic strength is precisely that anticipated for the reaction of a 3+ and 2+ ion. If this effect is valid, it should be even more difficult to observe this in the case of the 4+ charged organodichromium cations. Recall in the case of



$\text{HClO}_4/0.9 \text{ M NaClO}_4$ before 10% of the reaction went by direct attack while in this case 0.1 M HClO_4 was sufficient to observe this. The prediction is that direct attack will play the largest role for the substituted benzyl-chromium cations which contain uncharged electron withdrawing groups. Such an effect will be seen in the case of a related organochromium cation.

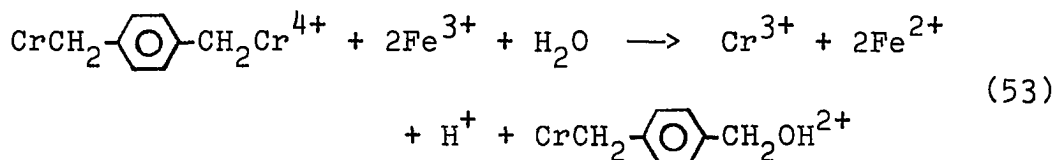
Some unusual chemistry is seen in the case of the reaction of the oxidizing agents with $\text{CrCH}_2\text{-C}_6\text{H}_3\text{(CH}_2\text{Br)}^{2+}$. The

anticipated products were $\text{HOCH}_2\text{-C}_6\text{H}_3\text{(CH}_2\text{Br)}$ for Cu^{2+} and Fe^{3+}

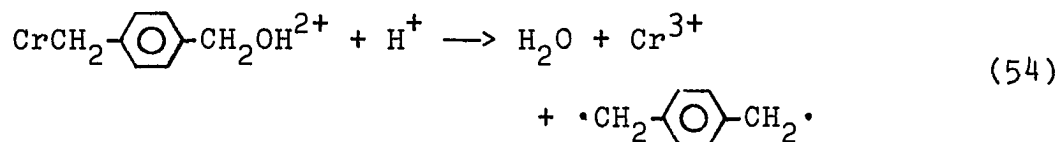
and $\text{C}_6\text{H}_3\text{(CH}_2\text{Br)-CH}_2\text{-CH}_2\text{-C}_6\text{H}_3\text{(CH}_2\text{Br)}$ in the case of $\text{Co}(\text{NH}_3)_5\text{Cl}^{2+}$.

Surprisingly, in all cases the product was a polymeric material, presumably poly-m-xylylene. This product suggested

manner analogous to the other benzyl-chromium cations from Cr^{2+} and $\text{BrCH}_2\text{-C}_6\text{H}_4\text{-CH}_2\text{OH}$. This compound was novel from the point of view that it represented total oxidation of one-half of $\text{CrCH}_2\text{-C}_6\text{H}_4\text{-CH}_2\text{Cr}^{4+}$. This fact is represented in equation 53. Since this compound represented a stoichiometry of



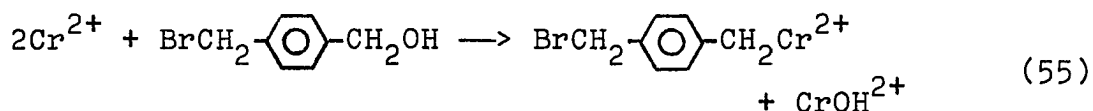
2 moles of Fe^{3+} per mole of organodichromium, it appeared to be an intermediate which should readily decompose to the product poly-p-xylylene. The kinetics analysis has shown the chromium-carbon bond homolysis to be the rate limiting step and so this intermediate should decompose relatively readily. In fact, it did decompose under acidic conditions to poly-p-xylylene, but the reaction required in excess of 24 hours to go to completion. A balanced equation for this reaction is presented as equation 54. An equation of this



sort does not represent a redox reaction and so implies no role for the oxidizing agents. Quite to the contrary, oxidizing agents accelerated this reaction markedly and also produced poly-p-xylylene. This type of experiment cannot be

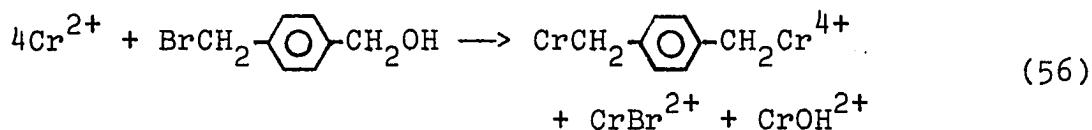
represented by a balanced redox equation, and so the identity of the substituted benzyl-chromium cation was questioned.

Several possibilities for new chemistry were considered. The first case was Cr^{2+} reacting at the benzyl alcohol group instead of the benzyl bromide group. This is presented as equation 55. This was quickly dismissed by adding excess



Cr^{2+} and noting no change in the observed product. The $2+$ cation shown is the midpoint in the reaction of $\text{BrCH}_2\text{-}\langle\bigcirc\rangle\text{-CH}_2\text{Br}$, and so it could never exist in the presence of excess Cr^{2+} . Thus, this formulation is impossible.

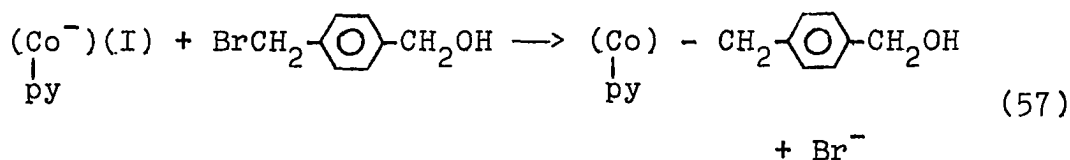
Another closely related idea is that the species is really an organodichromium. Such a reaction is presented in equation 56. This species would indeed produce poly-p-



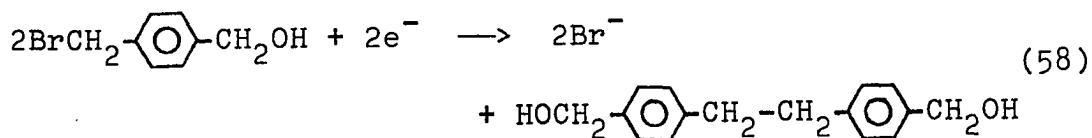
xylylene upon reaction with oxidizing agents as required. The problem is that its ion-exchange behavior was very different from a $4+$ species, and much more like that of a $2+$ cation. In addition, the kinetics of decomposition were very different from those observed for the organodichromium cation. The structure was finally proved to be

$\text{CrCH}_2\text{-C}_6\text{H}_4\text{-CH}_2\text{OH}^{2+}$ by decomposing it in base and isolating the product *p*-methylbenzyl alcohol. These results all suggested that this benzyl bromide had chemistry identical to that of other substituted benzyl bromides.

The chemistry of $\text{BrCH}_2\text{-C}_6\text{H}_4\text{-CH}_2\text{OH}$ was further investigated by performing several reactions. The first one was to attempt to prepare the substituted benzyl-cobaloxime according to standard procedures (24). The reaction proceeded according to equation 57 and produced an orange,

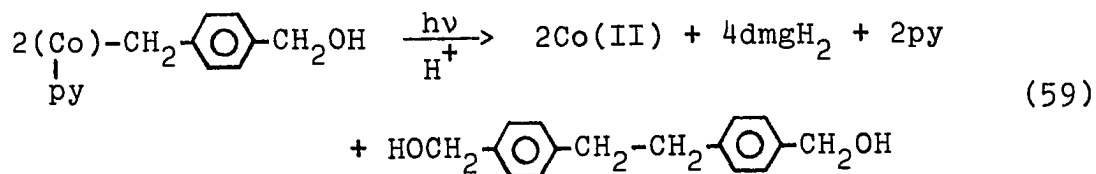


isolable solid compound. The compound was isolated, and it analyzed very well (see Table 2) for the compound of interest. Another type of experiment was electrochemical reduction. This sort of chemistry had been shown to produce polymer in the case of $\text{BrCH}_2\text{-C}_6\text{H}_4\text{-CH}_2\text{Br}$ (42), and so possibly this compound would exhibit such chemistry. The compound was reduced with one equivalent of electrons, but no polymer was produced. Although the product was not positively identified, it appeared to be a simple organic compound. A balanced equation for production of the coupling product is shown in equation 58. This is the



final line of evidence supporting this compound as a simple benzyl bromide.

Now that the structure of the 2+ cation was established, it remained to be shown how it decomposed to poly-p-xylylene. Since the reaction appeared to consume zero equivalents of oxidizing agent, it appeared necessary to study the homolysis reactions in the absence of the oxidizing agents. The first type of reaction to be investigated was photochemical homolysis. This type of reaction is well-documented for organocobaloximes (73) and was first attempted for $(\text{Co})\text{-CH}_2\text{-}\langle\text{O}\rangle\text{-CH}_2\text{-OH}$. The compound decomposed smoothly but did not produce any poly-p-xylylene. Although the actual product was not identified, a likely explanation is shown as equation 59. This certainly implies that the substituted



benzyl radical, $\cdot\text{CH}_2\text{-}\langle\text{O}\rangle\text{-CH}_2\text{OH}$, does not spontaneously produce poly-p-xylylene. This certainly complements the results from the electrochemistry experiment. The same photolysis was performed on $\text{CrCH}_2\text{-}\langle\text{O}\rangle\text{-CH}_2\text{OH}^{2+}$. The

cation did not photochemically decompose over the period of four to five hours under nitrogen (74). This suggests that visible light is not energetic enough to bring about the homolysis. Perhaps if ultraviolet radiation had been used, the reaction could be forced to proceed. Nonetheless, the experiments suggest that bond homolysis is not a sufficient condition to produce polymer.

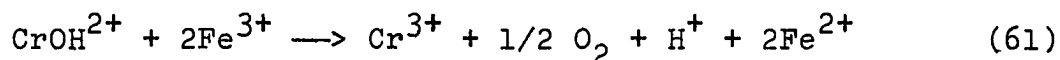
All of these negative results pointed to the need to show conditions under which homolysis could product polymers.

The compound initially studied was $(\text{Co})-\underset{\text{py}}{\text{CH}_2}-\text{C}_6\text{H}_4-\text{CH}_2-\underset{\text{py}}{(\text{Co})}$.

Photolysis of both cobalt-carbon bonds should produce p-xylene which is the most logical precursor for the polymer. This compound does indeed undergo photolysis under gentle conditions to produce poly-p-xylylene. The reaction is so facile that it can be brought about by ordinary room light. The same procedure was then repeated for $\text{CrCH}_2-\text{C}_6\text{H}_4-\text{CH}_2\text{Cr}^{4+}$. It was not photolyzed by room light, but could be readily photolyzed by the xenon lamp to produce poly-p-xylylene. These examples show the ability of photolysis to produce diradicals from these organodimetallics which are capable of producing polymers. The fact that $\cdot\text{CH}_2-\text{C}_6\text{H}_4-\text{CH}_2\text{OH}$ has no clear path to polymers is also amply proved by these experiments.

the initial step to occur, and it must also be consumed because stoichiometry experiments have shown that at least one mole of Fe^{3+} is consumed per mole of benzyl-chromium. This dilemma suggested further experiments.

The role of the oxidizing agent was most clearly spelled out in the case of Fe^{3+} . The data (Table 10) made it clear that Fe^{3+} was again showing enhanced reactivity over the other oxidants. In this case, the Fe^{3+} dependent path is contributing a substantial share to the overall reaction even at relatively low concentrations of Fe^{3+} . This constitutes a great proof for the notion that the Fe^{3+} dependent path is represented by direct attack by Fe^{3+} on the carbon-chromium bond. It was predicted that this effect would be seen most clearly in the case of a benzyl-chromium cation containing strongly electron withdrawing substituents precisely as this case shows. The only problem is proposing a redox step. From the sketchy mechanism developed, the only step which would meet the criterion is shown as equation 61. This is



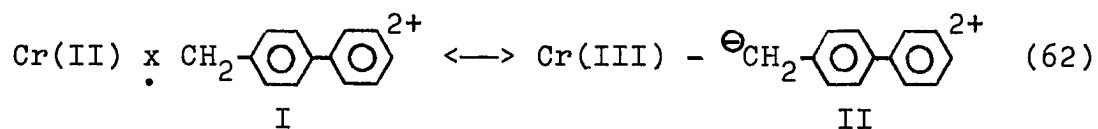
a redox reaction, but surely represents the only reaction proposed between Fe^{3+} and Cr(III) which is a redox process. As a result, there does not appear to be any satisfactory explanation for all of the experimental facts. Of course, one bothersome aspect of this problem has always been the

rapid decomposition of the $\text{BrCH}_2\text{-C}_6\text{H}_4\text{-CH}_2\text{OH}$. The possibility exists that regardless of how fresh the sample is, there is a small amount of impurity which determines the chemistry of the entire solution. The decomposition is even more troublesome since the decomposition product contains an orange-colored material, presumably bromine. This would suggest some sort of homolysis and the possibility of forming radical products which would react with Cr^{2+} . Thus $\text{CrCH}_2\text{-C}_6\text{H}_4\text{-CH}_2\text{OH}^{2+}$ reacted at reasonable rates, but produced unusual products exactly like $\text{CrCH}_2\text{-C}_6\text{H}_3(\text{CH}_2\text{Br})^{2+}$.

The only "normal" benzyl-chromium cation studied in this work was $\text{CrCH}_2\text{-C}_6\text{H}_4\text{-C}_6\text{H}_5^{2+}$. This compound exhibited many of the features seen in the original work on benzyl-chromium (9). The reaction with oxidants produced the products anticipated from the work on benzyl-chromium (Figure 21). This made for a nice comparison between the two systems, but created a problem for the kinetics. The alcoholic products in this case had such large organic substituents that the products were no longer soluble in water. This led to formation of cloudiness and so produced highly questionable kinetic results. As a result, general trends will be discussed without many specific details.


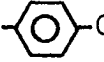
The value of k_1 for Cu^{2+} , $3.28 \times 10^{-3} \text{ s}^{-1}$, was very close to the value for benzyl-chromium ($2.63 \times 10^{-3} \text{ s}^{-1}$),

and in light of the uncertainty considered to be within experimental error. This value was well within the range anticipated from the σ_p value for C_6H_5 which is +0.03 (66). Thus, the phenyl has a slight electron withdrawing effect relative to hydrogen. The rate with Fe^{3+} did, however, seem to show quite a strong effect from the phenyl group. At the lowest $[Fe^{3+}]$ used, the rate was one-third faster than the rate for Cu^{2+} while at the highest $[Fe^{3+}]$ it was twice the rate. These results suggest a strong contribution by resonance structure II shown in equation 62, but there

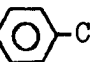
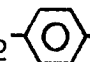
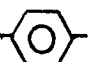
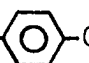




appears to be little related chemistry to support this idea. The closest analogy is the abnormally low basicity of aromatic amines. The explanation is that the aromatic π system aids in delocalization of the lone pair of electrons thus making them less accessible to protons. If this is a valid analogy, the pK_a for aniline is 4.60 (75) while that for *p*-phenylaniline is 4.35 (75). The smaller value of K_a , $10^{-4.60}$, represents the smaller amount of the basic amine while the larger K_a , $10^{-4.35}$, represents a larger amount in the deprotonated form. Thus, the phenyl group makes it a bit less basic but only by a small amount. This effect is very much in line with the σ_p value of +0.03 assigned to the

phenyl group. These results imply that structure II should not play a predominant role and so the Fe^{3+} results are attributed to problems in the kinetics caused by the precipitation problem.

This substituted benzyl-chromium cation was originally studied to serve as a basis for comparison with CrCH_2 -- $\text{CH}_2\text{Cr}^{4+}$. In the latter case, the kinetics were too rapid to be studied and it was desirable to locate the cause of the rapid decomposition. These results suggest that the phenyl group may play a role, but it is small at best. The key to the chemistry appears to be the second chromium site. It is obviously essential that the benzene be there because CrCH_2 -- $\text{CH}_2\text{Cr}^{4+}$ does not show this same effect. The role of the ring may involve its remaining coplanar to the other ring so that the two ends can communicate. It is hard to prove or disprove this idea, but these experiments suggest the benzene ring cannot bring about this effect by itself.

One final aspect of the project was the production of polymers. This is an area which was not thoroughly explored due to analytical problems. The products poly-p-xylylene and poly-m-xylylene were anticipated from the work of Lunk and Youngman (10). These authors identified their products by IR spectroscopy. This was fine for their work because they had two totally different substitution patterns on the

benzene ring to distinguish. In the cases studied here, there are subtle differences which need to be distinguished. CrCH_2 -- $\text{CH}_2\text{Cr}^{4+}$ and CrCH_2 -- CH_2 - CH_2 -- $\text{CH}_2\text{Cr}^{4+}$ both decompose to poly-p-xylylene (Table 16). CrCH_2 -- CH_2 -- $\text{CH}_2\text{Cr}^{4+}$ should produce a polymer with alternating two and one methylene group as opposed to the constant two of poly-p-xylylene. CrCH_2 -- $\text{CH}_2\text{Cr}^{4+}$ should produce a polymer with alternating two and zero methylene groups. These polymers are only slightly different and will be difficult to distinguish by IR spectroscopy. This problem is especially bad in light of the poor KBr pellets which result from these linear polymers. In light of these problems, other techniques were examined. The melting points were all so high (>300°C) that they provided little insight into the structure. The last technique examined was elemental analysis. Such a technique has been applied to polymers (45) with no apparent difficulties. The application of this technique to poly-p-xylylene produced terrible results (Table 4). The results were all exceptionally low for carbon and hydrogen. The entire source of the problem cannot be impurities because authentic samples showed the same effect. This suggested the possibility of incomplete combustion of the sample and so oxidation catalysts were added. The results improved slightly (Table 4), but they were still quite short of the theoretical values. The ratio of carbon to

hydrogen is always very close to 1:1 as it should be, but the low absolute values invalidated this as a suitable means of analysis. This lack of proper identification of the polymeric products made it difficult to assess the synthetic importance of these reactions.

Poly-p-xylylene has been synthesized by a wide variety of routes (31,42,45,76). The reactions studied here suffer from the fact that when the polymer is formed in solution it can occlude solvent, metal salts, and any other materials in solution. Thus, other routes can produce higher purity material (31) as well as much higher yields. The commercial use for this polymer is for coating electronics equipment (31). For this use thin layers of the polymer are required, and so the procedure described here is totally useless. Thus, the only advantage to these systems seem to be for synthesis of polymers not accessible by other routes. Thus, the new polymers (77) previously mentioned may be valuable modifications of the basic poly-p-xylylene structure. The original work (10) also suggests great ease in preparing copolymers which also could prove to be a valuable application. More work by people trained in this area will be required to verify these ideas.

BIBLIOGRAPHY

1. F. A. L. Anet and E. L. LeBlanc, J. Amer. Chem. Soc. 79, 2649 (1957).
2. J. K. Kochi and D. D. Davis, J. Amer. Chem. Soc. 86, 5264 (1964).
3. M. Ardon, K. Woolmington and A. Pernick, Inorg. Chem. 10, 2812 (1971).
4. W. Schmidt, J. H. Swinehart and H. Taube, J. Amer. Chem. Soc. 93, 1117 (1971).
5. H. Cohen and D. Meyerstein, Inorg. Chem. 13, 2434 (1974).
6. J. H. Espenson and J. S. Shveima, J. Amer. Chem. Soc. 95, 4468 (1973).
7. Cobaloxime is the trivial name for the bis(dimethylglyoximate) complexes of cobalt.
8. J. K. Kochi and D. Buchanan, J. Amer. Chem. Soc. 87, 853 (1965).
9. R. S. Nohr and J. H. Espenson, J. Amer. Chem. Soc. 97, 3392 (1975).
10. H. E. Lunk and E. A. Youngman, J. Polymer Science: Part A-1, 3, 2983 (1965).
11. For actual data see the Aldrich Catalog - Handbook of Organic and Biochemicals and the Aldrich Library of NMR Spectra.
12. J. A. Goodson, L. J. Goodwin, J. H. Garvin, M. D. Goss, K. S. Kirby, J. A. Lock, R. A. Neal, T. M. Sharp and W. Salomon, Brit. J. Pharmacol. 3, 62 (1945).
13. HBr was used from two different sources. The first was a gas cylinder from MCB. The second was from the reaction of bromine and tetralin. For the actual procedure see M. Schmeisser in Handbook of Preparative Inorganic Chemistry, Vol. 1; G. Brauer, editor, Academic Press, New York, 1963, p. 282. The results were identical with either source and so they were used interchangeably.

14. J. V. Braun, Chem. Ber. 70, 993 (1937).
15. S. Kögi and W. Marty, unpublished results, Iowa State University, Ames, Iowa.
16. R. E. Buhts, K. K. Chesney, J. R. Handly, F. D. Popp and D. C. Smith, Org. Prep. Proc. Int. 7, 193 (1975).
17. W. Marty and J. H. Espenson, submitted to Inorg. Chem, for publication.
18. W. Marty and J. H. Espenson, unpublished results, Iowa State University.
19. E. Hjelt and M. Gadd, Chem. Ber. 19, 867 (1886).
20. M. Bullpitt, W. Kitching, D. Doddrell and W. Adcock, J. Org. Chem. 41, 760 (1976).
21. J. T. Codington and E. Mosettig, J. Org. Chem. 17, 1035 (1952).
22. M. H. Felkin, C. R. Acad. Sci. (Paris) 230, 304 (1950).
23. M. Charpentier and B. Tchoubar, C. R. Acad. Sci. (Paris) 233, 1621 (1951).
24. S. N. Anderson, D. H. Ballard and M. D. Johnson, J. Chem. Soc. Perkins II, 311 (1972).
25. The acetone used was distilled from KMnO_4 to oxidize any impurities. As a result, an azeotrope of acetone-water was obtained and used without further purification. This procedure was necessary because most commercial acetone contains an impurity which reacts with Cr^{2+} to produce a green Cr(III)^{2+} species which ruins the ion-exchange procedure. In some cases methanol was used instead of acetone and the same results were obtained.
26. J. P. Leslie and J. H. Espenson, J. Amer. Chem. Soc. 98, 4839 (1976).
27. R. G. Coombes and M. D. Johnson, unpublished procedure, University College, London,
28. R. G. Coombes, M. D. Johnson and M. Winterton, J. Chem. Soc., 7029 (1965).

29. L. A. Errede and J. P. Cassidy, J. Amer. Chem. Soc. 82, 3653 (1960).
30. W. F. Gorham, J. Polymer. Science: Part A-1, 4, 3027 (1966).
31. W. F. Gorham, Encyclopedia of Polymer Science and Technology 15, 98 (1971).
32. D. W. Carlyle and J. H. Espenson, Inorg. Chem. 6, 1370 (1967).
33. J. Doyle and A. G. Sykes, J. Chem. Soc. (A), 217 (1968).
34. R. J. Angelici, Synthesis and Technique in Inorganic Chemistry, W. B. Saunders, Co., Philadelphia, Pa., 1969, p. 16.
35. H. Diehl, H. Clark and H. H. Willard, Inorg. Syn. 1, 186 (1939).
36. E. A. Guggenheim, Phil. Mag. 2, 538 (1926).
37. R. G. Wilkins, The Study of Kinetics and Mechanism of Reactions of Transition Metal Complexes, Allyn and Bacon, Inc., Boston, Mass., 1974, p. 22.
38. N. W. Alcock, D. J. Benton and P. Moore, Trans. Faraday Soc. 66, 2210 (1970).
39. B. A. Zabin and H. Taube, Inorg. Chem. 3, 963 (1964).
40. G. W. Haupt, J. Res. Nat'l. Bur. Stand. 48, 414 (1952).
41. A. E. Harvey, J. A. Smart and E. S. Amis, Anal. Chem. 27, 26 (1955).
42. F. H. Covitz, J. Amer. Chem. Soc. 89, 5403 (1967).
43. T. R. Crossley and M. A. Slifkin, Prog. Reaction Kinetics 5, 416 (1970).
44. D. O. Hummel, An Atlas of Infrared Analyses of Polymers, Resins, and Additives, Wiley-Interscience, New York, 1971, spectra #556.
45. J. M. Hoyt, K. Koch, C. A. Sprang, S. Stregovsky and C. E. Frank, Amer. Chem. Soc. Div. Polymer Chem. Preprints 5, 680 (1964).

46. J. H. Espenson, "Chemical Kinetics and Reaction Mechanisms", Iowa State University, Ames, Iowa, 1978, p. 25.
47. R. W. Kolaczowski and R. A. Plane, *Inorg. Chem.* 3, 322 (1964).
48. A. Adin, J. Doyle and A. G. Sykes, *J. Chem. Soc. (A)*, 1504 (1967).
49. Precisely the converse of this situation has been expressed by Jorgensen (50). "Qualitatively, a satisfactory description of these (electron transfer) bands may be given by saying that their wave number is the lower, the more oxidizing the central metal ion and the more reducing the ligands. This is exactly as expected for electron transfer from the ligand to the central ion during the optical excitation. It is a redox process, decreasing the oxidation number of the central ion by one...."
50. C. K. Jorgensen, *Absorption Spectra and Chemical Bonding in Complexes*, Pergamon Press, Reading, Mass., 1962, p. 146.
51. R. H. Abeles and D. Dolphin, *Acc. Chem. Res.* 9, 114 (1976).
52. Katon and Lippincott (53) present strong spectroscopic evidence that the angle between the two benzene rings is very close to 0° in solution as well as in crystalline compounds.
53. J. E. Katon and E. R. Lippincott, *Spectrochim. Acta* 15, 627 (1959).
54. J. E. Harriman and A. H. Maki, *J. Chem. Phys.* 39, 778 (1962).
55. R. P. A. Sneeden and H. P. Thronksen, *J. Chem. Soc. Chem. Commun.*, 509 (1965).
56. R. G. Coombes, M. D. Johnson and N. Winterton, *J. Chem. Soc.*, 7029 (1965).
57. D. Dodd and M. D. Johnson, *J. Chem. Soc. (A)*, 34 (1968).
58. F. A. Cotton and G. Wilkinson, *Advanced Inorganic Chemistry*, Interscience Publishers, New York, 1972, p. 523.

59. K. Bass, *Organomet. Chem. Rev.* 1, 391 (1966).
60. For a general review of the reactions of electrophiles with σ -bonded organotransition-metal complexes, see M. D. Johnson, *Acc. Chem. Res.* 11, 57 (1978).
61. J. C. Chang and J. H. Espenson, *J. Chem. Soc. Chem. Commun.*, 233 (1974).
62. For a review of Cr^{2+} reactions, see A. G. Sykes, *Adv. Inorg. Chem. Radiochem.* 10, 153 (1967).
63. J. M. Pearson, H. A. Six, D. J. Williams and M. Levy, *J. Amer. Chem. Soc.* 93, 5034 (1971).
64. J. R. Chipperfield, *J. Organomet. Chem.* 137, 355 (1977).
65. D. A. Buckingham, D. J. Francis and A. M. Sargeson, *Inorg. Chem.* 13, 2630 (1974).
66. O. Exner, *Colln. Czech. Chem. Commun.* 31, 65 (1966).
67. The value should be between the value +0.34 volts which is the estimated value for $\text{Co}(\text{NH}_3)_6^{3+}$ and -0.20 volts which is the estimated value for trans- $\text{Co}(\text{NH}_3)_4\text{Cl}_2^+$ (68).
68. P. A. Rock, *Inorg. Chem.* 7, 837 (1968).
69. The charge on Fe^{3+} depends on whether the reactive species is $\text{Fe}(\text{OH}_2)_6^{3+}$ or $(\text{H}_2\text{O})_5\text{Fe}(\text{OH})^{2+}$.
70. This compound has only been characterized by its melting point 154°C (71) and its boiling point $100\text{--}103^\circ\text{C}$ (0.2 mm) (72). The ^1H NMR spectra should indicate a peak in the vicinity of δ 2.80 with integration 4 corresponding to the two methylene groups. This is based on the spectra for $\text{O} \text{---} \text{CH}_2 \text{---} \text{CH}_2 \text{---} \text{O}$ which appears in reference 11,
71. E. D. Bergmann, I. Shahak and Z. Aizenshtat, *Tet. Letters* 31, 3469 (1968).
72. B. A. Hess, Jr., A. S. Bailey and V. Boekelheide, *J. Amer. Chem. Soc.* 89, 2746 (1967).
73. G. N. Schrauzer, J. W. Sibert and R. J. Windgassen, *J. Amer. Chem. Soc.* 90, 6681 (1968).

74. This negative result is not surprising since no references could be found for the photolysis of $(\text{H}_2\text{O})_5\text{Cr}(\text{alkyl})^{2+}$ types of compounds.
75. A. Albert and E. P. Serjeant, The Determination of Ionization Constants, Chapman and Hall, London, 1962, p. 94.
76. J. H. Golden, J. Chem. Soc., 1604 (1961),
77. These polymers have not yet appeared in the literature to our knowledge.

ACKNOWLEDGEMENTS

I would like to thank Professor James H. Espenson for his guidance and concern throughout the course of this work. Dr. M. D. Johnson provided several helpful procedures. Dr. W. Marty supplied several samples as well as organic purification procedures. Dr. A. Bakac provided much helpful discussion and many useful ideas. I would like to thank Ms. Sue Musselman for the excellent job of typing this thesis. I would also like to thank Garry Kirker and Debbie Ryan whose friendship and encouragement helped me make it through the many long Iowa winters. Finally, I am deeply indebted to my wife for her kindness, understanding, and love throughout the course of my graduate career.